3D printing system for ceramic materials: design and testing of an experimental rig

Armand Yahnn Fabrice Chefdor

Thesis to obtain the Master of Science Degree in

Mechanical Engineering

Supervisors : Prof. Marco Alexandre de Oliveira Leite

Prof. António Manuel Relógio Ribeiro

Examination Committee

Chairperson : Prof. Luís Filipe Galrão dos Reis

Supervisor : Prof. Marco Alexandre de Oliveira Leite

Member of the Committee : Prof. Bruno Alexandre Rodrigues Simões Soares

July 2018

Acknowledgements

Primarily, I would like to express my gratitude to my supervisors from the Mechanical Engineering Department, Professor Marco Alexandre De Oliveira Leite and Professor António Manuel Relógio Ribeiro, as well as Professor Ana Paula Valagão Amadeu do Serro from the chemical department. They all did an outstanding job by granting me support, knowledge and valuable insight into this interesting subject.

I would also like to thank my former colleagues from iMakr who introduced me to the capacities of additive manufacturing and took the time to provide me useful knowledge for this following topic.

I would likewise thank my colleagues from the chemical department and the Lab2Prod for their guidance and generous help with diverse tasks regarding my work.

Finally, I gratefully acknowledge all the people who allow the Erasmus exchange program to exist, and thus helped me to stay at Técnico for this semester. On the other hand, I do not wish to thank my Erasmus friends who often found a way to take my concentration away from this subject.

Abstract

In the context of a constantly growing additive manufacturing market, many processes are acquiring important statuses in the medical field. Particularly for dental restorations where those manufacturing techniques helped to produce more performant implants to solve both plastic and functional problems of deteriorated teeth. As restorative materials, ceramics became increasingly popular because of their aesthetics, inertness, mechanical properties and biocompatibility. Thanks to its inherent ability for complex geometries fabrication, additive manufacturing has thus gained significant interest to realise quickly available customized pieces with low material consumption, which led to lowering the costs of the most popular dentures. However, some uncommon prosthetics still remain impossible to produce or are overpriced.

The motivation of this study is to help filling this gap by adapting the economic advantages of the FDM process into a solution for the dental medical care.

To do so, the aim is to create an experimental rig for ceramic paste deposition, which purpose is to allow the testing of several parameters to assess the printability of the material. This prototype is done by designing a hardware adaptation of a 3D printer, originally operating with the method of fused deposition modelling, to make it capable of liquid deposition modelling process. A preliminary literature survey on rapid prototyping with 3D printing was led, with methodical tests on key factors of printed parts quality, in order to adopt an effective development strategy based on CAD.

A functional prototype was manufactured with positive overall results in terms of functions and geometric freedom for production. A maximum amount of original hardware and 3D printed parts were used to ensure an affordable reparability and modularity. Finally, this experimental rig is considered as a first iteration that can be improved and adapted to specific manufacturing needs in the future.

Key words: Design for manufacturing, additive manufacturing, liquid deposition modelling, zirconia pastes, manufacturing strategy, experimental prototype

Resumo

Com o mercado de manufatura aditiva em constante crescimento muitos processos estão a adquirir uma especial importância na área da medicina. Particularmente nos restauros dentários essas técnicas ajudaram a produzir melhores implantes para solucionar os problemas plásticos e funcionais de dentes deteriorados. Como materiais de restauro os cerâmicos tornaram-se cada vez mais populares, devido à sua estética, inércia química, propriedades mecânicas e biocompatibilidade. Graças à facilidade de produção de geometrias complexas, a manufatura aditiva ganhou um interesse relevante para construir rapidamente modelos personalizados, com baixo consumo de material, o que levou a uma diminuição dos custos das próteses mais comuns, apesar de algumas próteses incomuns continuarem a ser impossíveis de produzir ou não trazer grande vantagem fazê-lo desta forma.

A motivacao deste estudo é contribuir para preencher este hiato através da adopção das vantagens economicas do processo FDM a uma solução para a medicina dentaria.

Este trabalho pretende criar um equipamento experimental para deposição de pasta cerâmica, cujo propósito é permitir o teste de variados parâmetros para determinar a adequabilidade do material para impressão. Este protótipo foi desenvolvido por uma adaptação do hardware de uma impressora 3D, originalmente a utilizar o método de deposição de filamento fundido, convertendo-a para depositar materiais liquídos/pastosos. Foi efectuada uma pesquisa bibliografica preliminar em prototipagem rápida, e testes metódicos em factores chave da qualidade das peças impressas, de forma a adoptar uma estratégia eficiente de desenvolvimento por CAD.

Um protótipo funcional foi construído com resultados gerais bastante positivos em termos de funcionalidade e liberdade geometrica de produção. O máximo de hardware inicial e de peças impressas em 3D foi utilizado de forma a garantir uma manutencao acessível e modularidade. Por fim, este equipamento experimental é considerado uma primeira iteração que poderá ser melhorado e adaptado às necessidades especificas de manufatura no futuro.

Palavras-chave: concepção para fabrico, manufactura aditiva, fabricação de deposição líquida, pastas de zircônia, estratégia de fabricação, protótipo experimental

Table of content

List of figures

List of tables

List of abbreviations

AM	=	**A**dditive **M**anufacturing
SM	=	**S**ubtractive **M**anufacturing
FM	=	**F**ormative **M**anufacturing
CAD	=	**C**omputer **A**ided **D**esign
CAM	=	**C**omputer **A**ided **M**anufacturing
CNC	=	**C**omputer **N**umerical **C**ontrol
RP	=	**R**apid **P**rototyping
FDM	=	**F**used **D**eposition **M**odelling
FFF	=	**F**used **F**ilament **F**abrication
LDM	=	**L**iquid **D**eposition **M**odelling
SLS	=	**S**elective **L**aser **S**intering
STL	=	**St**ereo **L**ithography
SLA	=	**S**tereo **L**ithography **A**pparatus
DLP	=	**D**igital **L**ight **P**rocessing
PLA	=	**P**oly**l**actic **A**cid
ABS	=	**A**crylonitrile **B**utadiene **S**tyrene
TPU	=	**T**hermoplastic **P**oly**u**rethane
PETG	=	**P**oly**e**thylene **T**erephthalate **G**lycol
PFTE	=	**P**olytetra**f**luoroe**t**hyl**e**ne
Y-TZP	=	**Y**ttria-stabilised **T**etragonal **Z**irconia **P**olycrystalline

Chapter 1 - Preface

1.1 Motivations

The decade old introduction of Additive Manufacturing techniques in the medical field has marked a turning point in the prosthesis production technology, from the traditional hand made to the innovative automated approach. Particularly for the dental market, this manufacturing method offers advantages of being faster, more efficient and leads to less waste material compared to conventional machining. The speed and ease-of-use of those technologies open the possibility for dentists to design and produce custom dental crowns directly in their offices. The Figure 1.1 illustrates the progress of additive manufacturing breakthrough in the dental machining market, which gained a growth of 35% in number of sales between 2016 and 2017. Regarding the opportunities provided by additive manufacturing, new restorative materials have been lately developed and massively adopted. That is especially the case of dental ceramics, which presents outstanding biocompatibility properties along with excellent ratios between mechanical and aesthetics functions. However, the production of all-ceramic crowns and bridges is still quite incipient, which mainstream adoption is estimated to take place in at least 5 years (Peng et al. 2018). One of the main reasons is that additive manufacturing developments are mainly focused on metal alloys and polymers, while slower progress leave the ceramic fabrication market ruled by still overpriced high-end printers. This work thus intends to contribute developing this market, as well as to help affordable medical solutions progress in the long run.

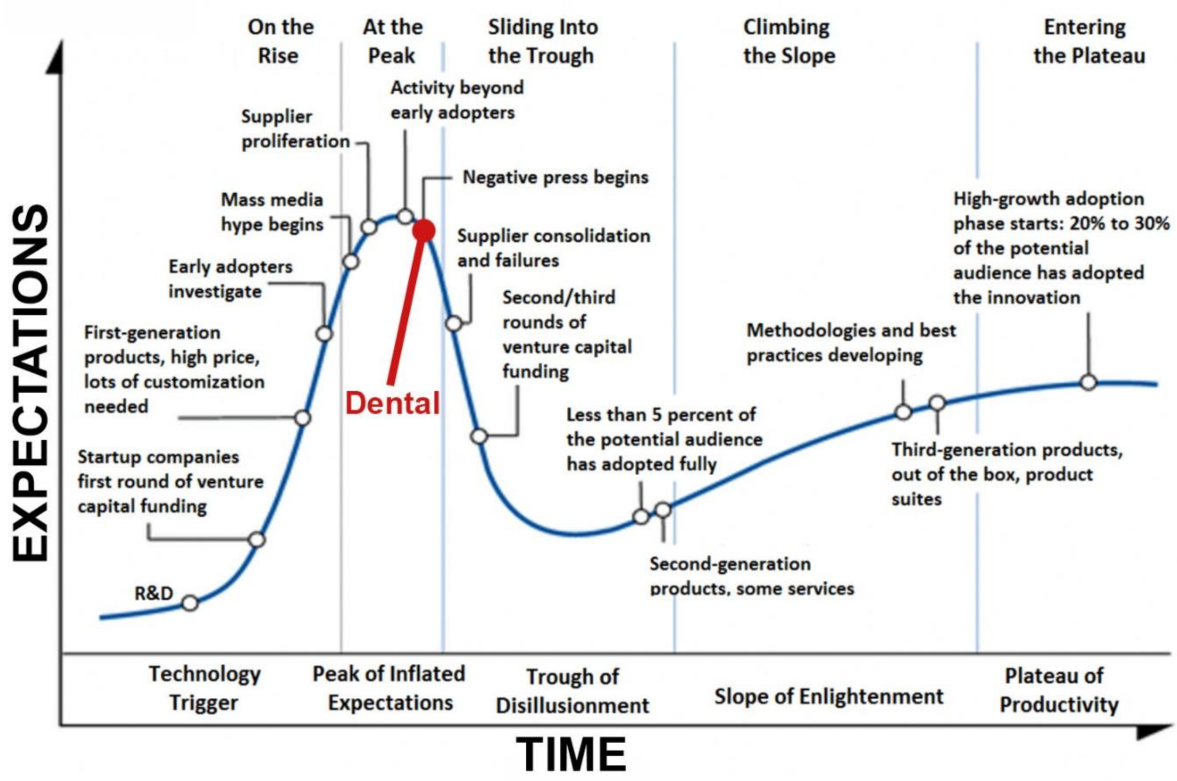

*Figure 1.1 : Evolution of additive manufacturing uses among dental industry (*Peng 2018*)*

1.2 Objectives

The aim of this work is the result of a common willpower of the Lab2Prod of the Mechanical Engineering Department and the BioMat Research Group of the Chemical Engineering Department of Instituto Superior Técnico Lisboa. The objective is to develop an additive manufacturing experimental rig for liquid deposition in the Lab2Prod, whose purpose is to work with a printable ceramic paste prepared by the BioMat Research Group. The overall product should allow the mastering of a maximum of additive manufacturing related parameters, in order to test the printability of the paste and determine a related range of correct production settings.

A functional prototype will be built from an existing 3D printer frame working with Fused Deposition Modelling. The tool head of the machine will be replaced on the actuated carriage by a Liquid Deposition Modelling-capable extruder, which needs to respect the original extruder build volume. Since the goal of the experimental rig is to test a small amount of ceramic paste at the time, the new extruder's operation will be based on standard syringe and short reservoir, chosen among those already in use in the BioMat Research Group. This adaptation will be done by reusing a maximum of the original components and realised largely thanks to parts that will be 3D printed in the Lab2Prod, to ensure modularity, ease of adaptation and maintenance of the prototype.

The chosen design strategy for additive manufacturing and the related CAD models will also be described to help further complementary works. Finally, propositions to help developing this experimental rig's first iteration will be discussed, considering both interests of the Lab2Prod and the BioMat Research Group.

Chapter 2 - Theoretical background

2.1 Additive manufacturing

The aim of this section is to present a global overview of the Additive Manufacturing (AM) technologies, in order to clarify some terminologies, concepts and relevant features to the work that will be developed in the next sections.

2.1.1 Global knowledge

2.1.1.1 Production methods comparison

Since the arrival of computers in the manufacture world a few decades ago, traditional machining has been highly improved, and a plethora of new production processes has been developed in the manner of AM tools. Nowadays a same object can be produced in many ways, each method with evolving drawback and advantages regarding the others, allowing manufacturers to constantly improve production times, energy consumptions and material wastes.

One of the most ancient production method on the market is the Subtractive Manufacturing (SM), which is still widely used in plentiful of fields. The basic principle of SM is to cut progressively material away from a large solid block until reaching the desired shape of the product (see Figure 2.1). In practice, this process is mainly embodied by the Computer Numerical Control (CNC) conventional machining, using power-driven tools such as lathes, saws, milling machines and drill presses. CNC offers great repeatability, high accuracy and a wide range of materials and surface finishes, making it a popular method of manufacturing for both small one-off jobs as well as medium to high volume production. Some unconventional machining, such as chemical and heat-based tools may also be used.

All those machining techniques have limitations, that the engineers are forced to have in mind when designing parts. Although it is a widely used technology based on Computer Aided Design (CAD), this method leads to great wastes because of the enormous quantities that are removed compared to what is used in the final product. It also involves tools wear, which require periodic substitution. In this way, on a large scale, this results in relevant environmental problems (Le, Paris, and Mandil 2017).

Commonly used for high-volume production, Formative Manufacturing (FM) is another of the oldest production methods, embodied by the Injection Moulding (IM) technique. The principle here is to create a component by injecting under pressure molten material into a die (or mould). Once injected, the melted material takes on the mould cavity’s shape, then cooled and ejected as a solid part (see Figure 2.1). The main strength of this process is its excellent repeatability, where almost all steps can be fully automated to reach very high production rates. Mainly used to produce thermoplastics polymers products it can also be adapted to every fusible material such as glass, metal and even several of them at the same time by co-injecting (Haque 2016).

However even if it produces less waste than CNC machining, this method does have its pitfalls. For instance, dies can be reused to make hundreds of thousands of parts, but represents a large upfront investment in time, development and cost. As a result, an inflexibility comes with needing to create a new mould for every new or modified part.

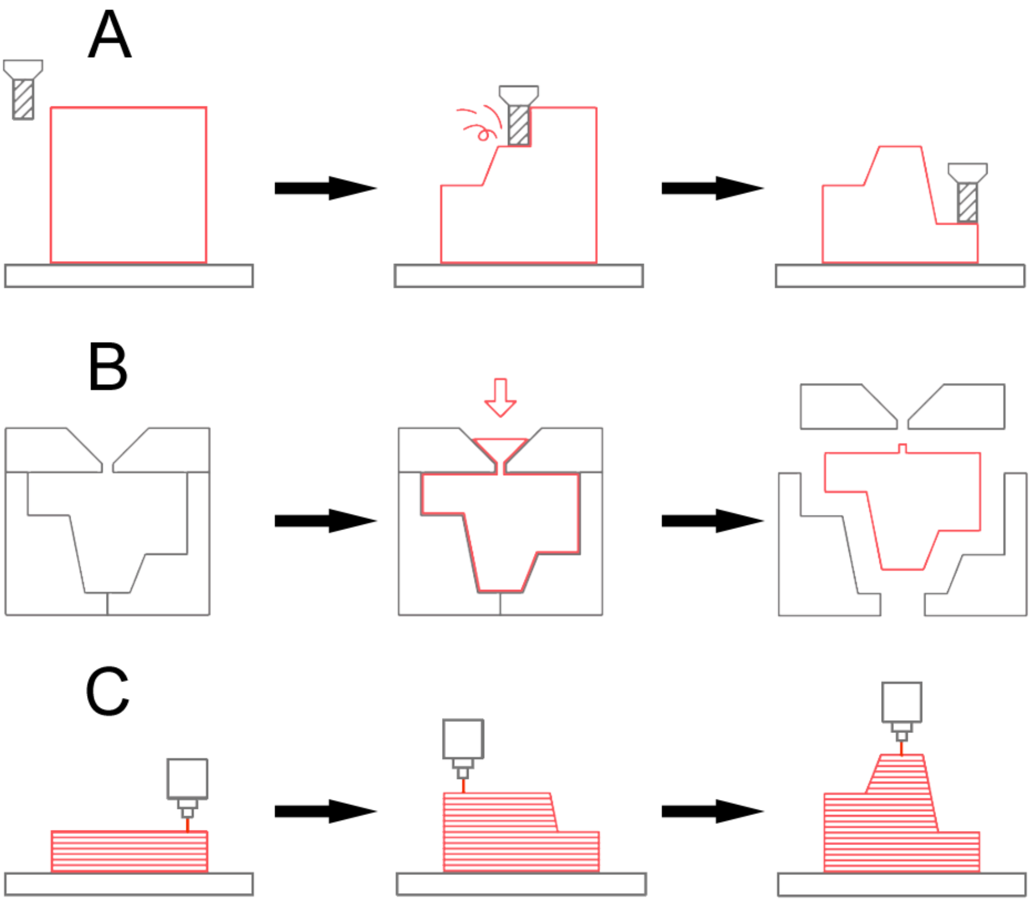

Figure 2.1 : Subtractive (A), formative (B) and additive (C) manufacturing methods (3DHubs)

Most recently introduced to the large public, Additive Manufacturing is a method of manufacture where layers of a material are build up one after another to create a three-dimensional object. It is an inevitably computer-assisted technology whose actions are originated on a digital 3D model of the object to be manufactured. Through machines based on various technologies, materials such as plastics, metals and even ceramics can be processes through this layer-by-layer method. This unique method allows the creation objects of almost any shape and geometry with virtually no upfront machining nor production lead development.

However, it is a low cost but typically slow and non-scalable method, meaning that increasing number of units for production does not decrease price per unit. Thus, AM use is restricted to rapid prototyping, single units or small batch production. On top of that, the mechanical properties of produced parts depend on lot of parameters and are still hard to predict because of lack of knowledge about it.

2.1.1.2 Evolutions and relevance of AM technologies

One of the first additive manufacturing equipment and materials were developed by Charles Hull in 1984, elaborated on an abandoned patent by the former French General Electric Company. The device, called the stereolithography fabrication system, was able to generate plastic objects by curing successive layers of photopolymers with ultraviolet light lasers. Hull's contribution was the STL file format, directly named after “stereolithography”, as well as the digital slicing and infill strategies common to many current processes. This file format allows the AM machine to interpret CAD files data, carrying information such as shape, colour, texture and thickness of the object to be printed. Today the majority of 3D printing solution operating on the market are based on this file format (Bird 2012).

In 1988, S. Scott Crump develops a special application of plastic extrusion technology, the Fused Deposition Modelling (FDM). His own company Stratasys marketed the first FDM machine in 1992 to become the most used technology by desk-sized 3D printers to date, especially for hobbyist and consumer-oriented models. In 1993, MIT research workers invent the term "3D Printing" to refer to a powder bed process they developed employing standard and custom inkjet print heads. From now on this term encompass all technologies using the AM method. In 1995, the Fraunhofer Institute developed the Selective Laser Melting (SLM) process, allowing the AM capabilities to open to a wider range of materials that were until then restricted to polymers (André Mateus de Marques Frutuoso 2017).

Since the first 3D printing process patents expired in 2009, a plentiful of improvements have been made thanks to multinational companies knowledge, along with a wide community of private buyers helping each other thanks to internet based open-source projects (Schoffer 2016; ACMA 2014). This exponentially growing AM machinery market thus satisfies needs from personal plastic objects to future ISS auto-repair prints (NASA and Bean 2017), by way of aircraft parts and buildings themselves. In this way, we can discuss the main advantages and drawbacks that AM approach globally provides over the traditional manufacturing methods, around several relevant points at the scale of this work.

➔ **Practically:**
  + **Geometries** and articulated designs impossible to replicate with FM and SM methods are usually easy to produce with AM, without any machinery adaptation.
  ± **Materials** and colour options are more and more available to AM, but some are still impossible to print, like specific metal alloys.
  − **Mechanically**, SM and FM products have better properties, whose are depending on layer’s orientation in AM. Production volumes and speeds are also limited in AM.

➔ **Financially:**
  + **Upcoming investments** are virtually non-existent in AM and the costs to produce both simple and complex-shaped parts are the same.
  • **Scale economies** are quasi impossible to realise in AM.

➔ **Environmentally:**
  + **Wastes** are limited by using only required amount of energy and material to print parts. Expendable supports use is significantly lower than in SM and FM.

2.1.2 Goals and strategies of use for AM method

The strengths of AM lie in those areas where conventional manufacturing reaches its limitations. The technology gains its full interest by enabling a way of production where the design determines the manufacturing, and not the other way around. All through its enhancement, AM acquired more and more accuracy and is working with an always wider material range. Especially when combined with other process AM is very likely to enter numerous types industries during the following years. What is more, AM allows overly complex structures that can still be extremely light and stable, which is a particularly important characteristic for medical bio engineering. It provides design freedom, optimisation and integration of functional features as well as manufacture of small quantities at a high degree of customisation for a reasonable unit cost (Atala and Murphy, n.d.).

For example, medical models are already 3D printed as well as laboratory tools and AM technologies are experimented to create stem cells capable of generating new tissues and organs in living humans. Many medical devices such as hearing aids, dental crowns and surgical implants are relatively small and therefore suitable for the production available through common AM systems. As shown in Figure 2.2, the global strategy of AM uses suits perfectly the orthopaedic field that already uses printed but expensive dentures.

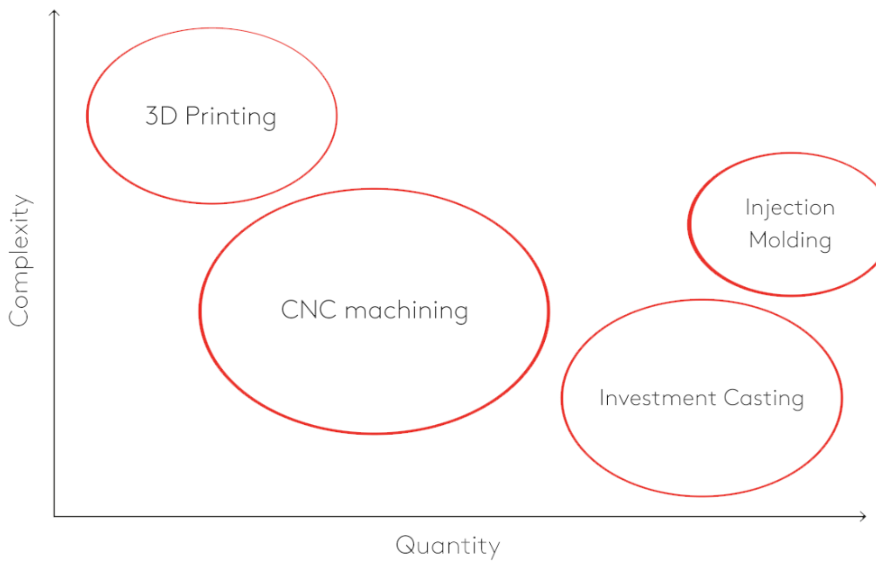

*Figure 2.2 : Global strategies of uses for the main manufacturing methods (*Varotsis 2018*)*

This graph shows the global tendencies of manufacturing method's use considering only one process, yet nowadays it makes more sense to couple those methods to obtain both brief time of development and advantageous production costs. For instance, the Printed Injection Mould Tools (PIMT), or the use of 3D printed metal dies for formative plastic production perfectly suits medium-sized batch production. As well as enrobing plastic printed parts with cement and then melt them to build cost-effective moulds for metal pouring. Thus, developing an AM experimental rig for the growing demand in dental applications makes just as much sense as using AM to build the prototype of the rig itself, before considering conventional manufacturing.

2.1.3 3D printing processes

Although AM is sometimes referred to as “Rapid Prototyping” or “3D printing”, those designations are umbrella terms that encompass a lot of individual processes which vary in their way of layer manufacturing. Those individual procedures will differ depending on the material and machine technology used. Hence in 2010 the American Society for Testing and Materials group ASTM F42, formulated a set of ISO standards that classify the range of Additive Manufacturing processes into 7 categories (ASTM International 2012).

2.1.3.1 Vat Photo-polymerisation

A vat of liquid photopolymer resin is cured through selective exposure to light, via a laser or projector, which then initiates polymerization and converts the exposed areas to a solid part. Depending on machines specifications, this method is also known as “Stereolithography Apparatus™” (SLA), “Digital Light Processing™” (DLP), “Scan, Spin, and Selectively Photo-cure™” (3SP) or “Continuous Liquid Interface Production™” (CLIP). The typical used materials are UV curable photopolymer resins with the strength of reaching elevated level of accuracy and complexity, smooth surface finish and accommodate large build areas.

When used with specific photo-polymers this technology suits the needs of dental prosthesis production field. Either by directly manufacturing customised definitive splints, either dies that will help the production of a final denture. Both technologies are used, DLP where projectors allows to process a whole layer at the same time being usually faster yet less accurate than SLA that reaches precisions of about 10 microns by using a laser beam to solidify only one point at a time (Lo Russo et al. 2018).

2.1.3.2 Powder Bed Fusion

Powdered materials are selectively consolidated by melting it together using a heat source such as a laser or electron beam. The powder surrounding the consolidated part acts as support material for overhanging features. The main technologies using this process are Selective Laser Sintering™ (SLS), Direct Metal Laser Sintering™ (DMLS), Selective Laser Melting™ (SLM), Electron Beam Melting™ (EBM), Selective Heat Sintering™ (SHS) and Multi-Jet Fusion™ (MJF).

It allows the production of parts with prominent level of complexity for virtually no wastes since powder acts as support material. Moreover, because it can work with a wider range of materials than in vat photo-polymerisation, such as plastics, metals and ceramic, it is commonly used to manufacture definitive dental implants (Azari and Nikzad 2009).

2.1.3.3 Binder Jetting

Liquid bonding agents are selectively applied onto thin layers of powdered material to build up parts layer by layer. The binders include organic and inorganic materials able to produce parts made of plastic, metal, ceramics, glass, and sand. Metal or ceramic powdered parts are typically fired in a furnace after they are printed. With strength as high productivity, wide range of materials and full colour production, the term “3D Printing” was named after this technology.

2.1.3.4 Material Jetting

Also known as Polyjet™, Smooth Curvatures Printing™ (SCP) or Multi-Jet Modelling ProJet™ (MJM). Here, droplets of material are deposited layer by layer to make parts. Common varieties include jetting a photo curable resin and curing it with UV light, as well as jetting thermally molten materials that then solidify in ambient temperatures. Usually working with polymers, photo-polymers and waxes, it provides high levels of accuracy, full colour parts and multiple materials in a single part.

2.1.3.5 Sheet Lamination

Sheets of material are stacked and laminated together to form an object. The lamination method can be adhesives or chemical (paper/plastics), ultrasonic welding, or brazing (metals). Unneeded regions are cut out layer by layer and removed after the object is built. It has as alternative names Laminated Object Manufacture (LOM), Selective Deposition Lamination (SDL) and Ultrasonic Additive Manufacturing (UAM) and operates on materials like paper, plastic sheets and metal foils or tapes. Its main advantages are high volumetric build rates, relatively low cost (for non-metals) and possibility for combinations of metal foils, including embedding components.

2.1.3.6 Material Extrusion

Material is extruded through a nozzle or orifice in tracks or beads, which are then combined into multi-layer models. Common varieties include heated thermoplastic extrusion (similar to a hot glue gun) and syringe dispensing. Also known as Fused Filament Fabrication (FFF) or Fused Deposition Modelling™ (FDM), this technology can be used in an office environment. Easily working with multiple colours, it allows the production of inexpensive parts with relatively good structural properties. It usually works with thermoplastic under the form of filaments (FFF) or pellets, but syringe-based machines are developed to print liquids and slurries such as chocolate or clay. More and more specific filaments are also experimented like the ones containing wood's fibre, rubber or metallic particles.

2.1.3.7 Directed Energy Deposition

Its alternative names are Laser Metal Deposition (LMD), Laser Engineered Net Shaping™ (LENS) or Direct Metal Deposition™ (DM3D). Here, metal powder or wire with ceramics is fed into a melt pool that has been generated on the surface of the part, where it adheres to the underlying part or layers by using an energy source such as a laser or electron beam. This is essentially a form of automated build-up welding that is not limited by direction or axis. Since it has the highest single-point deposition rates of the AM categories, this method is particularly effective for repairs and adding feature to existing parts, as well as creating multi-materials objects.

Of course, all those aforementioned categories can be mixed with each other as well as with traditional manufacturing methods. For instance, the Laser metal deposition (a form of DED) is often combined with CNC machining, which allows additive manufacturing and ‘subtractive’ machining to be performed in a single machine so that parts can utilize the strengths of both processes.

2.2 FDM process

By combining both previously explained AM benefits and low-cost easy to use materials, the Fused Deposition Modelling process allows highly customable fast prototyping. Those characteristics are a solid match for the needs of this project to develop, test and confirm solutions in a short span of time as well as for building main parts of a functional prototype. All of that with reduced costs and easy to repair parts by re-printing them on site.

2.2.1 Details of the process

2.2.1.1 Modelling the part to print

As for every AM process, the first step of FDM produced parts always starts by the design. This step can be sometimes realised by 3D scanning (those technologies and hybrid combinations may vary among different industries) or more often by modelling it thanks to Computer Aided Design (CAD). Since it is important for AM systems to work with accurate models that are fully enclosed, the preference is for solid modelling CAD. This ensures that all models have fully enclosed surfaces and therefore by definition a fully defined volume that fits in the build volume of the machine.

Once the design done, the next action is usually to set this design into a standard file in order to ensure the transition between CAD and CAM. A few standards exist that can be processed by CAM software associated to the printer, but for the FDM this is usually done using STL files, the one originally created for the stereolithography process (see section 2.1.1.2).

As seen in Figure 2.3, the STL format works with assemblies of triangles, the simplest convex geometrical shape. Those unit triangles are defined by 3 vertexes plus a normal vector that indicates the inner and the outer directions, for a total of 12 relative coordinates. In this way, the STL format discretises an original CAD file where curved shapes are coded as loss less vectors. Thus, to ensure a decent discretisation and obtain a good file size to loss of shapes ratio, the numbers of triangle used in the STL are usually set just a little under the precisions that can be reached by the machine.

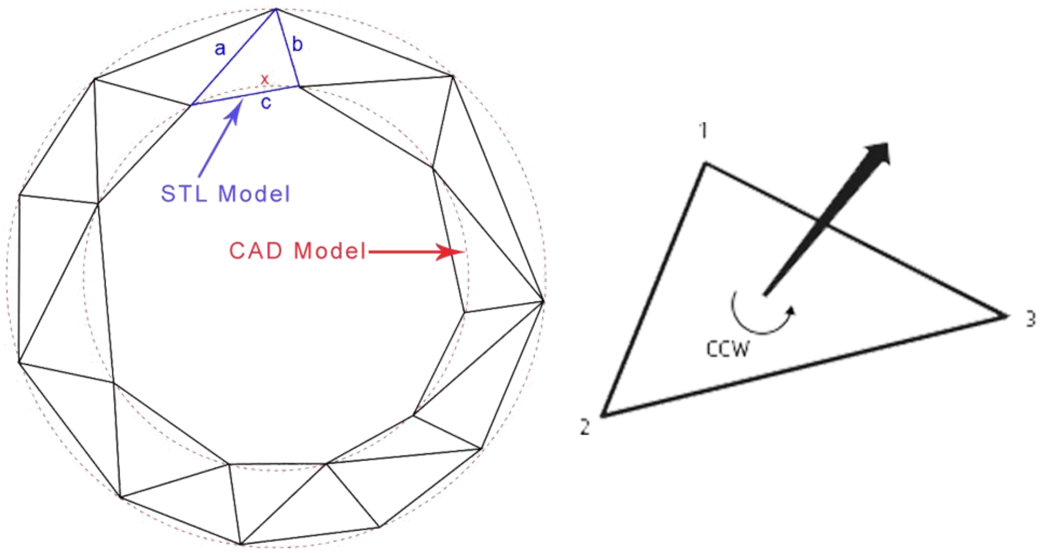

Figure 2.3 : The STL file format, adapted from Materialise Cloud

2.2.1.2 Slicing the model

Usually for AM technologies, the link between CAD and CAM is made by processing the STL file through a software that will then give orders to the machine. This main CAM software is called a slicer because that is where the STL file will be divided into virtual layers, which with the printer will then work. We can see this step as a virtual environment of the machine were all the printing parameters are decided. This allows the designers to operate a first check before printing, estimate the use of materials and can play the role of a monitor for live controlled printing (Materialise Cloud 2015).

The first goal is to interpret the data of STL file and place them with chosen scale and position in the coordinates of the printer. Those can be polar but usually Cartesian, where the Z-axis is always collinear to the direction of the extruded filament. Then the strategy is to slice the object with layers that are normal to the Z-axis. Those layers are defined by the boundaries of the object and a filling pattern that can vary on form and percentage of surface occupation. Of course, this slicing method depends on lot of parameters such as layer's height, material used and speeds the machine will work with.

The data are then directly send to the printer or stocked in a file as a succession of basic commands. Those command controls coordinate, motors speed or material extrusion. As in conventional machining, those commands are expressed in a language known as gCode.

2.2.1.3 Printing the part

Physically the FDM machines functions with material stocked under the form of pellets or filament. This second form, the Fused Filament Fabrication (FFF) process, is so common that it is generally confused with the FDM appellation. Most of the FFF printers, as the one used in the Product Development Laboratory “Lab2ProD”, are built on a similar architecture that is presented below:

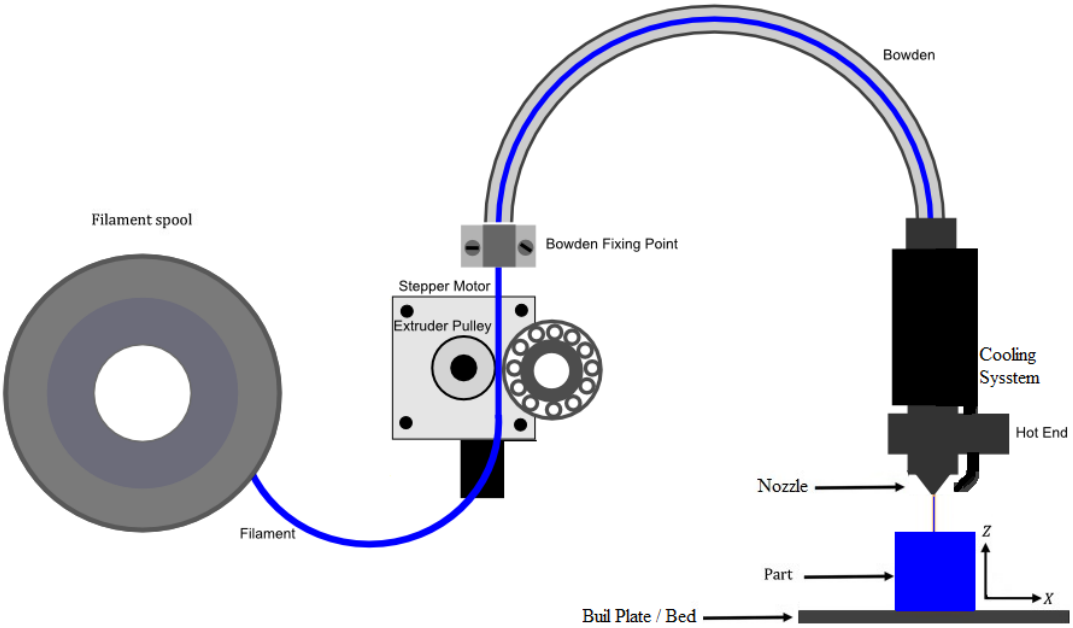

Figure 2.4 : FFF process standard architecture

- ➔ The material is stocked as a filament usually of 1.75mm or 2.85mm of diameter, on a spool that is free to rotate.
- ➔ A mechanism called the extruder puts the filament in movement thanks to a ribbed pulley attached to a motor and a tensioner.
- ➔ The filament then travels into a sheath from the extruder to the hot end.
- ➔ A hot end sets the temperature of the material above its melting point. A cooling system prevents the heat to spread in the filament located in the sheath.
- ➔ The molten material then flows through a nozzle of a specific diameter, to be dropped off on the object to build and quickly cooled down to solid material.
- ➔ Motors allows the printing head, composed of the hot end, the nozzle and the cooling system to move according to the shape of the object to form a layer.
- ➔ Once a layer is finished, the bed or the printing head moves of a layer's height and the process start again to form another layer.

The first layer is dropped on the bed that can also be heated to provide better adhesion conditions. Usually all the motors are steppers controlled by the same board and are able to displace the bed and the printing head thanks to timing belts and pulley. The vertical displacement of the Z-axis is often made thanks to threaded rods. The extruder can also be mounted right next to the hot end, in order to work with flexible filaments that does not have enough stiffness to be carried by a sheath. However, this configuration puts more weight on the printing head and can add dynamic perturbations while printing.

There is virtually no number limit of printing heads per machine, allowing then to print from different filaments. Finally, temperature and position sensors allow controlling the right execution of the gCode.

2.2.1.4 Post processing

Due to their complexity, some parts need support structures. Because this is a layer-based manufacturing, without support structures under over hanged areas, accuracy might be compromised, or the part can collapse over itself. When the printer can print simultaneously two materials, one of them can plan the role of support. In this configuration, a material that can be dissolved in a bath after the print is the most justified choice. Else, the support can be realised with the same material as the part with considerably lighter density and continuous pattern making it easier to be manually removed after the print.

After this first post-processing step of removing the supports, the finished object still needs cleaning, since raw FDM prints can show fairly visible layer-lines. The products can then be finished to a very high standard using various post-processing methods, such as sanding and polishing, priming and painting, cold welding, vapour smoothing, epoxy coating or even metal plating. Those three last methods can even provide better mechanical properties by creating a continuous shell around the raw object. Thanks to the quality of those finishing, big industry names like BMW and Nestlé are using FDM on a daily basis (Armstrong 2016).

2.2.1.5 Materials used

FDM systems are capable of printing with diverse fusible materials, yet the most common are thermoplastic polymers. For a given material, even if the raw form comes from the same element, mechanical properties may vary with composition, working temperatures and the manufacturer's formula. Some interesting plastics for this project are presented below, based on data from Ultimaker for the finest materials and compared by 3DHubs under same printing parameters (3D Matter 2017).

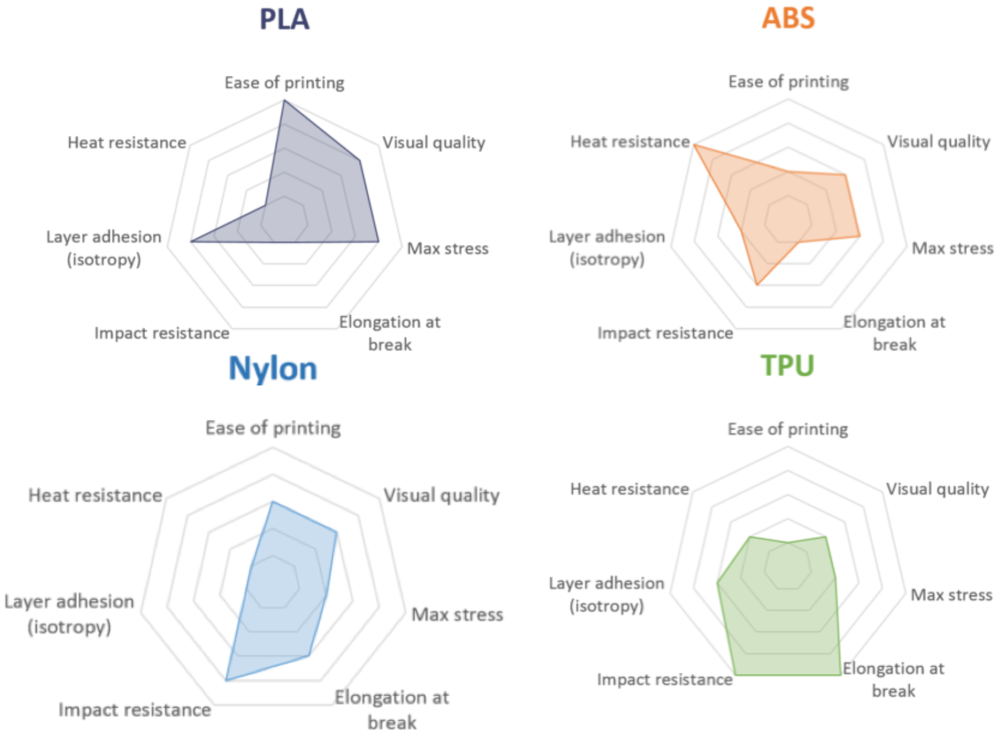

Figure 2.5 : Comparison of main thermoplastics used in FFF

2.2.2 Common problems

Beyond the obstacles that are nowadays impossible to solve with 3D printing, we will talk here about the limitations and recurrent complications that can occur in the FDM process. From the global expectations that takes form during the design phase to the troubles that appears in the machine, some of those anomalies can be avoided or planned to be non-disruptive regarding the final object.

2.2.2.1 Inevitable problems

Due to the very principle of layer manufacturing, some effects that can be observed on every AM process are particularly clear when manufactured with FDM. The main reason for that is the way of using the circular nozzle, as well as the relatively coarse layers aspect regarding some printed object's small dimensions (Hudson 2016).

One obvious but important limitation is the layers orientation when 3D printing a part and lot of complications can occur because of the bad management of this aspect. First on a mechanical point of view, FDM components are inherently weaker in one direction due to the anisotropic nature of layer orientation. Since the layers are printed as a round-ended rectangle, the joints between each layer are actually small valleys where a crack can easily form. Those stress concentrations and the lack of continuous material paths contribute to the object's weakness. The Figure 2.6 below illustrate this weakness aspect in the case of bending forces applied to the same part, printed along two orthogonal direction. The same attitude can be observed for tension, compression and shearing loads.

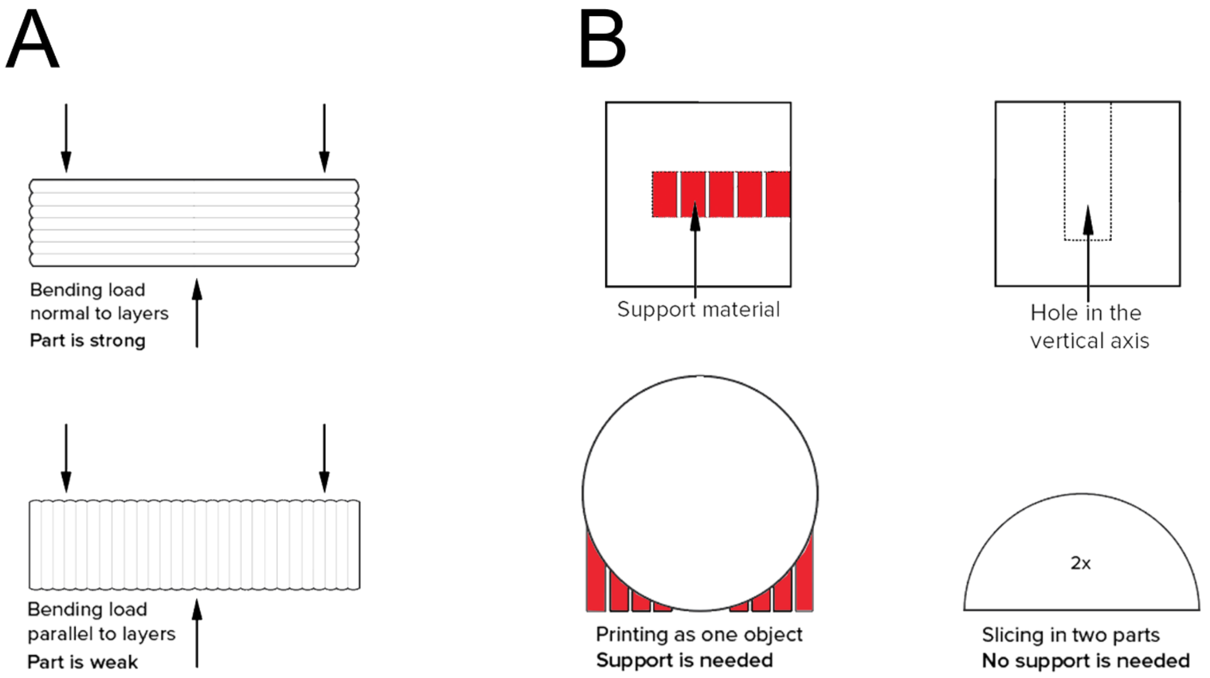

*Figure 2.6 : Layer orientation consequences for mechanical strength (A) and support (B)(*3DHubs*)*

Of course, the first aspect to deal with when orienting a part on the build platform before printing should the mechanical strength of the part. That said another important aspect to consider is the amount of support the object will need, with direct consequences on the printing cost and the surface finish of the backed areas. In order to reduce manufacturing time and recurrent complication due to the excessive use of supports, the strategy here is to reduce support use at the maximum. Since we often work with thermoplastics that are easy to glue, a good approach is to split the model (see Figure 2.6). It generally allows to suppress support as well as to print on several machines, thus allowing saving time and preventing crashes that can occur on long prints. The other classic way is to change the layer's orientation to fit the hole's directions. However, this can sometimes conflict the required orientation to obtain desired mechanical properties.

Another problem of this process is linked to the machines resolution along different orthogonal directions, which directly depends on the nozzle diameter for the X and Y-axis and on the capable layer height for the Z-axis. The first limitation that comes out of this resolution is the staircase effect. As the Cartesian system of the machine interpolates curvatures into a discretised number of layers, the CAM object cannot exactly follow the CAD file. This effect can be observed in the X and Y directions where it depends on the motors step but is particularly marked in the Z direction because of the minimal reachable layer's height that is more significant than motors steps. The Figure 2.7 below depicts this effect, as well as the precision problem that the layering FDM process imposes.

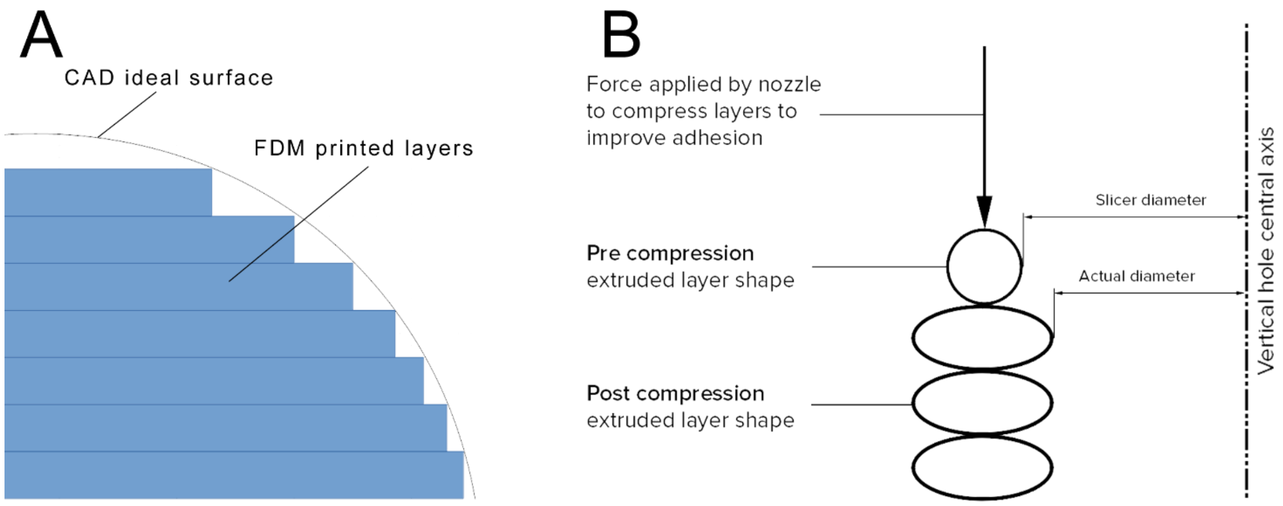

*Figure 2.7 : Staircase effect (A) and geometrical errors due to layers compression (B)(*3DHubs*)*

As shown above, the staircase effect impeaches the printed object to follow the exact CAD design. On the same way, the compression of layers while printing slightly changes the actual dimensions of the printed object. Depending on the printer, the slicer, the material, the speeds and temperatures those variations can be more and more important. This can be of particular issue when printing small diameter holes where the effect is greater due to the ratio of hole to nozzle diameter. Test prints are often needed to bypass this problem, and if high precision is needed, post-process drilling may be the only option. This aspect can also be problematic for parts that require precise mechanism plays, where small dimensions and curved areas are often undersized (Armstrong 2016).

2.2.2.2 Preventable recurrent problems

With the knowledge of previous problems, it is this possible to adapt designs to fit the required expectations, at both the CAD and slicing step. However, in practice, some other issues can appear and those depends on the printing conditions in the machine. The situation in the printer is determined by a plentiful of parameters that are usually controlled by the slicer during printing or through the gCode file. Here is a list of the parameters that usually have the most impact on the overall print quality, supposing a print with only one material (Simplify3D 2018):

- **Layer height** for the entire print, that can be set on a different value for the first layer
- **Temperatures** of the Hot-End and the bed that are usually constant during the print
- **Extrusion** flow and **Retraction** of the filament, different for walls, infill and support
- **Speed** of the travelling of the print head and of the build plate
- **Fan's speed** to cool the currently printing layer that can vary along the print
- **Thickness** of the walls, top and bottom layers of the printed object, usually constant
- **Infill** of the object, which the percentage and pattern can vary
- **Support** amount, pattern and overhang angle to hold up
- **Adhesion** strategy adopted to stick to the build plate, raft, brim or skirt and their amount

A bad calibration or a combination of those parameters can cause many printing defaults. As those also depends on the materials used, the geometry of the object and specificities of the slicer and the machine itself, a few experience and test prints are required to obtain decent parts. Below is a non-exhaustive list of the most common problems encountered with the FFF process:

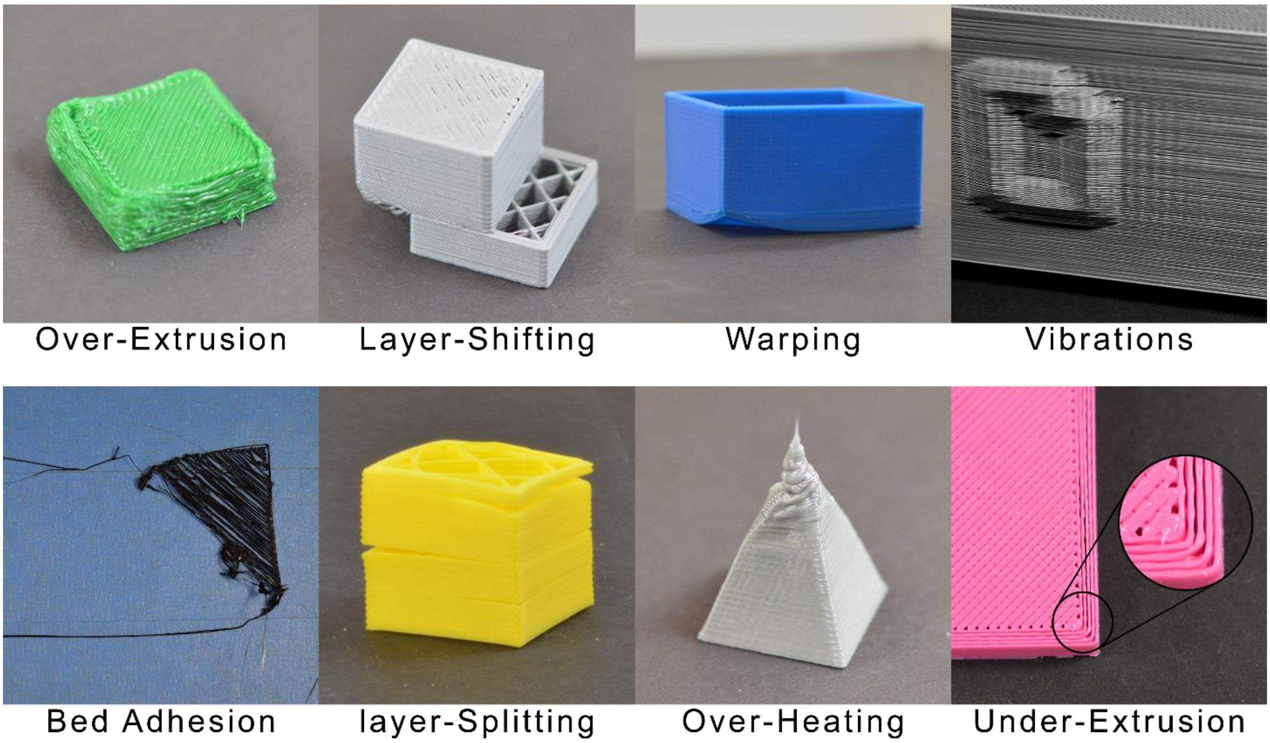

Figure 2.8 : Illustration of common FFF printing problems, adapted from Simplify3D

2.2.3 Adapted design advices

As several strategies exists and are usually appropriate to specific defaults or design complexities, the first step is to get to know the tools at our disposal. Desk-sized FFF printers as the one in the Lab2Prod are commonly used with different filaments, several software and of course by many people who almost every time set different configurations. In order to limit human factors as much as possible and master the printing parameters, it is often necessary to check cleanliness of the tools, software updates and previous print failures causes. In the very beginning, this rigour also helps to identify a cause of fail and thus to understand faster the specificities of a machine through a few simple tests, like printing small cubes and hollow cylinders with each time different parameters (Hudson 2016).

Those first prints will have on purpose to calibrate the machine, especially for the bed levelling to guarantee a correct first layer, on which all the object will depend. Those will then help to understand several software differences. For instance, it is easy to slice thin features with Cura where it can be more difficult with Simplify3D, yet Simplify3D usually manages better the support generation. Those first prints will also allow understanding infill and materials properties for mechanical purpose. That is thus a good strategy to convert a bit of printed materials into knowledge, when this waste of material can be later saved on a fail of a ten hours print. Once able to identify a problem and solve it by acting on layer dimensions, temperatures, speeds or materials based on estimates, we can focus on functional designs of parts to print. Beyond appreciation of the tools, understanding the application of a component and how it is built are critical to the success of a design. One of the hardest part here is maybe to abolish the way of thinking that includes conventional machining limitations, to think the designs freely during the CAD and then arrange them at the best during slicing (Micallef 2015). Following this principle, beyond the looking for the best slicing configuration possible, a few general production tips can improve the way of creating with FFF process. It will be particularly useful for Chapter 4 to know that:

- Draw with equations to simplify adaptation of a whole design to a specific configuration.
- Include ribs and fillet in the CAD where the slicer would use supports to improve strength.
- Design shells to be a multiple of nozzle diameter to avoid dimensions shift.
- Consider using a clearance hole and bolting with washers instead of direct screwing.
- For applications with small vertical pins, add a small fillet at the base or consider instead inserting an off the shelf pin into a printed hole.
- Divide large parts into simpler shaped small fraction to avoid crash of long time print, save support and re-print only the concerned fraction in case of design changes.
- Considering printing an entire object at 45° may increase the printing time but can guarantee a good mechanical behaviour as well as a good support to surface finish ratio.
- Include chamfers to edges touching the build plate to reduce post processing of surfaces.
- Rectangular infill is usually quick to print but honeycomb and triangular are stronger.
- Index the geometrical adaptations and the plays used for articulation or mechanical purpose in a specific configuration, share and use the data made by worldwide communities.

2.3 Zirconia pastes for prosthesis

This section's intention is to both get knowledge about human tooth and state of the art on nowadays denture's materials as well as awareness of the environmental conditions of the mouth.

2.3.1 Natural tooth and mouth environment

2.3.1.1 General architecture

Human teeth are playing a vital role in human daily life, by providing an important masticatory function but also by being strongly associated with the pronunciation and facial aesthetics. With ageing, pathological factors and traumas inevitably generate dental lesions that are treated thanks to artificial dental materials in a constant evolution. Understanding and evaluating the structure/property relationships of the human tooth is imperative to develop new dental restorative materials. In order to rehabilitate the functions of tooth at well as possible, it is also important to study its intrinsic mechanical and microstructural properties as well as the mechanisms by which tooth structures resist to functional forces that are present in the mouth.

At macroscopic scale, human teeth are composed of two distinct parts, the crown and the root, being attached in a strangulated intermediate portion called the colon. These parts are made of two anisotropic structures: a non-calcified called the pulp and a calcified one comprising external enamel and subjacent dentine. Thus, those two last elements are the most important to determine tooth resistance to the conditions of the mouth environment, enamel being harder than dentine. From materials science perspective, a tooth is a functionally graded composite material with mineralized matrix and organic reinforcement. Since we can only synthesise mineralised matrix yet, the restorative materials are exclusively based on the enamel and dentin properties (Zhang et al. 2014).

Enamel contains on average by weight 1% organic substances, 4% water and 95% inorganic texture that is mainly constituted of a crystalline calcium phosphate called hydroxyapatite. Enamel's structure consists of approximately 5 µm diameter rods made of a mesh of crystallite encapsulated by thick protein-rich sheaths. Those rods are oriented from the dentin-enamel junction to the outer enamel surface, with a higher concentration near the junction. On the other hand, dentine is considered an elastic and soft part of the tooth that contains dentinal tubules, which extend through its entire thickness. Those are composed of about 12% water, 18% organic material and 70% inorganic material, forming a hydrated biological composite mostly made of phosphoric apatite crystallites.

2.3.1.2 Mechanical characteristics

There is still a lack of correlation between microstructure and basic mechanical properties for enamel and dentin, but it has been experimentally verified that both have a fragile behaviour with an anisotropic fracture mode regarding impacts. However, resultant from rod orientation and the presence of organic components, the microstructure of the enamel controls the way a crack will spread. Because enamel is about 5 times hardest than dentin with a Knoop hardness of about 250 – 500 KHN (Zhang et al. 2014), it can easily break if it loses the support of the flexible dentin below. That is this combination of the two materials that will reduce their brittle characteristics to withstand about 20 MPa occlusion pressure approximately 3000 times per day (tooth fracture resistance properties are displayed in Table 2.1). Therefore, replacing damaged dental tissues is primordial to help enamel retaining its fracture and wear resistance during load-bearing function of all an individual's life.

After identifying the imperatives mechanical forces and behaviours the replacement materials will be submitted to, another important property to understand is the tribological behaviour to mimic natural tooth. The contact between hard pieces of food and teeth or teeth with themselves creates transmission of forces, alteration of the mechanical and chemical properties as well as an eventual removal of material. This tooth property is commonly characterised by both its wettability and its friction and wear behaviour (Xu et al. 1998).

Tooth friction and enamel wear are multifactorial phenomena involving the interplay of biological, mechanical and chemical factors. Which means the aetiology of tooth wear and restorations vary depending upon joint pathology, occlusions force and frequency, muscle tune, individual dietary and hygiene habits and the type of restorative material used. In this way, friction and wear for replacement materials are often considered for the worse possible cases. In addition to that, the oral environment through saliva provides protection against chemical wear and acts as a lubricant to reduce mechanical harm. On the other hand, this buccal environment can damage replacement materials on the long run because of chemical fatigue wear. This characteristic is highlighted by wettability, usually quantified by contact angle of a water drop at the three-phase boundary on a horizontal test surface of the material. Experimental tests on enamel wettability is considered highly hydrophilic, yet without absolute quantification due to its natural way of production. Wettability depends on chemical composition, structure of the material as well as the surface finish. Thus, replacement materials will be developed to have a high raw wettability and the smoothest surface condition as possible to guarantee a good resistance long-term fatigue due to oral environment.

2.3.2 Ceramic materials characteristics

2.3.2.1 Why ceramics?

Various artificial materials have been developed for dentistry, to replace missing teeth or non-aesthetic but healthy tooth tissue and enamel. Usually dental materials can be grouped into four categories: metals and their alloys, polymers, ceramics and composites. The selection among materials depends on the mechanical and corrosion behaviour of the prosthesis, but also on costs, availability, biocompatibility and aesthetic values. Nowadays, the use of composite ceramics is increasing compare to classic metal alloys, especially for their excellent combination of mechanical and aesthetic properties. They also are highly resistant to acid and corrosion attacks and are therefore regarded as exceptionally biocompatible and chemically durable on a very long term (Sarasota 2017).

However, in addition to prohibitive costs and relatively long manufacturing time of ceramics, there are relevant issues related to their potential for brittle fracture and for abrasion of opposing natural teeth or weaker restorations. The development of a 3D printable ceramic paste thus aims to improve conditions on those issues. Firstly, by letting dentists to design and produce dentures in the same office, thus limiting human errors due to interactions, interpretations or delays. Secondly by lowering costs and production time thanks to limited materials wastes and machining phases. Thirdly by allowing production of complex shapes that could allow more resistant composition of materials.

2.3.2.2 Mechanical properties

In order to minimize damage from brittle fractures, many efforts have been made in the last decades to develop high strength dental ceramics. For instance the best known are leucite reinforced feldspathic porcelain, magnesia based porcelain, lithium disilicate glass-ceramic (Shen 2014). Lately, a family of tetragonal polycrystalline base ceramic reinforced with yttria-stabilized zirconia (Y-TZP) was developed as an alternative to porcelain and glassy matrix-based ceramics with significantly higher resistance to fracture and an excellent biocompatibility. The Table 2.1 below shows main mechanical properties of the most common dental ceramics to compare their behaviour regarding fracture resistance and propagation, based on the Invibio Biomaterials Company's data.

*Table 2.1 : Fracture resistance properties for several dental ceramics (*Invibio Biomaterials*)*

material system	**Reinforcing material**	**Flexural strength (MPa)**	**Fracture toughness ($MPa.m^{-1/2}$)**	**Fracture Force (N)**
Natural tooth	*Deteriorate with ageing*	~ 160	~ 2.6	~ 1300
Crystalline	Glass-infiltrated alumina	236 - 600	3.1 - 4.6	659
Crystalline	Zirconia toughened alumina	421 - 800	6 - 8	770
Glassy matrix	Lithium disilicate	300 - 400	2.8 - 3.5	950
Polycrystalline	Y-TZP	900 - 1200	9 - 10	1331

Thanks to their significantly high fracture force, zirconia-reinforced ceramics were chosen as the main component of a custom 3D printable paste currently developed at Técnico Lisboa. Experiments also shows that raw data are not the only parameters to take into count but global structure, surface conditions and position of the implant in the mouth also matters. For instance, there is an enormous difference of long-term wear between teeth exposed to implants with different conditions, rough finish being more threatening than correctly polished surfaces. Thus, developing the overall manufacturing finish through 3D printers is equally important as improving the paste inner characteristics.

2.3.2.3 Zirconia-based ceramics

Since the discovery of the transformation toughening capabilities of zirconia in the mid-1970s, its excellent mechanical properties let it hold a unique place amongst ceramic oxides. Considerable research has been led on its different phases during process, as well as on effects of additives. Under ambient pressure, pure zirconia assumes three crystallographic forms: monoclinic phase (**m**) at ambient temperature to 1170°C, tetragonal phase (**t**) from 1170°C to 2370°C and cubic phase (**c**) above 2370°C and up to melting point. The best mechanical properties are achieved only if some grains transform from **t** to **m** under stress thanks to phase transformation toughening. In other words, zirconia can be used as a structural bio ceramic only if it is not completely stable. In addition, upon cooling to obtain this instable phase, the **t** → **m** transformation will induce a substantial increase in volume (~4.5 %), which will lead to catastrophic failure. Even so, this necessary meta-stability in a moist environment may cause a spontaneous transformation from **t** to **m**, decreasing the strength of the material, phenomenon called aging or low temperature degradation (Afonso Vilar de Castro Paredes 2017).

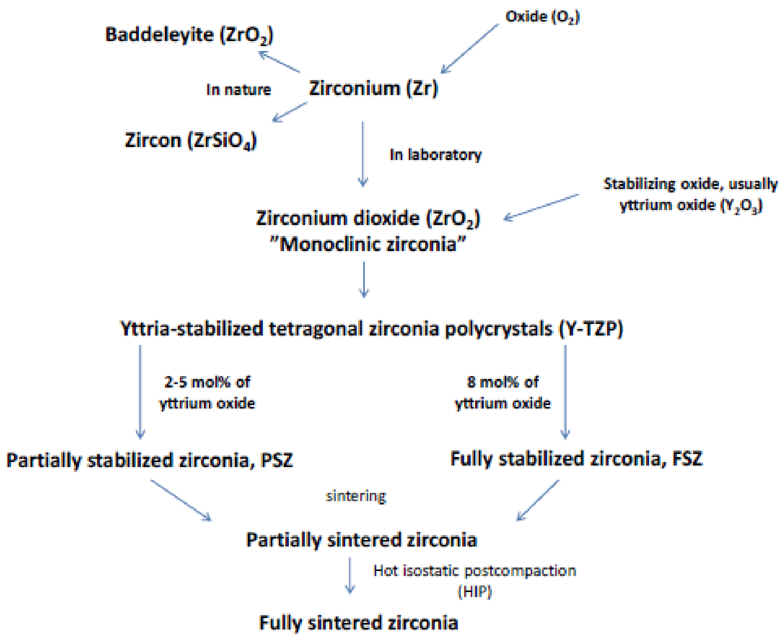

*Figure 2.9 : The various states of zirconia (*Pihlaja 2016*)*

However, as shown on Figure 2.9, treatments and addition of oxide to zirconia-alloys allows retention of the tetragonal structure at room temperature. This will control the compressive stress-inducing **t** → **m** transformation, thereby closing the crack tip to prevent further propagation and leading to high toughness. The addition of stabilizers can also prevent or decrease aging. Although there are several types of zirconia-containing ceramic systems currently available, to date only three are used in dentistry (Ivoclar Vivadent n.d.). These are yttrium cation-doped tetragonal zirconia poly-crystals (3Y-TZP), zirconia-toughened alumina (ZTA) and magnesium cation-doped partially stabilized zirconia (Mg-PSZ), whose properties are presented in Table 2.2. By comparing the various parameters of this table and through some literatures, we learn that stabilizing zirconia with yttrium generally enhances its mechanical properties more than with other oxides. Zirconia can be fully stabilized by 8 mol% of yttrium oxide although dental zirconia is usually partially stabilized by 2-5 mol% of yttrium oxide.

*Table 2.2 : Mechanical properties of zirconia-based ceramics for dentistry (*Castro Paredes, 2017*)*

Property	3Y-TZP	ZTA	Mg-PSZ
Young Modulus (GPa)	210	380	210
Compressive strength (GPa)	2		2
Density ($Kg.m^{-3}$)	6000	4150	5850
Flexural strength (MPa)	950		600
Flexural strength ($MPa.m^{-1/2}$)	10.5	4 - 5	5.8
Vickers Hardness ($HV_{0,5}$)	1250	1600 (HV_{30})	1250

A few clinical problems related to zirconia restorations like discoloration or chipping can occur on crown microstructures to cause surface characteristics loss and environmental influences in the mouth. When the difference of properties between tooth and degraded ceramics is too obvious, abrasiveness of these materials raises concerns in dentistry especially when they increase healthy teeth wear process. Those degradations also make implants more sensitive to the complex inter-oral chemical environment and makes their surfaces more sensitive to bacterial adhesion leading to dental plaque.

2.3.2.4 Fabrication of ceramics

In order to avoid the previously described complications and to obtain correct materials properties, the fabrication techniques of ceramics requires mastering elements homogeneous transformations as well as the surface finish. Traditionally made with conventional machining in large blocks of material, the methods are evolving towards increasingly AM techniques to limit wastes and improve complexity of implants. Another argument in favour of AM is also the highly customisable crowns that can be printed at the same time, therefore improving a lot in the production costs and delays (Le, Paris, and Mandil 2017). However nowadays only a few techniques are precise enough to guarantee a decent surface finish of the implants, like DLP or SLS used for moulds (see section 2.1.3) or direct modelling like the Lithoz LCM-Technology®.

Since the investments for operating the previously mentioned AM processes are still high, the idea behind developing a ceramic paste is to lower prices and intricacy of the manufacturing techniques by using a material extrusion process. Even though current FDM-like precisions do not allow yet a precise enough surface finish for final dental implants, the technique is quickly improving, and structures thus created could work as inner carrier for composite prosthesis. The developed cement to be printed by Liquid Deposition Modelling (LDM) is actually a suspension of about 90 % weight solids formed by a mixture of ceramic powder, water and additives that act as chemical modifiers.

2.3.3 State of the art on paste printing

From basic chocolate 3D printers to complex bio-extrusions to form stem cells, many applications illustrate paste-based manufacturing techniques. However, most of the ceramic paste printing is nowadays dedicated to macro-scaled lab ware production or pottery, for instance by extrusion of green objects that are then put to furnace. Thus, dimensions of ceramic printed objects are usually larger than the ones required for dental application. One of the most advanced process that embodies high precision ceramic extrusion is the robocasting (Lewis, Smay, and Stuecker 2006).

2.3.3.1 Robocasting

As for many of the Materials Extrusion family processes (see section 2.1.3), Robocasting or Direct Ink Writing (DIW) technique works with deposition of a paste or "ink", which is extruded through a small nozzle into a filament shape to form the successive AM layers. From CAD design to CAM printing, the entire process of robocasting looks like the FDM one (see section 2.2) in the sense it generally works with Cartesian based machines wherein the nozzle is moved in relation to a flat build frame, without using additional tools like moulds. The slicing step is also familiar, difference being made by the dimensions of the extruded material seam and the speeds occurring in the machine.

The main difference relies in the use of liquid based printing materials as well as the printing conditions of the build plate. Instead of relying on solidification or drying to retain its shape after extrusion like in FDM, the ink exploits rheological property of shear thinning after it exits the nozzle in a liquid-like state. Allowing many advantages regarding materials, that method nevertheless implies a few differences in the printing process due to the liquid properties of the ink. For instance, the ink can generally pass through the nozzle in only one direction with consequences on the general print quality. As shown on Figure 2.10, the bed can also be submerged in an antifreeze liquid or oil bath to control temperature and stabilise extruded material. Those have consequences on the support, large spanning and overhang areas of printed parts, which are usually more restricted than in FDM.

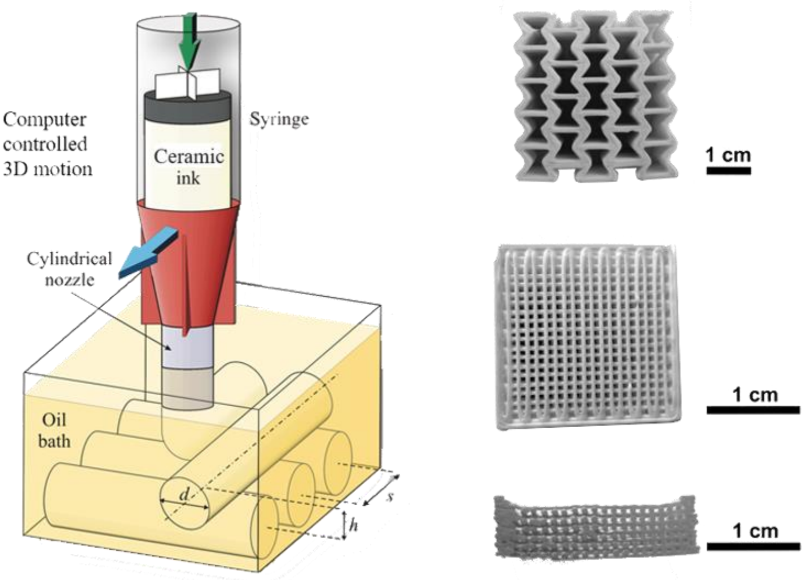

Figure 2.10 : Robocasting process with dried and sintered samples (Euroceam 2017)

Robocasting's strength are its flexibility regarding the range of materials that can be printed as well as possibility to print several at one time into graded composite structures (Cesarano 1998). This allows for instance intricate periodic 3D scaffolds to be printed with ease, a capability that is not possessed by other additive manufacturing techniques. This approach has shown extensive promise in fields from photonic crystals to bone transplants, by electronics, catalysts and filters. However, in return of good mechanical quality of produced material, this technique is somewhat limited in the shapes it can form. Firstly, by the radius of the printed filament, typically being around 300-500 µm, while other techniques such as stereolithography may reach one-tenth that size. Also, a bit more visible than in FDM because of liquid extrusion, the pieces will always have step edges due to the layer wise nature, printed supports and overhangs. In order to limit those unwanted shapes and lower the printable dimensions to reach the standard sizes of dental market, the ink must respect specific properties.

2.3.3.2 Double process machines

Some machines are capable of both FDM and LDM extruding systems with a few adaptations on their actuated carriage. Even if there are almost no theoretical differences between FDM and LDM processes regarding designing, slicing and printing, extruding shear thinning liquids instead of thermoplastics imposes some adaptations in practice. The Delta Wasp 2040® 3D printer is a good example to illustrate those changes, since it is able to use both LDM and FDM on the exact same hardware frame. It is also a system with dimension, precision and price range similar to the experimental rig which will be developed. The only differences are that this machine uses a delta actuation system and pressurised liquid tank with endless screw instead of Cartesian coordinates and a syringe as the tool head. The Table 3.1 shows the main distinctions of machine's abilities between its LDM and FDM modes. As we can see there is a difference in the capable printing dimensions, LDM ones being usually coarser than FDM ones. That's why this or equivalent machines are most of the time used for large dimension prints, which layers dimensions and global print quality are not mandatory criteria. Such dimensions also impose a few adaptations in practice, where for instance hollow objects printed in spiral are less sensitive to overlapping when printing than the ones sliced with infill. A good application is in the field of pottery, to produce green products with printable clay to form geometrical shapes with greater precision than handmade ones. Those green products are then sintered in a kiln to partially melt clay particles and obtain a hard ceramic object, that can be veneer or plated in the end.

2.3.3.3 Global ink requirements

Properties and composition of the paste are crucial factors to ensure mechanical abilities of prints. During extrusion, the paste should be homogeneous and free of air bubbles, contain a high-volume fraction of ceramic powder, flow properties suitable for extrusion and still be capable of maintaining its shape after printing. Thus, inks should be highly shear thinning to allow extrusion through fine nozzles and retain a degree of stiffness to prevent from collapsing and allow self-supporting during printing. Furthermore, aqueous inks are preferred due to their simplicity, lower toxicity, lower cost and slower drying, while low concentration of organics are desired to allow rapid firing, low volume reduction and high densities.

Various approaches have been explored to satisfy those criteria, such as very high solids loading pastes that dry during printing or polymer-solvent based inks dependent on solvent volatility (Peng et al. 2018). In this case, the yttrium-zirconia house made paste is a colloidal ceramic suspension where the average sized 150 nm particles interact by van der Waals forces to form a weak network, which abilities will have to check the following properties. To ensure that a paste is suitable for Liquid Deposition Modelling, and later in section 5.3.2 to plan the printing experiments, it is required to comprehensively control:

- Paste viscosity and rheology
- Percentage of solids in the ceramic powder suspension
- Dispensing rate of the slurry through the orifice
- Drying kinetics of the dispensed bead of slurry, determining the optimum build parameters
- Volume reduction after sintering

Chapter 3 - Experimental rig design

3.1 FDM to LDM

After gaining fundamental knowledge on Additive Manufacturing and the specifications applied to FDM, the goal of this section is to establish imperatives to ensure transition from Fused to Liquid Deposition Modelling suitable for the house made zirconia paste.

3.1.1 Target identification

As described in the section 2.3.3 some machines already exists using the LDM process. However, the one described as robocasting are most of the time custom made hardware and therefore not available on the market. Or, if so have sales prices that does not fit this project's budget because they offer a multitude of functions, often adapted to the medical research field or to bio-printing. On a lower range of prices, we can find machines as the Delta Wasp which machine's distinct abilities between its LDM and FDM mode are shown on the Table 3.1 below.

Table 3.1 : Delta Wasp 2040 printing properties for FDM and LDM adapted from DeltaWASP®

Process	Nozzle diameter (mm)	Layers resolution (µm)	Maximum speeds (mm/s)
FDM	0.4	50 - 300	300
LDM	1	200 - 700	150

The LDM parameters for this machine are thus much coarser than FDM ones. Since the slicer used is the same for both process, changing process induces significant changes in the geometry and slicing method, where walls with the same thickness or features thinner than nozzle diameters can be skipped. Preliminary stages of the design must take care of those alterations, mainly by considering wall dimension as multiples of the nozzle diameter, as advised in section 2.2.3. The layer resolution also influences design phase with problems related to staircase effect, first layer dimension and adhesion to the build plate. This adhesion problem can be countered by adjusting speeds while slicing, which could however induce over-extrusion and vibration related problems when set too slow, because of the slower drying time of the paste. Due to late arrival of this technology on the large-scale market and the multitude of inks with each their own characteristics, there is also a lack of knowledge on printing parameters leading to higher rates of print fails. Moreover, if a paste does not show distinct shear thinning aspects it can drop out of nozzle and thus impeach retraction, leading to an inferior printing finishing. Thus while robocasting machines have unsuitable prices and features to this experiment rigs needs, the clay LDM printer does not have precise enough outputs to test the ceramic paste in good condition for further dental prints. A more precise solution thus needs to be considered for the experimental rig.

3.1.2 Constraints and objectives

The main goal here is to design and build the experimental rig for ceramic paste deposition, by transforming an existing FDM hardware into an LDM capable machine. Intention being to obtain a machine able to work with several ceramics having distinct properties, to study their behaviour and test associated printing parameters to ensure correct deposition of each layer. This will be done by conceiving a paste dispenser operating with a syringe and needles, which is then intended for replacing the tool head on the actuated carrier of a FDM printer. In order to allow physical modifications supposedly compatible with the associated software and without breaking any costly guarantees, the FDM machine will dispose of an open source system.

The chosen FDM printer is the Lulzbot Mini that was made available at the Lab2Prod just before the beginning of this work. The machine to be built also needs to respect objectives set by the BioMat Research Group who wishes to test materials and operate this system by its own in the future. In addition, of constraints set by adaptations to ensure transition from FDM software to LDM hardware, those requirements mostly concern precision and ease of use of the machine. The list below highlights the main expectations:

- The paste extruder of the machine should use syringe and needles that follow medical standards to ensure compatibility with probable supplementary systems and allow stock orders from several suppliers.
- A choice should be possible among those standardised needles to allow several extrusion diameters. This will be useful to adapt the system to the different rheological natures of future pastes or simply to allow fine and coarse extrusion for both precision prints and time saving prints.
- The system should provide control over a maximum of printing parameters to obtain decent prints for several inks and under different conditions.
- The maximum precision the overall system can reach should be able to fulfil the dental market sizes requirements.
- Design the hardware to make it as easy to manipulate as possible and thus avoid misuse, shocks with glass parts and premature deteriorations.
- If possible, adapt the FDM software to take in count as much LDM parameters as possible, like the change of needle sizes, and to be simple to use.

The expectation concerning the dental market imposes to obtain similar precisions between both processes, although LDM is usually used for coarser prints than FDM as seen with the DeltaWasp example. Along with the FDM precisions, common functionalities that the LDM extruder needs to keep regard control of ink flow and temperatures, retraction and bed auto-levelling.

3.1.3 Available equipment

3.1.3.1 Hardware to be modified

The Figure 3.1 below shows the chosen micrometric syringe (B), a Cole-Parmer model Gilmont GS-1200, picked among a few syringes model that were already used in the chemistry department. It has advantages over regular linear syringes to be more compact and the amount of dispensed liquid is much easier to control. The plunger is mounted on a micrometric screw, right over a removable glass tank with a capacity of 2.0 mL. This means that for one revolution of the main sleeve, the plunger moves of 1 mm and the syringe dispenses 0.1 mL. Hypodermic needles (C) can be mounted on the end of the glass tank, which is compatible with the international Birmingham gauge norm for medical purpose. In our case, those needles will play the role of the LDM nozzle with inner diameters ranging from 4.5 mm to 0.2 mm.

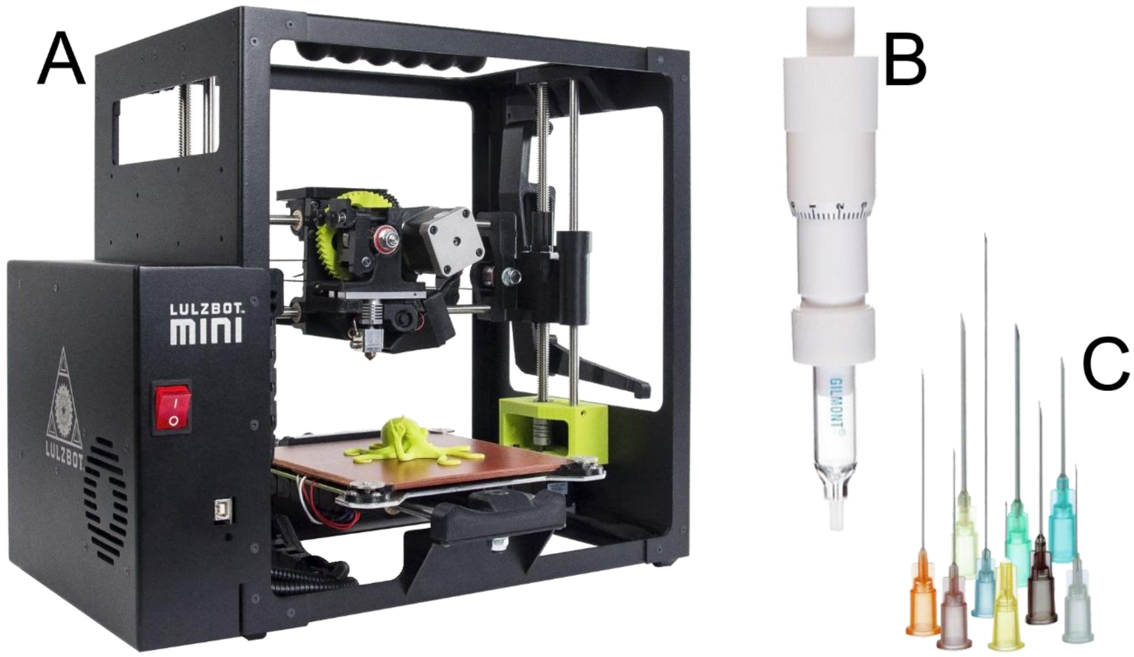

Figure 3.1 : FDM printer (A) to transform, micrometric syringe (B) and hypodergenic needles (C)

Considering the micrometric syringe has been designed to be used manually, there is a lack of data on its mechanical properties with only access to a non-sized plan of a cut view of the syringe. It was thus impossible to calculate the tightening forces that the sleeve can handle, so it was later experimentally determined. However, since this syringe costs about 300 € it was interesting to estimate the twist torque that we could operate on the sleeves without damaging the inner micrometric screw. The minimal diameter of this screw was optically measured on the plan and reduced with safety margin at d = 7 mm. We also know the screw's material is Polytetrafluoroethylene (PFTE) of which the young's modulus is estimated at on the worst case at E = 300 MPa and Poisson coefficient at v = 0.46, considering we don't know if this material has been reinforced with other components. We can then calculate the max torque for resistance condition (T_1) and rigidity condition (T_2):

$$T_1 \leq \frac{(\pi * d^3 * \tau)}{16} \quad \& \quad T_2 \leq \frac{(\pi * d^4 * \mu * \alpha)}{32}$$

The material's characteristics come from the database of CES Edupack (GrantaDesigns 2015), with respectively the shear yield stress τ = (ε*E)/2; the shear modulus μ = E/2(1+v) and the maximum torsion angle imposed α = 0.35 rd.m^{-1}. This gives us the values T_1 = 4,041 N.m and T_2 = 0,083 N.m. The difference of 2 orders of magnitude between those values shows that the PFTE have a very high range of elastic deformation before rupture, thus even a small applied torque could permanently damage the inner micrometric screw. Since those values have been vaguely estimated, they could not be take into account for more precise calculation, but shows rough size that can be compared to future motor's capable torque what is enough for the present work.

Finally, the selected 3D printer is the Lulzbot Mini v1 from Aleph Objects. As previously mentioned, the main advantage of this system is its open-source based development allowing easy physical modification, good software compatibility and plenty of documentation. The Lulzbot also have decent mechanical properties for its range of dimension with a quite small print area of 152x152x158 mm. The borosilicate glass heated build platform can reach 120°C when the hot end is able to stand 300°C for a max speed of 275 mm.s^{-1} allowing the print of a wide range of material that are compatible with 2.85 mm of diameter filaments. It is also interesting to note that extrusion stepper has a holding torque of 55 N.cm, a maximum torque of 25 N.cm at a speed of 150 rpm and is able of a constant 24 N.cm torque for speeds between 270 and 360 rpm. The overall printing resolution is also quite good with layer height between 0.05 and 0.5 mm and a nozzle diameter of 0.4 mm.

The Z-axis step is defined by the minimal layer's height definition and the X and Y-axis by the nozzle diameter, but can virtually reach more accurate precision when thinner needles are mounted on. This will be limited by the actuation system of the X and Y-axis, which are using the same system of belts and pulley while the Z-axis uses two parallel endless screws. Those motion systems are mounted along with a support structure composed of two parallel round rails on which the moving elements are travelling supported by two linear bearing sliders. The Figure 3.2 below shows the X-axis motion mechanism based on a timing belt of a 6 mm width with GT2 tooth profile that is actuated by a 16 teeth pulley directly mounted on a custom-made stepper motor using NEMA 17 size. This motor has a step angle of θ = 1.8° and the pulley have a radius of 5.09 mm, calculated with the number of 2mm pitch teeth according to r = (16*2)/(2π). The minimal displacement of the belt thus corresponds to (rθπ)/180 = **0.160 mm**. Because the precision of material deposition is even coarser, it means the maximum X and Y precision this machine can theoretically reach is now limited by steppers, because according to the Birmingham gauge, the hypodermic needles can have inner diameter as small as 0.08 mm.

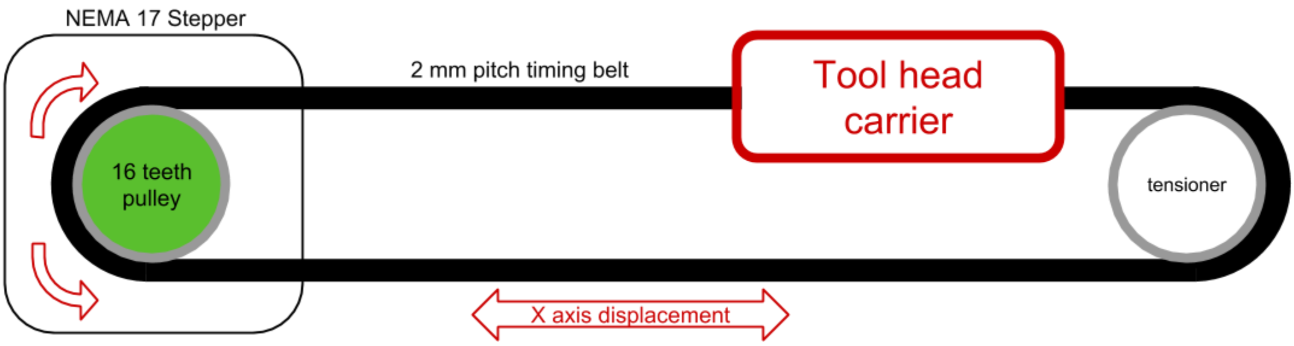

Figure 3.2 : Schema of the X-axis actuation system of the Lulzbot Mini

However, the estimation of this minimal precision does not consider the vibrations and dynamic problems that are inevitably present on this motion mechanism, and it can have a substantial impact on printing precision at such small dimensions. In addition, the Birmingham gauge explains the sizing of needles is made with dimension tolerances as displayed on Table 3.2:

*Table 3.2 : Birmingham gauge inner-diameter sizing for hypodermic syringe (*Sigma Aldrich*)*

Gauge	22	23	24	25	26	27	28	29	30
Inner Ø (mm)	0.413	0.337	0.311	0.260	0.260	0.210	0.184	0.184	0.159
Tolerance (±mm)	0.019	0.019	0.019	0.019	0.019	0.019	0.019	0.019	0.019

As we can see, the gauge 30 corresponds to 0,159 mm, which is remarkably similar to the 0,160 mm minimal precision theoretically reachable by the machine. Yet the tolerance says this inner diameter may vary between 0,140 and 0,178 mm and tests of the early version of the paste does not pass through such small diameter. With a smallest inner diameter of 0.165 mm, gauges 29 or 28 (difference being on the outer diameter) could be used, but a problem of position and vibration due to machine precision could appear at those dimensions. Larger needles as gauge 22 have similar dimensions to the original FDM nozzles, so it would not be advantageous to use broader gauge regarding printing precision.

Another observation is about the operating system of the Lulzbot, managed by a motherboard called Rambo v1.3 and based on Arduino components. Firstly, this is a non-upgraded version of the board that cannot read external micro SD card, meaning that it cannot autonomously print, the only way being by connecting a computer to send the gCode line by line. Secondly, this motherboard does not have electrical security preventing to power the machine with unplugged components. It can be a problem in case of misuse of the machine but that is more an advantage for this project, where a few of the original components will need to be removed. That also allows disconnecting the whole tool head and still being able to drive the X, Y, Z carriage position as well as the bed temperature with the Lulzbot version of the slicing software.

However, this software is not designed to manage any other processes than FDM, creating some issues for this project. Even if it can pilot the carriage, the only way to move the extrusion stepper is by virtually extruding filament. This require the hot end to be heated at least to 150 °C, which means some components needs to be connected on the tool head to give the slicer required temperature data. On the tool head it represents 15 wires, 4 for the stepper motor, 2 for the heater, 2 for the 24V fan, 2 for the 5V fan, 2 for the thermistor, 2 for the X-axis stop sensor and 1 for the zero-volt reference. Regarding the next steps of the project, the immediate solution is to keep both FDM tool head and future LDM extruder plugged on the machine. Yet to avoid problems related to this large amount of useless wire in the future, idea would be to fake signals sent by those components to the slicer by physically adding resistors or even recoding the software. This may be a next step improvement of the project, for instance while changing interface or improving tool head and motherboard.

3.1.3.2 Manufacturing tools

Since the manufacturing phase of this project took place in the Lab2Prod, which is specialised in Additive Manufacturing, most of the parts of the functional prototype have been 3D printed. A few conventional machining could eventually be made in the case their building time, cost or mechanical function would get the upper hand on AM properties for prototyping stated in section 2.2. The most used printer was an Ultimaker3® because of its high reachable displacement precision of 20 µm, its fast print speed of 300 $mm.s^{-1}$, its quite large build volume of 215 x 215 x 200 mm and overall good print quality. The main materials used to build this prototype were PLA and ABS thanks to their favourable mechanical properties, their ease of printing and availability as well as their fair price to quality ratio.

3.2 Design method

3.2.1 General organisation

With the previously mentioned advices about Additive Manufacturing in mind (see section 2.2.3), a design strategy was adopted before beginning the search of solutions for the adaptations from FDM to LDM. The main idea here was to plan the design phase in a way to respect the short limit of time imposed by the ordering delays, as well as respecting cost effectiveness and simplicity of manufacture. Research of solution for the syringe based liquid extruder were thus divided into subsections aimed at solving one problem at a time, the first one being to get to know the manufacturing equipment. This also allowed limiting FDM print failures by understanding limitations of the printers and materials as well as providing ease of adaptation by redesigning and reprinting only a fraction of affected solutions. The subdivision vas decided according to the previously identified adaptation from FDM to LDM (see section 3.1.2) as well as kinematics requirements set by the micrometric screw of the syringe. Finally, the state of mind while designing was also to think solutions and printable pieces as simple as possible to limit weak parts and hard maintenance work, due to elevated number of components or too complex shapes. Although some tests were made during manufacturing stage since this is a dynamic process, the list below explains main points of the strategy adopted during the designing stage:

- ➔ First step before conceiving any solutions is to understand limitations of the tools regarding overall mechanical properties of printed parts, times of print, finishing qualities and be able to estimate the failure chances of a print. It is thus necessary to take time to get accustomed to the different 3D printers and slicers. That will also help during the CAD stage to avoid designing future complex parts behind complications or errors leading to loss of time and materials and even tools degradation. In practice, it goes through calibrations and prints on both production tools and machines to be modified, in the form of samples testing angles, supports needs, holes dimensions…

- ➔ Second key point is to design with versions (see Chapter 4), a version being a practical design of the whole project, embodied by CAD files divided in sub folders, each of them focusing on one of the identified problems. Starting with version 0.0 for the test prints to determine the useful dimensions for the next steps, the versions 1.x are entire solutions. For instance, version 1.0 was designed before reception of the Lulzbot Mini thus allowing starting solution inquiry, but after reception, version 1.1 corrects dimensions that were until then estimated. The other main thought behind those versions is the idea of creating knowledge and relying on results that have been proved effective. It also helps to keep tracks of explored solutions and remember why some were abandoned, useful if someone external wished to take over this project.

- ➔ Specially to avoid poor mechanical properties the idea now is to design parts with geometries that are as simple as possible. Since we are producing most of the parts with FDM, complex shapes are much easier to obtain than with conventional machining, thus it will more be a small CAD step than a CAM complication. We will therefore favour fillets and rounded shapes instead of sharp angles to limit weaken parts due to stress concentration. In this mind, the layer orientation and global position of the part while printing will also be taken care of during the design stage. This step is at the origin of overall smooth geometries visible on the liquid extruder's body (see section 4.2).

- ➔ To avoid future problems of compatibility and stocks concerning the basic fastenings present in the conception, it was decided to limit the use of different screw sizes by adopting a uniform dimension for screws, bolts and nuts (determined in section3.3.1). This strategy also allows to determine once the corresponding holes dimensions on a test print, then repeat them on CAD files without running tests each time, as well as avoiding maintenance confusions for future co-workers. Of course, this does not apply for the imposed items with different dimensions like the sensors and tool head fixations. This strategy avoids as well thermal inserts as the ones present on the Lulzbot Mini, which can weaken the part when badly mounted and are expensive due to their few presences on the market. That said this solution could be considered for future improvements to lighten and simplify the whole-body structure.

- ➔ Materials used were also picked according to the availabilities and regular orderings of the Lab2Prod as well as their overall quality print on the Ultimaker3. Even if standard materials are globally compatible with the machine, some unofficial supplier's brand can give bad finishing and mechanical properties. See further information on materials in section 3.2.3.

- ➔ Finally, the available post-processing techniques for 3D printed objects in the Lab2Prod are only subtractive processes, unlike coating or vapouring, thus their use was limited at the maximum. In addition, those manual processes are not perfectly repeatable, which can be an issue in case of re-manufacturing or maintenance interventions.

3.2.2 Global kinematics

In order to identify the subsections of the CAD versions, determination of the global kinematic started straight away with the first test prints, before receiving the Lulzbot and picking the definitive syringe type. First ideas were based on a timing belt drive to actuate a regular syringe, in the style of a crossbow were the arrow would be replaced by the syringe's plunger, with the advantage to adapt to several type of linear syringes. However, those solutions were rapidly ruled out because of the impossibility to move the plunger in both directions, thus skipping any chances for retraction. It could have been possible with a system of twin belts, but this solution would have been too complex to implement. Since retraction was a requirement for the future machine to be able to experiment a maximum of different ceramic pastes, solutions then found were inspired from pinion and rack or screw mechanisms. Fortunately, the syringe with integrated micrometric screw that was chosen in the meantime allowed to simplify actuation’s kinematic, leaving the linear solutions behind. The Figure 3.3 below explains kinematic requirements imposed by the syringe to the future extrusion system.

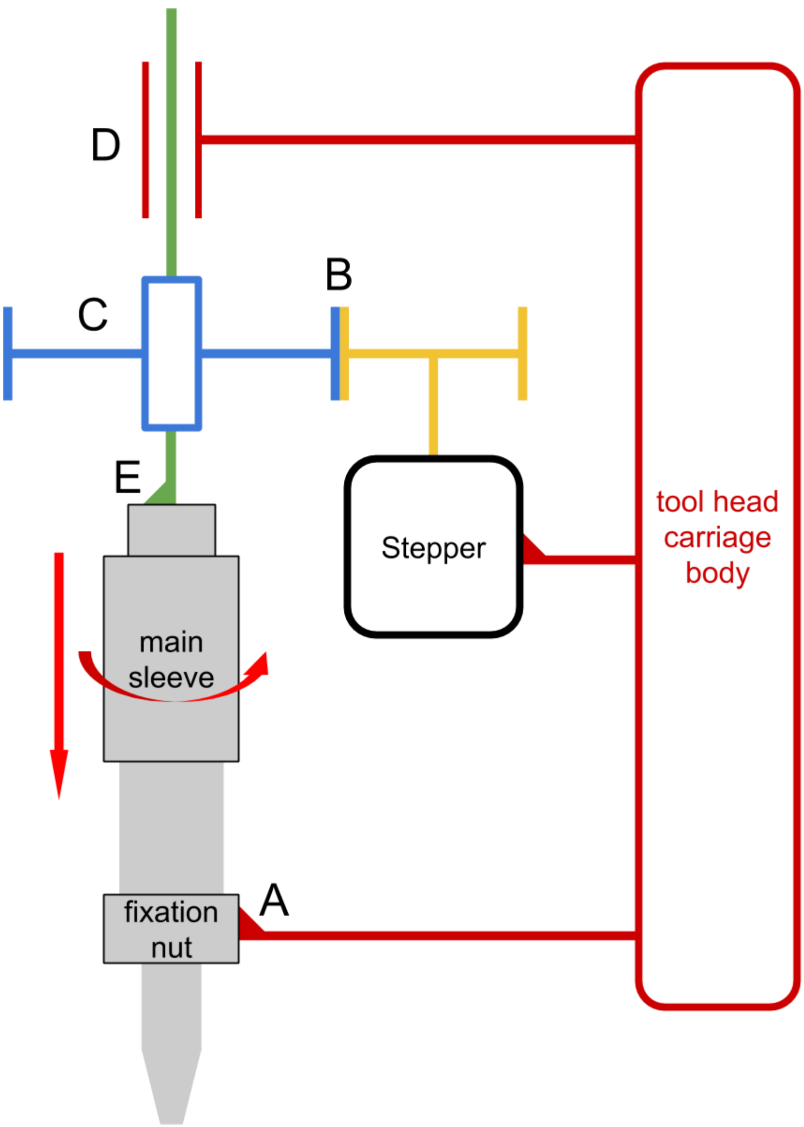

Figure 3.3 : Kinematic diagram for LDM extruder with micrometric syringe

On Figure 3.3, red part represents the frame of the carriage on which the system will be mounted. The syringe's nut is embedded to it in **A** thanks to a recessed connection because it needs to be fixed to the frame to allow the screwing movement of the syringe's sleeve. The yellow one embodies the stepper that was originally used for the filament extrusion, which is directly mounted on the carriage's body. This stepper actuates the blue component through a gear reduction connection in **B**. This component plays the role of a transition part that transmits the rotation movement of the motor and allows the translation movement of the green shaft. It is thus linked to the green shaft with a sliding connection in **C** that prevents rotation movement between blue part and green shaft. This green shaft then actuates the syringe's main sleeve, being guided in rotation relative to the frame in **D** and embedded to the sleeve with a recessed connection in **E**.

This schema displays the first functional solution that was considered for technical design solutions. However, interface **C** was a space demanding solution, problematic for the LDM extruder that needs to be installed in an area limited in height. Meant to transmit rotation while being maintained to carriage body, the **D** connection was also leading to elevated level of complexity for printable parts or elevated price for commercially available solutions. This diagram thus evolved into a simplified adaptation, which suppressed the **D** pivot by integrating it into the blue/green parts connection in **C**. To initiate its development, this last solution was divided into sections corresponding to sub-folders of the CAD versions (see 3.2.1). With the search of cost effective upgradable solutions in mind, those sub-sections were identified to focus on the interfaces technical realisation, and their realisation divided into design and manufacturing phases with a first iteration that was successively improved.

➔ **Designing** phase of the first iteration of the experimental rig:
  - **Fastenings** for **A** and **E** connections, which were distinct solutions considering their different attach location on the syringe. A solution to make the fastenings between printed parts as uniform as possible, and more generally in the whole mechanism.
  - **Transmission** of power to the syringe's sleeve that is embodied by the shaft. Several fastening relations will appear on this part, as well as **C** and **D** interfaces solutions.
  - **Reduction** of the stepper's speed to match its effective range, through a gear transmission solution in **B**. Number, shape, teeth properties and materials of those gears impact the whole mechanism.
  - **Protection** of the syringe while using the mechanism. That means avoiding degradation on both the expensive inner micrometric screw and outer thin needles.

➔ **Manufacturing** of the functional prototype with successively adapted design, especially of the main body of the LDM extruder (see Chapter 4).

3.2.3 Printing tests for designing

Figure 3.4 : Up and bottom view of the first print, made with PLA on the Ultimaker3

This Figure 3.4 shows an avatar used in the Lab2Prod, which is the first print of this project, done with PLA from Lulzbot on the Ultimaker3 and using basic manufacturer's printing profile with the Ultimaker Cura slicer. The goal here was to get familiar with both the slicer and the machine as well as their limitations by printing an object containing multiple shapes. Sharp and smooth geometries, layers orientation or supported areas, were key features to observe for identification of several design-related factors that will help to prepare future parts for good print quality. For instance, on this avatar we can see regular finish defects like the layer staircase effect on the head of the upper view of the avatar, over-hanged areas inferior quality on the bottom view due to placement of supports or the difference of smoothness between vertical, horizontal and bed-touching surfaces.

3.2.3.1 Determining correct printing settings range

As soon as the Lulzbot Mini was received and operational, other simple objects such as dices were printed on both machines using both Ultimaker Cura and Lulzbot Cura slicers with different parameters. That allowed to put in practice advices to improve finishing, find out parameters impacts or experience that Ultimaker slicer usually provides better finishes even when used on the Lulzbot machine. This first practice also enabled understanding of problems shown in section 2.2.2.2, such as precision or vibrations, and more particularly the actions needed to attenuate them. This step was thus useful to estimate manufacturing durations, mechanical qualities of surfaces and infills, adaptation of parameters to minimise chances of print fails and perception of future printing complications.

An important part in the understanding of print fails and overall aspect was to know about printing properties of the main materials to be used during manufacturing step. The Table 3.3 below compares values found after calibration and experimentation with the ranges given by suppliers supposed to adapt to most machines. To ensure low print fail rates for this project, raw supplier's data were not precise enough because they rely on many parameters that were fixed in our case. For instance, they consider nozzle diameters variations that impose increasing extrusion temperatures with bigger diameters to ensure homogeneous flows. Those materials were thus compared on the Ultimaker3 except for the TPU that requires a specific extruder and was tested on the Lulzbot Taz6 with the help of Francisco Dias Pinheiro who worked with this material for his master's thesis (C. B. Dias Pinheiro 2018).

Table 3.3 : Adjusted printing parameters for a layer height of 0.15 mm on the Ultimaker3

Material	Supplier	Recommended		Adjusted		
		Nozzle (°C)	Speed range ($mm.s^{-1}$)	Nozzle (°C)	Bed (°C)	Max speed ($mm.s^{-1}$)
PLA	RepRap	195 - 215	30 - 90	210	60 - 65	70
	Lulzbot	190 - 210	15 - 70	205	60	60
ABS	Ultimaker	225 - 250	20 - 80	235	85 - 90	50
Nylon	Ultimaker	230 - 260	20 - 60	240	70	50
TPU	Recreus	215 - 250	10 - 70	230	50	15 - 30

3.2.3.2 Printing simplicity

After finding the parameters to obtain correct prints, the global observations were concerning the ease of use of those materials to later decide of their adoption for specific parts. Nylon density is quite sensitive to ambient humidity variation and thus needs to be stored in a specific dehumidifier closet, which can lead to important print flow variations when storage time is too short to properly dry the Nylon before use. Even when extruded under decent conditions, printing with Nylon remains hard to master because of regular issues with layer adhesion and a tendency to warp. Manufacturing phase will favour ABS and PLA since they have quite comparable mechanical properties but are easier to print with. TPU printing also depends on humidity and is as hard to use as Nylon, but its rubber like aspect could be nevertheless interesting for joints, pads and potential flexible parts.

Since the geometrical differences between CAD and printed parts does vary with the materials, a few dimension tests were also led. For instance, a dimension shift can appear when slicing, due to impossible match between desired length and discretisation that fits layer's height or nozzle diameter. As stated in section 2.2.2, those shifts must be taken into account while designing to avoid thin features skipping, infill problems and incompatible dimensions. That is particularly important for fastening holes, where it can be either impossible either dangerous for mechanical properties to re-machine wrong dimensions. The tests allowed to notice a regular shift of 0,3 mm on the inner diameters, as well as shifts on small dimensions of about a layer's height, further complementary tests were led in section 4.1.1. Having those difference in mind before starting solution design was useful to anticipate future dimension changes that could weaken parts.

3.2.3.3 Printed materials properties

After finding a range of correct printing settings, the goal was to understand the properties of each materials in order to allocate them to the various parts to be produced, in particular those of the body to be designed. To do so, materials were compared according to their properties furnished by Ultimaker for the raw printed materials (Ultimaker 2017). According to the supplier, those materials have been tested under the same conditions with a speed of 50mm/min, following the test norm ISO 527 for the PLA, ABS and Nylon, and ASTM D638 for the TPU. The Table 3.4 below display the properties that helped choosing among those materials. However, those value are not representative of the actual filaments used in the Lab2Prod, which is particularly true for the PLA, since they are measured with high-end manufacturer's materials. The last row of the table presents values of standard PLA, similar to the used one, which is way more flexible than the upmarket PLA provided by Ultimaker. It was measured by Optimatter for test specimens with a 100% infill and 0,2 mm layer height in linear pattern, following the ASTM D638 standard for the tensile tests (3D Matter 2017). As a general rule, ABS has a chemical composition that makes it more heat and UV fatigue resistant than PLA. In the case of the materials used in the Lab2Prod, the ABS had an improved impact resistance over PLA as well as a lower ductility.

Table 3.4 : Mechanical properties of Ultimaker filaments for FDM adapted from Ultimaker.com 2018

Material (Ultimaker)	Tensile modulus (MPa)	Tensile stress at yield (MPa)	Elongation at yield (%)	Flexural modulus (MPa)	Hardness (Shore D)
PLA	2346,5	49,5	3,3	3150,0	83
ABS	1681,5	39,0	3,5	2070,0	76
Nylon	579,0	27,8	20	463,5	74
TPU	26,0	8,6	55	78,7	46
Regular PLA	~ 1900	32,0	6,2	~ 2500	_

Those properties, crossed with the previously tested printing ergonomics for the same materials, allowed to apprehend their sturdiness for different infills and wall thickness values. For instance, it was decided to use TPU exclusively for gaskets or pads to protect the glass parts. After that, ABS was chosen for stiff parts like supports where precision is needed. Those supports will be completed with smaller connections printed in softer PLA to adapt to X carrier geometries. Since PLA and ABS both have a good raw finish and are usually stable regarding the defaults listed in section 2.2.2.2, both could be selected for mechanically useful surfaces in the mechanism, depending on the different parts functions.

3.3 Fastenings

3.3.1 Standardisation

In accordance with the strategy adopted in 3.2.1, most of the assemblies were designed to use bolt and nuts instead of thermal inserts, imposing a few adaptations. First one is to anticipate the place used by bolt's head and nuts in the global design, which can impeach desired contacts between parts when badly positioned. Then the design must make sure there will be enough space to operate tools to assemble those fastenings along with the other parts of the prototype. If not this problem can be bypassed by integrating a nut-cap in the design, which will block the nut in rotation thus allowing to screw the bolt without having to use two spanners. Finally, there is also a problem due to brittleness that makes those thermoplastics quite sensitive to cracks when fastened with small metallic parts. A few solutions can attenuate this problem, like dividing loads onto several fastening points or use washers to extend contact surfaces on bolt heads. Manufacturing issues explained in section 2.2.2 can also create misalignment or gaps that could be corrected by combining round and oblong holes in the design. For the same reason of brittleness, oblongs will be favoured for ABS parts that are slightly stiffer than PLA.

Since there are lot of those fastenings, decision was taken to use a standard size for as many bolts as possible with the help of Table 3.4. First argument to choose the bolt size was to pick it among the regularly ordered metric standards used in the Lab2Prod, from M1 to M6, to minimise the out-of-stock and tools compatibility issues. The second criterion was based on practicality to handle standard items and their bulkiness, like bolt heads or flat washers (EngineersEdge 2018). By experimentation, bolts smaller than M2,5 were bothersome to work with and sizes over M4 were judged too bulky for small features requiring nut-caps and potentially dangerous regarding cracks. So far since it is the size already used to fasten the steppers, the best compromise was M3. Then a final check of tensile resistance was done to ensure those fastenings could handle a minimum load L, which was estimated after the heaviest element in the new extruder, the stepper of 365 g with a safety coefficient s = 3. According to properties of AISI 304 stainless steel the maximum tensile yield strength at a 0.2% strain is S_{all} = 215 MPa (MatWeb 2007). The stress σ at the area A was calculated with the formula $\sigma = (s*L)/A$. In this case every sizes suit the expectation since $\sigma < S_{all}$ for all of them, so M3 was adopted as standard.

Table 3.5 : Standard bolt sizes choosing for the LDM extruder adapted from EngineersEdge.com

Sizes	d_{min} (mm)	A (mm^2)	σ (MPa)	Round head D_{max} (mm)	Hexa nut l_{max} (mm)	Flat washer D_{max} (mm)
M1,6	1.28	1.29	8.35	3	3.41	4
M2	1.41	1.56	6.90	3.8	4.32	5
M2,5	1.64	2.11	5.09	4.5	4.45	6
M3	2.47	4.8	2.24	5.5	6.01	7
M3,5	2.97	6.93	1.55	6	6.84	8
M4	3.27	8.41	1.28	7	7.66	9
M5	4.27	14.33	0.75	8.5	8.79	10

3.3.2 Discarded ideas

The next step regarding fastenings was to find solutions for interfaces A and E described in Figure 3.3. As for many decisions, a first approach was to observe existing solutions and adapt them to the syringe dimensions. In the very beginning, the objective was to design a maximum of pieces to be manufactured by FDM, along with the idea to build most of the prototype in the Lab2Prod to reduce production delays and ensure repair solutions. That led to looking at systems from areas such as cycling and conventional machining, as shown in Figure 3.5. The Initial idea was inspired from bike seat clamp was to block the syringe's nut by retrieving both strong seizing and ergonomic of the clamp. Then clamping device for the sleeve was traced after lathe's jaw chuck with intention to ensure concentricity of motored axis and syringe's sleeve. This part was developed while finishing the tests described in section 3.2.3 and a few adaptations were necessary to obtain a functional printable design. For example, since the first tests showed difficulties to print small features with decent quality, so round large helixes were designed instead of standard thread to ease the print. To bypass bracing problems and allow printing without support, inner jaws were added with thin flexible PLA blades.

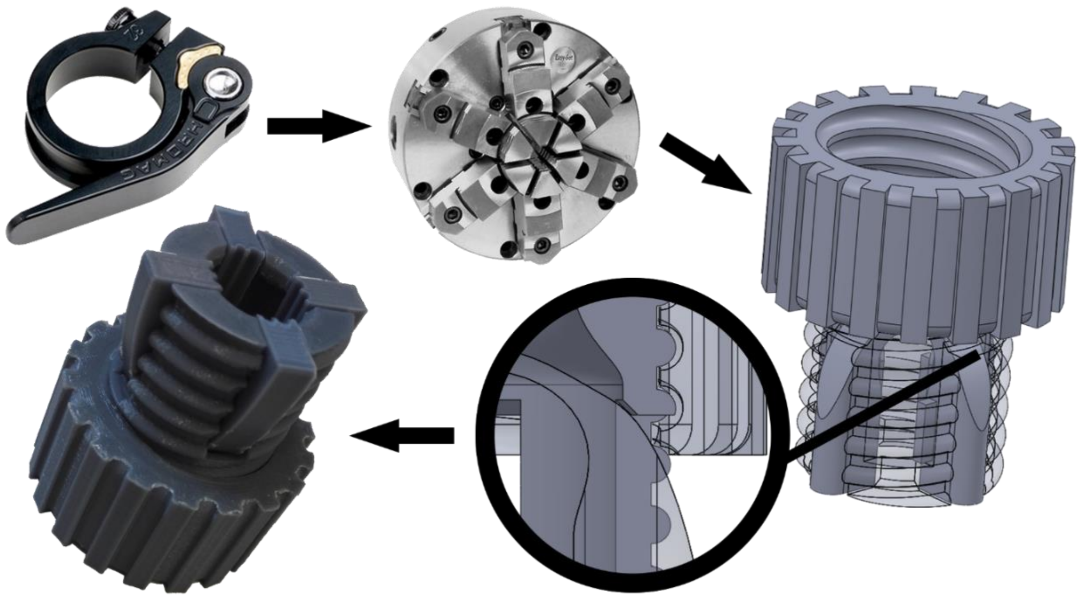

Figure 3.5 : Inspirations and first discarded draft of syringe fastenings

3.3.3 Final clamps

Unfortunately, the seizing of this chuck was not powerful enough to correctly maintain the sleeve, in addition to some printing flaws that made it uncomfortable to use. For the same reasons and to avoid fragile parts the bike inspired clamps were cut down into hinged clamp relying on a long M3 bolt and without rapid fastening arm. Those clamps were applied with adapted dimensions in A and E, respectively named main and top clamps and thought to be printed in PLA for its ease of print and better tolerance to flexion than ABS (see section 3.2.3). This also allowed to add a guide on the main clamp to both protect and ease manipulation of the syringe. Those stronger simplified versions were later successively enhanced until final form with the design versions (see Chapter 4).

3.4 Transmission shaft

3.4.1 First inspirations

As explained in section 3.2.2, the intention for the main transmission piece, the green one on Figure 3.3, is to use a shaft. Initially this part needed to be associated to the carrier's body by a pivoting link in C and at the same time allow translation and block rotation compared to the blue part in D. But since it was decided to simplify this kinematic diagram by removing the D connection, the shaft now only has one sliding connection in C, the rotation and maintain to the body being delegate to the blue part. It also needs to be linked to the previously established hinged clamp for interface E. The simplest solution to do that regarding print fail chances was to design small parts linearly sliding along a ribbed axis. As displayed in Figure 3.6, this ribbed shaft was first designed as in a motor's gearbox. However, in this case FDM was not an appropriate tool for production of such a shaft, which needs a rigid material with a surface finish as smooth as possible.

3.4.2 Existing solutions

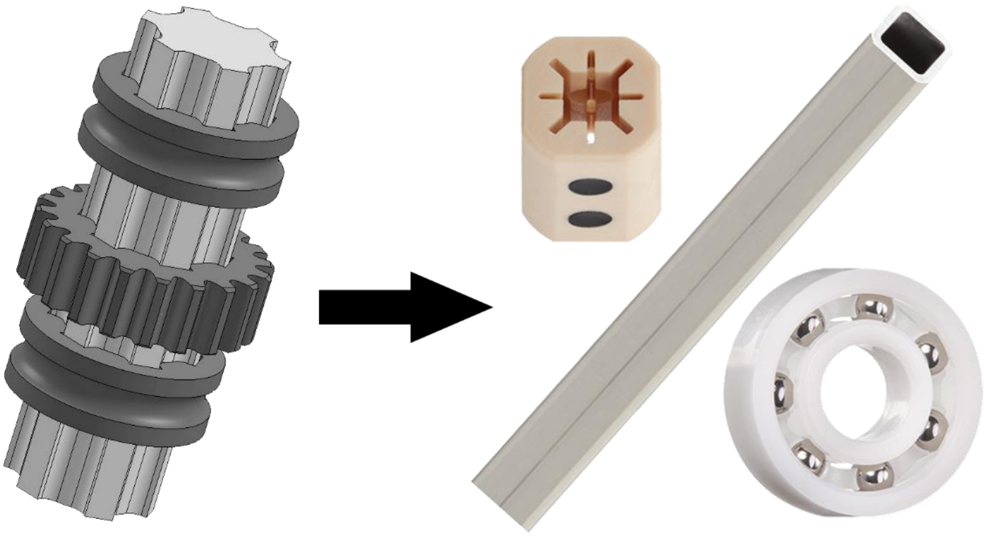

Figure 3.6 : Transmission from ribbed shaft to aluminium square profile

Since the function of this shaft imposed a conventional machining, it was interesting to look for existing solutions from suppliers, like the DryLin® assortment of plastic linear bearing from IGUS. This provider was chosen for attractive prices (detailed in section 4.3.2) and because of the availability of each items that could be grouped with a regular order of the Lab2Prod. The shaft is an aluminium square profile that plays the role of a rail on which a plastic bearing will be mounted. Both can support a torque up to 3000 N.cm that is way superior to the stepper holding torque, and the square profile was ordered with an extra margin to ensure its future integration in the overall design. To anticipate the next step of the C liaison design, a pair of ball bearing was also ordered with an inner diameter superior to the square profile to ensure the blue part maintain in rotation (see section 4.2).

3.5 Motorisation and reduction

3.5.1 Gears type selection

Regarding overall kinematic, this section focuses on realisation of the interface between the stepper and the square shaft. For this transmission with reduction gears were chosen over belt-based solutions because it was impossible to manufacture such solutions at the Lab2Prod. Then 3D printing the gears in plastic in the Lab2Prod offered a cheaper, faster and easier solution to redesign in case of mistake than conventional machining or ordering them. On top of that, high degrees of complexity do not affect prices, allowing to manipulate more efficient gearing shapes than with conventionally produced gears in the same conditions. Of course, printing gears using the available plastics is a sacrifice in surface finish and durability compared to injection moulded or machined plastic parts. But when designed correctly, printed gears can provide efficient and reasonably high load transfer (Graham 2017). Considering that the original Lulzbot Mini FDM extruder also uses printed gears and regarding the relatively slow torques and speeds that will occur in the mechanism, printing gears was thus an ideal compromise in our case.

Since it was possible to work with all range of gearing for the same amount of price and time, the choice of the main shape stopped on the herringbone. This presents the advantages of helical gears that allow more teeth to come into contact simultaneously to work more quietly than spur gears. Yet those helical teeth also create axial thrust force leading to problems concerning alignment of the gears. But the herringbone uses both right-handed and left-handed helical teeth to balance those undesired inherent forces, which gives it at the same time the peculiarity of being self-aligning. Finally, the choice of the printed material was made regarding their raw mechanical properties (see section 3.2.3). Usually the choice of materials from the perspective of strength / finished gear quality ratio is Nylon>PLA>ABS>PETG (Graham 2017). However, the first tests highlighted the difficulties to print with Nylon and its tendency to absorb humidity, and PETG was not an appropriate mechanical choice because of its low scratch resistance and relatively high flexibility on thin parts. Finally, even if they have similar quality finish, ABS was chosen over PLA for its higher stiffness and impact resistance.

3.5.2 Reduction ratio calculation

After the decision to realise this reducer with ABS printed gears, the idea was to reuse the same stepper as the previous FDM extruder and drive it with similar speeds to take advantage of its best performance range. To match the simplicity driven strategy, it was decided to design the mechanism with the minimal amount of gears, the driving one being the pinion directly attached to the stepper's shaft. Then the end larger wheel was thought to fit precisely on the slider bearing, between supports for the ball bearings of the C interface. The next step was to compare FDM and LDM extruder's mechanism to understand the relations between the driving speeds and extruded material's velocity as displayed on Figure 3.7, in a way to adjust the future reduction ratio to match similar stepper's momentum.

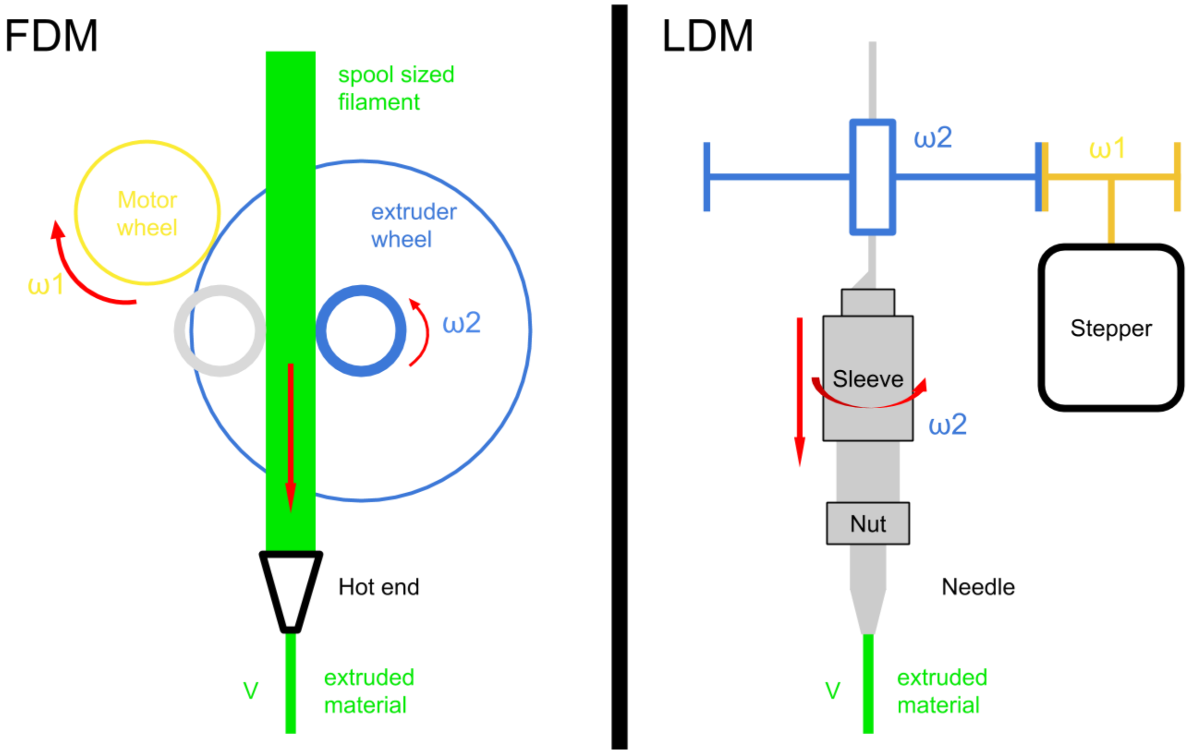

Figure 3.7 : LDM and FDM reduction mechanism between stepper and output printing speeds

As shown on the figure above, several elements are considered to calculate the total reduction. For the FDM it starts with an angular velocity reduction thanks to printed gears of respectively 9 and 47 teeth. Then this rotational movement is transmitted to the large diameter filament thanks to a ribbed tensioner of a diameter of 8 mm. Finally, the filament diameter is reduced through the nozzle from 2.85 mm to 0.5 mm with conservation of extruded volume. That gives an overall reduction of $v = 0.0249*\omega_1$ with v the linear extrusion speed in $m.s^{-1}$ and ω_1 the stepper angular speed in $rd.s^{-1}$.

For the LDM, starting from the end, the needle mounted on the syringe imposes a similar reduction on extruded materials, which can be calculated on the same way depending on the needle's inner diameter. To do the estimation we will consider here a needle of gauge 23 with an inner diameter of 0.337 mm. Then there is the reduction of the syringe, where one entire rotation of the sleeve corresponds to the dispense of 0.1 mL or 100 mm^3. Finally, the sleeve angular speed is equivalent to the large wheel of the geared reduction whose reduction ratio will be called **X**. This gives a total reduction ratio of $v = 0.1777\ \omega_2$, also in $m.s^{-1}$ and $rd.s^{-1}$. Since we want both ω_1 to be in the same ranges, it means the ratio needed here for the gears to design is **X** = 249/1777.

However, even if gauge 23 is supposed to be the most used, partners from the chemical department intend to use needles with gauges from the Table 3.2 to test the future ceramic pastes under several conditions. It thus changes the whole reduction ratio of the LDM extruder, which varies by a factor of 5 between the gauge 22 and the gauge 29. It is also planned to start trying those inks with significantly lower printing speeds than for polymers in FDM, which are using in any case maximum speeds around $v = 90\ mm.s^{-1}$ corresponding to $\omega_{1} = 40$ rpm for the stepper. So, choosing a reduction ratio X about two times higher than the calculated one would be a better choice to fit to a wider field of gauges and still remain in the stepper's efficiency range.

The next criteria to determine the reduction ratio was concerning the gear design itself. Usually the first rule to respect is the one of interferences induced by incompatible number of teeth. The Table 3.6 illustrates this with Z_a as the pinion and Z_b embodying our large wheel (Michalec 1994). If we follow this rule it would impose to work with a pinion with at least 16 teeth, which would either give enormous dimensions to our gears either make them too fragile to be printed. But since this rule is important for European standard gears with a pressure angle of α = 20°, all we need here is to adjust parameters to free the gears from this constraint since they will be printed. The Figure 3.8 below shows test prints realised to help decision of those parameters.

*Table 3.6 : Interference rule for given teeth number at a pressure angle of 20° (*Michalec 1994*)*

Z_a	13	14	15	16	17
Z_b	13 – 16	13 – 26	13 – 45	13 – 101	14 – ∞

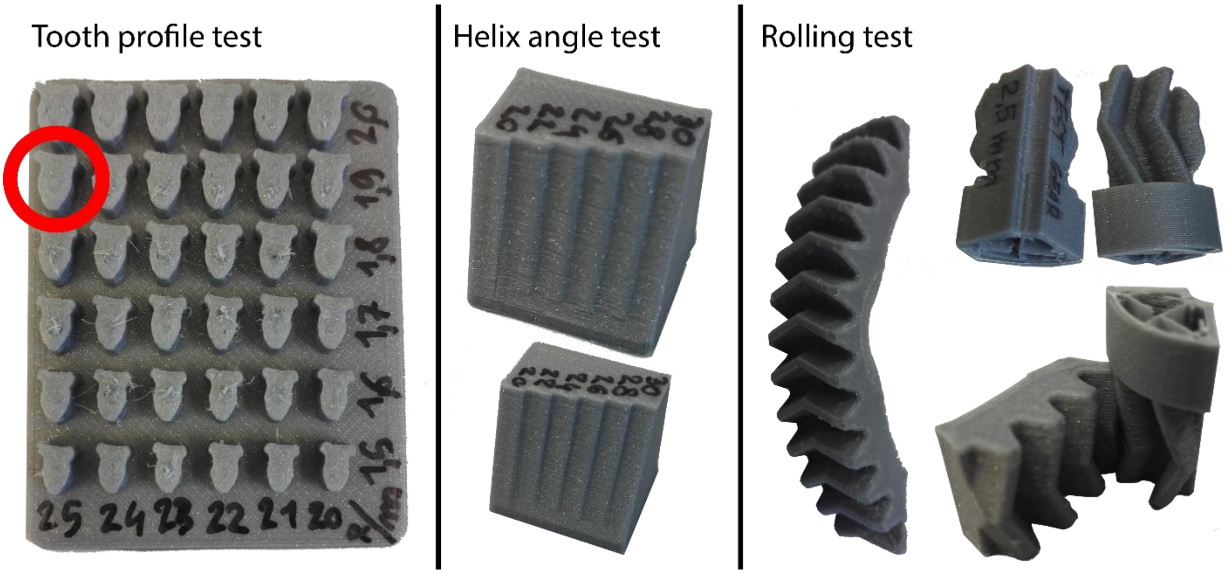

Figure 3.8 : FDM printing tests for gear design

Those tests combined with Solidworks® simulations allowed to choose an involute tooth profile with a pressure angle of α = 25°, as the American standard, and an unstandardized module of 1.9. Besides avoiding backlash issues, this combination provides a good bulk / strength ratio that will thus allow a choice among a larger range of ratios. Similar designs have been tested, confirming that for 3D printing a 25° angle is a good balance of chunkiness and efficient motion transfer on a palm sized gear (Graham 2017), plus that original Lulzbot printed gears are using this same pressure angle with 9 and 47 teeth. Then a helix angle of 22° was chosen by comparison with original gears, also being a good compromise for the staircase effect. Then the idea was to pick prime numbers to obtain a homogeneous distribution of wear, as displayed on Table 3.7 expressed in the form 1/x to show round ratios. The pinion will therefore wear faster than the wheel but is also easier to reprint and to access for replacement on the global mechanism. Finally, the ratio was determined as being a rational number that could also be a rational, to limit the errors while calculating the total reduction ratio when changing needle's gauge. The 47/10, or 4.7 ratio was then a good compromise regarding the overall LDM extruder volume.

Table 3.7 : Gear ratios for homogeneous distribution of wear

	Pinion								
Wheel	**8**	**9**	**10**	**11**	**12**	**13**	**14**	**15**	**16**
35	4.375	3.889	X	3.182	2.917	2.692	X	X	2.188
36	X	X	X	3.273	X	2.769	X	X	X
37	4.625	4.111	3.700	3.364	3.083	2.846	2.643	2.467	2.313
38	X	4.222	X	3.455	X	2.923	X	2.533	X
39	4.875	X	3.900	3.545	X	X	2.786	X	2.438
40	X	4.444	X	3.636	X	3.077	X	X	X
41	5.125	4.556	4.100	3.727	3.417	3.154	2.929	2.733	2.563
42	X	X	X	3.818	X	3.231	X	X	X
43	5.375	4.778	4.300	3.909	3.583	3.308	3.071	2.867	2.688
44	X	4.889	X	X	X	3.385	X	2.933	X
45	5.625	X	X	4.091	X	3.462	3.214	X	2.813
46	X	5.111	X	4.182	X	3.538	X	3.067	X
47	5.875	5.222	4.700	4.273	3.917	3.615	3.357	3.133	2.938
48	X	X	X	4.364	X	3.692	X	X	X
49	6.125	5.444	4.900	4.455	4.083	3.769	X	3.267	3.063
50	X	5.556	X	4.545	X	3.846	X	X	X
51	6.375	X	5.100	4.636	X	3.923	3.643	X	3.188
52	X	5.778	X	4.727	X	X	X	3.467	X
53	6.625	5.889	5.300	4.818	4.417	4.077	3.786	3.533	3.313
54	X	X	X	4.909	X	4.154	X	X	X
55	6.875	6.111	X	X	4.583	4.231	3.929	X	3.438

3.5.3 Design for FDM printing

More than giving information on tooth profile's geometry and its inherent resistance, those printing tests allowed to anticipate complications that could occur during the production phase (more details in section 4.2). First, a few imperfections on the surface finish related to vibrations and layer under-extrusion were observed, so the final gears will need to be printed with smaller layer height and slower speeds than the one used during those tests, to reach a better quality finish. The other reason in favour of a better finish was that Lulzbot Mini's gears were printed in Nylon that is stiffer than ABS, but in a coarse way leading to potential cracks that can be avoided with a better printing quality. To do this, the design was based on a Solidworks® CAD template developed in common with the colleagues of the laboratory, that was build using involute gears equations shown in Figure 3.10 (Michalec 1994). According to adjustments found while printing tooth profiles tests, standard involute gears were adapted with:

- Oversized teeth height compared to original gears to improve the contact surface's area.
- Holes and cuts to lighten the wheel, to reduce its printing time and inherent errors
- Full circular base to stiffen the pinion where printing time is not an issue.

- Revolved cut on pinion’s helix middle edge to avoid misalignment due to imperfections.

Item	Symbol	Formula	Example	
			Pinion	Gear
Normal Module	m_n		3	
Normal Pressure Angle	α_n		20°	
Helix Angle	β		30°	
Number of Teeth & Helical Hand	z_1, z_2		12 (L)	60 (R)
Radial Pressure Angle	α_t	$\tan^{-1}\left(\frac{\tan\alpha_n}{\cos\beta}\right)$	22.79588°	
Normal Coefficient of Profile Shift	x_{n1}, x_{n2}		0.09809	0
Involute Function α_{wt}	inv α_{wt}	$2\tan\alpha_n\left(\frac{x_{n1}+x_{n2}}{z_1+z_2}\right)+\text{inv}\,\alpha_t$	0.023405	
Radial Working Pressure Angle	α_{wt}	Find from Involute Function Table	23.1126°	
Center Distance Increment Factor	y	$\frac{z_1+z_2}{2\cos\beta}\left(\frac{\cos\alpha_t}{\cos\alpha_{wt}}-1\right)$	0.09744	
Center Distance	a_x	$\left(\frac{z_1+z_2}{2\cos\beta}+y\right)m_n$	125.000	
Standard Pitch Diameter	d	$\frac{zm_n}{\cos\beta}$	41.569	207.846
Base Diameter	d_b	$d\cos\alpha_t$	38.322	191.611
Working Pitch Diameter	h_{a1}	$\frac{d_b}{\cos\alpha_{wt}}$	41.667	208.333
Addendum	h_{a2}	$(1+y-x_{n2})\,m_n$ $(1+y-x_{n1})\,m_n$	3.292	2.998
Whole Depth	h	$[2.25+y-(x_{n1}+x_{n2})]m_n$	6.748	
Outside Diameter	d_a	$d+2h_a$	48.153	213.842
Root Diameter	d_f	d_a-2h	34.657	200.346

*Figure 3.10 : Helical gears equations for tooth profile caculation (*Michalec 1994*)*

When informing the module, the number of teeth, the pressure angle and the helix angle, those equations allow to calculate automated value to adapt the template until reaching the herringbone gear stated in 3 on Figure 3.9. This automation was a time saver to print and test tooth profiles, as well as for apprehending gears bulkiness by comparing their outside diameters. Then, once the tooth profile and the ratio decided, the template was adapted for printing as in step 4 for instance here in the case of the pinion. That final designing step saw the apparition of the full circular base, the revolved cut and the fastening system composed of a through screw on the steppers axis, which is maintained with and embedded hexagonal nut.

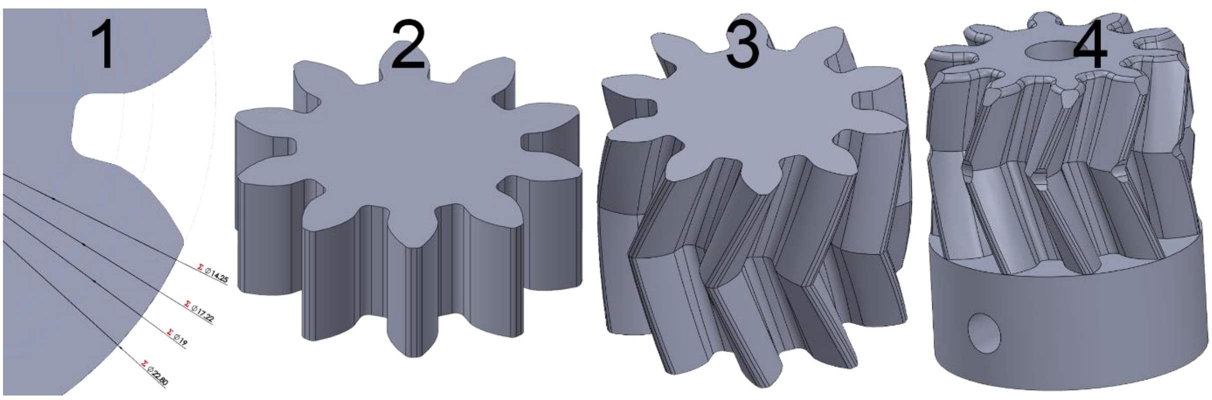

Figure 3.9 : Gears template progression and adaptation on Solidworks®

3.6 Syringe protection

This section focuses on an important function for the mechanism long-term operation by preventing syringe's early degradation and guaranteeing a good use of it. The goal here is to both avoid damaging the micrometric syringe that is the costliest part of the extruder as well as the needles of which degradation could lead to severe malfunctions in the whole mechanism.

3.6.1 Needle protection

3.6.1.1 First prototypes

Hypodermic needles are cheap thus considered as expendables, but since they are extremely thin they also are acutely fragile, especially for smaller diameters than gauges 23. A simple shock can badly bend them or damage the output surface and compromise the overall printing precision. Firstly, if the out printing end is impaired the paste will uncontrollably flow considering both speed, direction and sprawl changes. Then if the needle bends, the tool head end reference will be altered by changing its relative position to the bed level and modifying the X and Y coordinates, thus resulting wrongful building of the printed part.

In addition to that, the necessary automatic bed-levelling process is also the first source of vertical shocks on the extruder and thus of possible needle's deteriorations. On the Lulzbot Mini for the FDM mode, this operation is realised thanks to an electrical contact between the nozzle and the metallic washers that are located at the four corners of the bed. The Z level is thus detected when the nozzle-washers contact closes an electrical circuit called the zero-volt sense that is wired with a harness on the hot end. Consequently, it was needed to consider a solution in order to both protect the needle while printing and provide the same auto levelling function as FDM for the LDM mode.

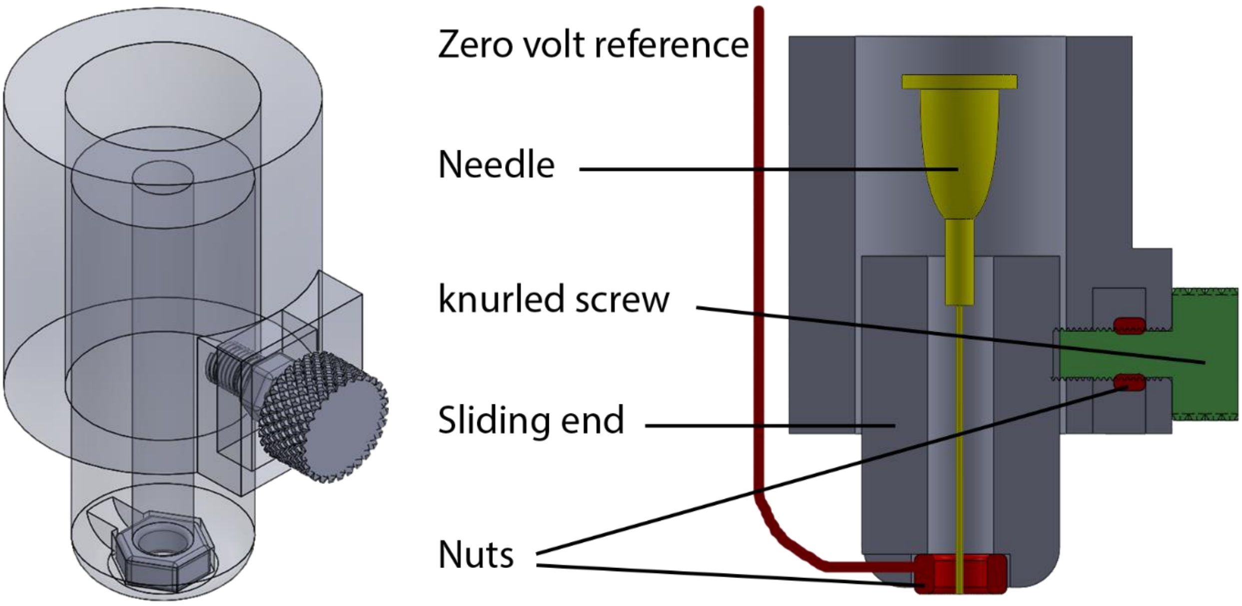

Figure 3.11 : First functional solution for needle protection

The firstly considered solution was to place a small metallic rod attached to the zero-volt sense circuit in a parallel way to the needle to make the electrical. This would have been easy to realise by integrating a hole with a through screw in the main clamp, as a support allowing to adjust the rod to the needle's Z position. However, this solution would have required the rod to be placed next to the needle's end, that would have weakened the clamp and especially would have not protected the needle from lateral shocks and offset impacts from the rod. The idea was then to replace this rod by a printed part that could encircle the needle for a better protection, on which a metallic washer or nut would be glued at the extremity and liked to the electrical circuit. This last version shown on Figure 3.11 above is very similar to the printed one, see section 4.2. The main advantage here is the possibility the remove the sliding part to help needle placement along and adjust it to the right length. It also allows to precisely adapt the protection to each needles length, depending on the gauges and the bevel that was cut. Since the needle is somewhat flexible, it can be slightly bended by compressing it along the Z axis before returning to its original form. That is why the protection can be placed just above the needle's end to avoid touching the paste once extruded and still protect the needle during bed auto-levelling.

3.6.1.2 Permanent solution

For the case of a more advanced version of the experimental rig, a more durable solution was examined. The needles are considered as expendables for their price but are quite hard to work with due to their bevel's cut, an operation which is manually made in Técnico to limit the expenses but that is hardly repeatable. This gives needles with different output surfaces and length to which the protection needs to adapt. Plus, the previous system imposes to use one needle per print because of the difficulty to clean them, which demands great deal of manipulations each time the syringe is changed, as well as preventable wastes. The idea here is thus to replace the needles and inherent protection by an all-in-one piece that is easier to use and to clean to avoid risks of shocks when manipulating.

It was then justified to think about this solution with conventional machining on a single metallic part. This would allow the LDM extruder to be stronger, more compact and therefore to access a bigger build volume, particularly by shortening the Z offset after the syringe's tank that was imposed by needles. The first draft mainly looked like a cylinder that could be manufactured on a lathe to be adapted to the syringe's reservoir following the needles standard and directly linked to the zero-volt sense harness. It also allows to insert a joint that can be compressed within the main clamp to ensure a hermetic connection with the syringe and avoid leakage or popping problems that can occur with needles. However, this solution presents the main default to be totally permanent thus complicated to clean and remove. The machining of such small hole also requires laser pulse or electron beam drilling, which consequently swells the price of this part, a bad argument if replacement is needed. Instead of drilling micro holes, a better solution is to directly screw FDM metallic nozzles on a similar part to be easily manipulated, cleaned and replaced. Such a piece retains the advantages of the previous one but would also be cheaper to produce and entirely manufacturable in the mechanical department workshop. Then nozzles from 0,5 to 0,1 mm of diameter usually cost about 0,5 € a unit and perfectly fit this cheap solution.

3.6.2 Syringe's body protection

As for the permanent needle protection, this section relates to a future version of the experimental rig. The actual version contains slacks that allow a few adjustments, but those plays in the mechanism may disappear in a more performant adaptation of the LDM system.

3.6.2.1 Protect the micrometric screw

The biggest danger for the syringe is to see its micrometric screw damaged by high torque applied on the motor shaft, with drastic consequences on material extrusion. In order to protect it, the simplest found idea was to insert a mechanical fuse between the square shaft and the top clamp. Regarding the small range of torque applied on the mechanism the easiest way to produce this fuse was to print it, knowing that it would also be easier to remanufacture if needed. After comparison of materials mechanical values (see section 3.2.3), the ABS has been selected for its stiffness and its neat way of breaking. Another argument in favour of ABS was also its good printability, especially for small parts like this one, which will allow to limit defaults in printed surfaces to better control the location of the crack. In order to do so, the geometry was based on a cylinder as shown on Figure 3.12, to obtain an equally distributed stress in the surface to break and thus ease the dimension estimations based on printed ABS mechanical properties (Ultimaker 2017). For a print with a 100% infill we can estimate the ABS properties as polar orthotropic at the breaking surface, even if a few test will be needed to adjust the calculated diameter because of the layer orientation and inherent printing weaknesses. Thanks to the formula of strength of materials for torsion we can determine the maximal diameter to break for an applied torque T on the estimated flexural stress at break for printed ABS τ_e = 19,5 MPa:

$$d \ll \sqrt[3]{\frac{16 * T}{\pi * \tau_e}}$$

The previously determined minimal torque for permanent deformation of the micrometric screw was 83 N.mm and the maximal motored holding torque is 550N.mm, which respectively corresponds to diameters of 2,73 and 5,24 mm. The exact diameter to be tested is therefore between those two theoretical values, the highest one also serving as protection for power consumption peaks of the stepper. Since this smallest diameter was already underestimated and that the crack surface will correspond to a weaker interface between two layers, the final diameter will more likely be around 4 mm to ensure a minimum of rigidity in the transmission of the fuse.

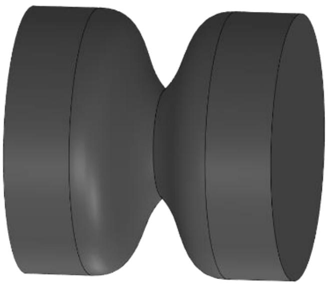

Figure 3.12 : Representation of the ABS mechanical fuse

3.6.2.2 Protect the axis alignment

The second protection needed is the one related to misalignment of the sleeve's revolution axis with the motored shaft, that can lead to distortion in the inner mechanism of the syringe. The first idea to realise this link was to produce a part using flexible filament that could bend along X and Y axis while transmitting Z rotation, in the manner of a soda straws elbow. Such a part can be produced in the Lab2Prod with the Lulzbot Taz 5 printer thanks to its duct free Flexystruder® tool head that can print low stiffness filaments like the Thermoplastic Polyurethane (TPU) based NinjaFlex® and FilaFlex®. Considering a cylindrical shaped link, the main difficulty here is to estimate the dimensions needed. It can be done by a finite element analysis on Abaqus using an Ogden model, thanks to data on NinjaFlex® filament provided by NinjaTek®. Even if the data of FilaFlex® filament, the one currently used in the Lab2Prod, are considered similar to the one used for simulation, the problem lies in the mechanical comportment of the TPU materials. Indeed, those materials have a very ductile behaviour making them perfect for joints, but imprecise to use for rigid transmission. The simulations results were thus inconclusive for cylindrical parts, which required large dimensions to ensure a decent Z rotation transmission. So a possible adaptation would rely in infills and shapes modification, but would be thus impossible to correctly analyse with finite elements because of lack of data on the materials. In addition to that, difficulties to print with TPU filaments and their multitude of inherent imperfections led to put this solution aside. However, since the angle between shaft and sleeve is really small-scaled, the actual slacks between the slider, the square shaft and the top clamp are big enough to absorb this misalignment, it is thus not a problem for this experimental rig.

Chapter 4 - Prototype manufacturing

This chapter focuses on the building phase of the prototype, from identification of the definitive printing parameters to the assembly of previously designed solutions to manufacture the functional LDM extruder.

4.1 Version 0.0

This very first version was designed at the same time as the theoretical documentations were led. In parallel of providing designs for the early tests of section 3.2.3 to determine decent printing parameters ranges, its purpose was to gain a maximum of knowledge about printed parts mechanical properties to save time on design of the parts to be printed.

4.1.1 Prior tests for production

After testing printing properties and understanding small parts proportions requirements in section 3.2.3, the idea was to go into dimension testing in depth, to design both the body parts and the forthcoming adaptations. Those adaptations from CAD to CAM went through setting adjustments on Ultimaker Cura until reaching the compromises displayed on Figure 4.1 below.

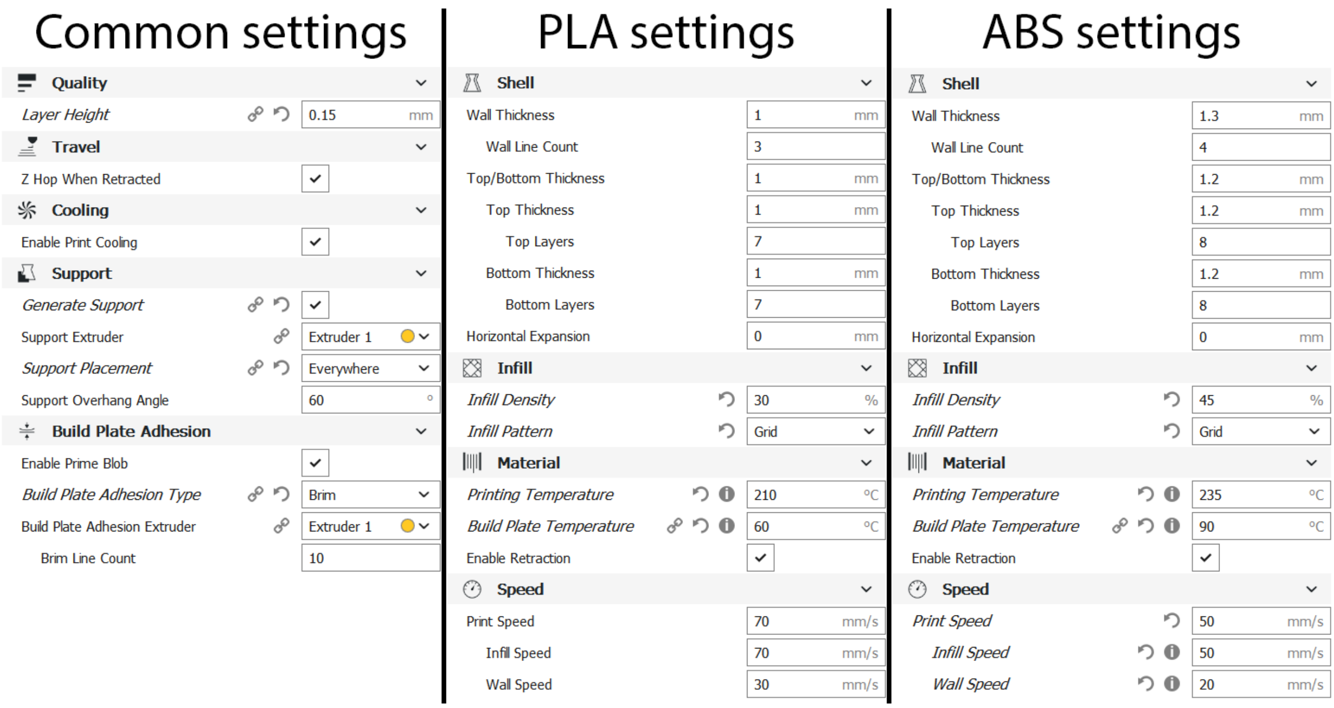

Figure 4.1 : Determined global Cura parameters for PLA and ABS

Among those settings, the strength of parts at macro scale will mainly depend on the shell and infill properties, but considering cracks and local defaults the temperature and speeds will have a bigger impact. Those last settings can thus be adjusted in the case where the piece has localized weaknesses, but broadly corresponds to a good surface finish. Since ABS was chosen to realise stronger parts than PLA the infill percentage generally keeps the same values as the ones above, knowing that beyond 60% the mechanical properties only improve in very little amount (Ligon et al. 2017). In addition to this, the risk of print crashes increases significantly because of layer cooling that is then more difficult to manage.

Then the supports and bed adhesion requires a bit of post processing to obtain mechanically useful surfaces. For bed adhesion, the raft provides a good adherence but the worst surface, the skirt is sometimes insufficient for decent adherence on large parts and the brim gives a good compromise, the only post processing being to cut detach it after print. For supports the idea is to cut and sand the surplus of extruded matter, but it is often located in hard access areas and sometimes can be a destructive technique. The idea is to orient le layers to avoid a maximum of support and avoid to use it for small dimensions. The Figure 4.2 below shows some important tested dimensions for the design of ball bearing supports and the realisation of the body.

Figure 4.2 : final dimension adjustment tests with PLA and ABS on the Ultimaker3

The figure displays the most important tests for adapting design dimensions, that were made after the design has been terminated and all the required parts received. For instance, the nut slot test allowed to correct every M3 nut caps in the design dimensions from 7,0 mm by 3,0 mm to 7,2 mm by 3,3 mm for full nuts and a depth of minimum 8,5 mm. That granted the exact insertion of nuts in the caps by giving them freedom in two directions to avoid misalignment issues, while blocking the rotation in the other direction thus allowing the tightening. Since the ball-bearings were mounted tight on the outer diameter, the ball-bearings inner diameter test allowed to find that the diameter needed to mount them fit was 19,8 mm instead of the theoretical 20,0 mm. Finally, the outer slider test also allowed to determine the fit mounting of the ABS links between the slider and the ball bearings. This shape was the most difficult one, since it is a square which fillets are made by a centred circle, with final dimensions of 19,60 mm for the square side and a radius of 14 mm.

4.1.2 LDM extruder's body first iteration

The design of LDM extruder's body follows the general versions organisation and the idea of keeping designs as simple as possible as stated in section 3.2.1. This first draft, of which the main supports are shown on the Figure 4.3 below, never went beyond the phase of CAD but constituted the starting point of the final body that integrates all the sub solutions. It was designed on Solidworks based on automatic equations in order to adapt dimensions to any changes quickly and safely. That was particularly useful for the standardised M3 fastenings to place the holes with adapted sizes and shapes to materials, as described in section 3.3.1.

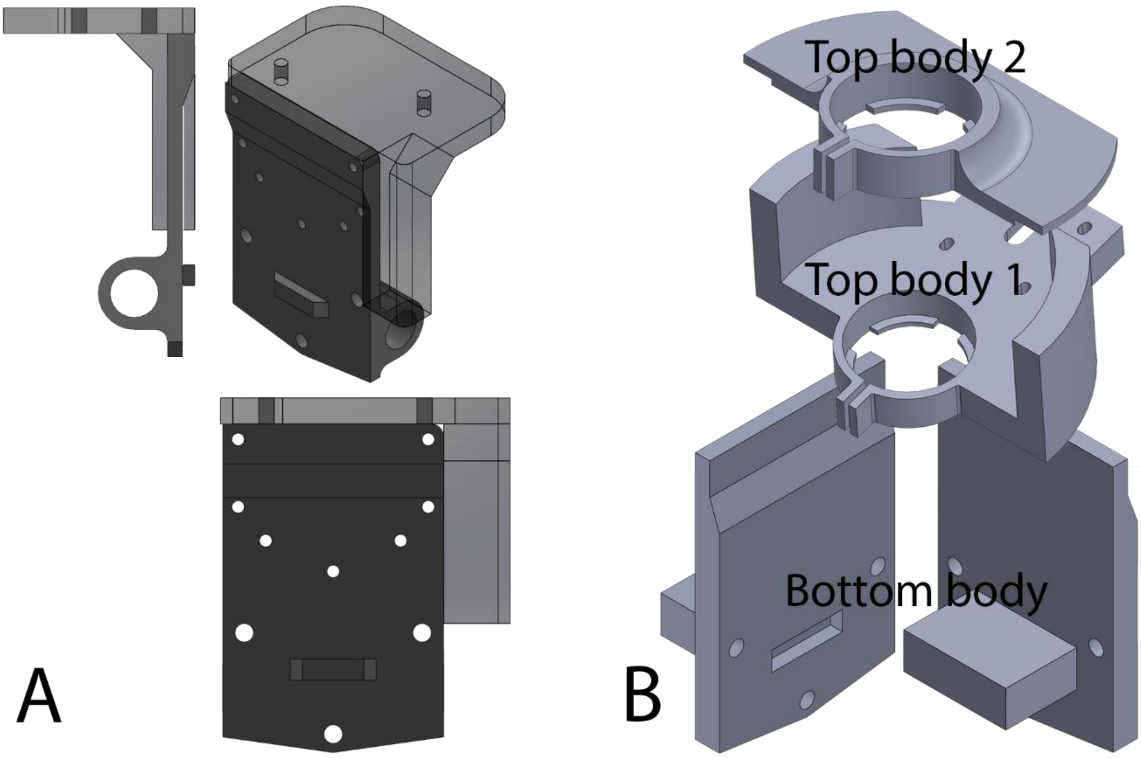

Figure 4.3 : First iteration of LDM extruder body (B), drawn to fit on the X carriage (A)

4.2 Version 1.X

Those 1.X versions embody the development of the whole prototype, with cyclical improvements on the LDM mechanism and successive adaptations to the Lulzbot Mini frame, until printing of a fully functional version. The Figure 4.4 below highlights this iterative design strategy.

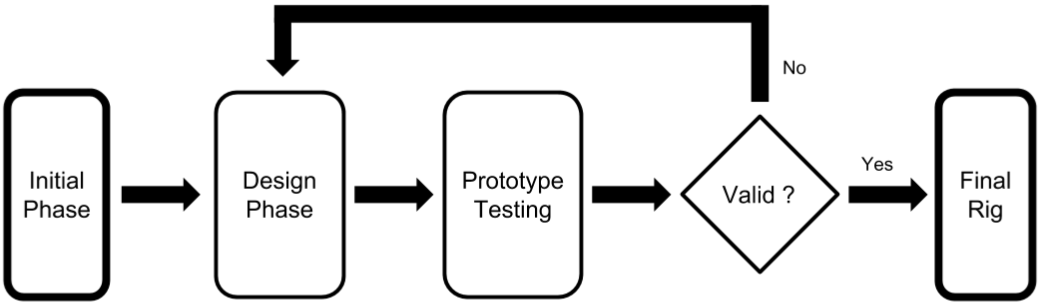

Figure 4.4 : Iterative design strategy corresponding to the work with versions

4.2.1 Adaptations of version 1.1

The first step in version 1.1 was to make sure every sub-solution could be correctly inserted in the LDM extruder body and that this body fits perfectly to the X carriage, before printing the prototype. To do so, the first adaptation was to redesign the bottom body so that its shape better fits the one of the X carriage and avoid eventual collision due to fastenings positioning. The second one was to create accurate fastenings following the strategies of section 3.2.1, with adapted nut caps to ensure the tightening of the M5 bolts imposed by the previous tool head fasteners to the X carriage. Then the automatic hole dimensions were adapted to all other M3 screws to create the attachment points of the body connections to be adapted, as well as an anchor to attach the main clamp centrally to the X carriage, as displayed on the Figure 4.5 below. This figure also shows the creation of a middle body to replace the cap of the X-carriage, the transparent piece of A on Figure 4.3. The goal here was to create better anchor points for the body supports while improving the rigidity of the whole extruder by fixing it to two perpendicular surfaces of the X carriage.

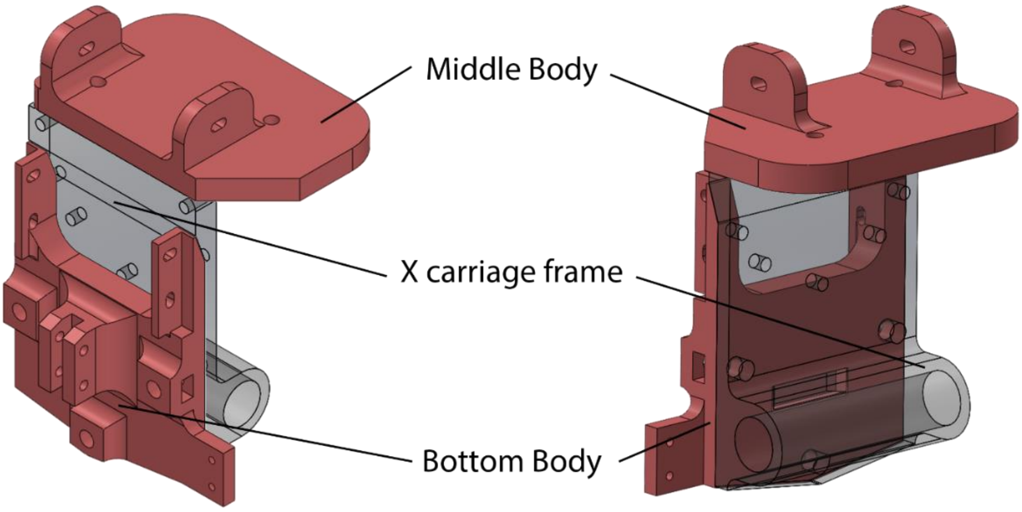

Figure 4.5 : Adaptation of the body by redesigning the bottom creatin a middle part

The second adaptation concerned the main clamp, whose first design had geometrical errors on the closed position, as framed in red on Figure 4.6. Those errors led to presence of an angle that caused problems for the positioning of the syringe's axis of revolution in the whole extruder and weakened the closing strip. That was solved by offsetting the hinge on the two parts of the clamp. After a test of the first version, the printed dimensions were measured and compared to the CAD ones to better adjust the clamp diameter to the syringe's nut. This trial has also highlighted some roughness in the hinge, which have been corrected by chamfers and larger slacks in version 1.1. It also allowed to change outer diameter dimensions to fit to the previously determined wall thickness to obtain a good strength / flexibility ratio for the tightening function. Those dimension adapted, the anchor strip for the fixation with the bottom body was designed.

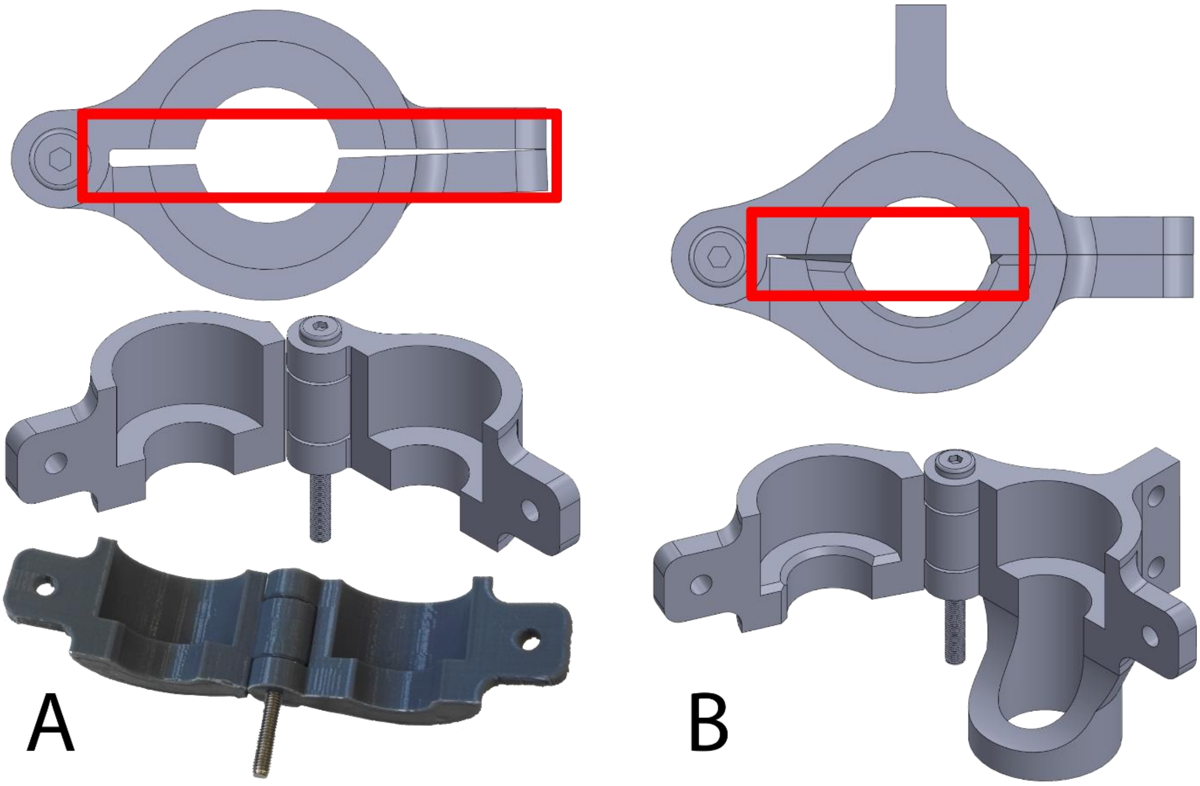

Figure 4.6 : Main clamp improvement from version 0.1 (A) to 1.1 (B)

4.2.2 Contribution of version 1.2

With a few dimension adjustments, the main contribution of version 1.2 lies in the motorisation and the reduction mechanism. As shown on Figure 4.8, the first step was to design the links between the slider and the ball bearings, thanks to knowledge on printed dimensions acquired in the version 0.0. That allowed adaptation of the top body parts and the design of their inherent connection parts. The following action was to print the gears, starting with the large wheel that will be inserted on the linear slider, between the two ball bearing supports (called links on Figure 4.8). Thanks to the complementary profile, the wheel will therefore put the slider in motion, which will itself drive the shaft in rotation while leaving it sliding along. It that sense, the linear slider, the ball bearing supports and the large gear are forming the blue part described in the kinematic diagram on Figure 3.3.

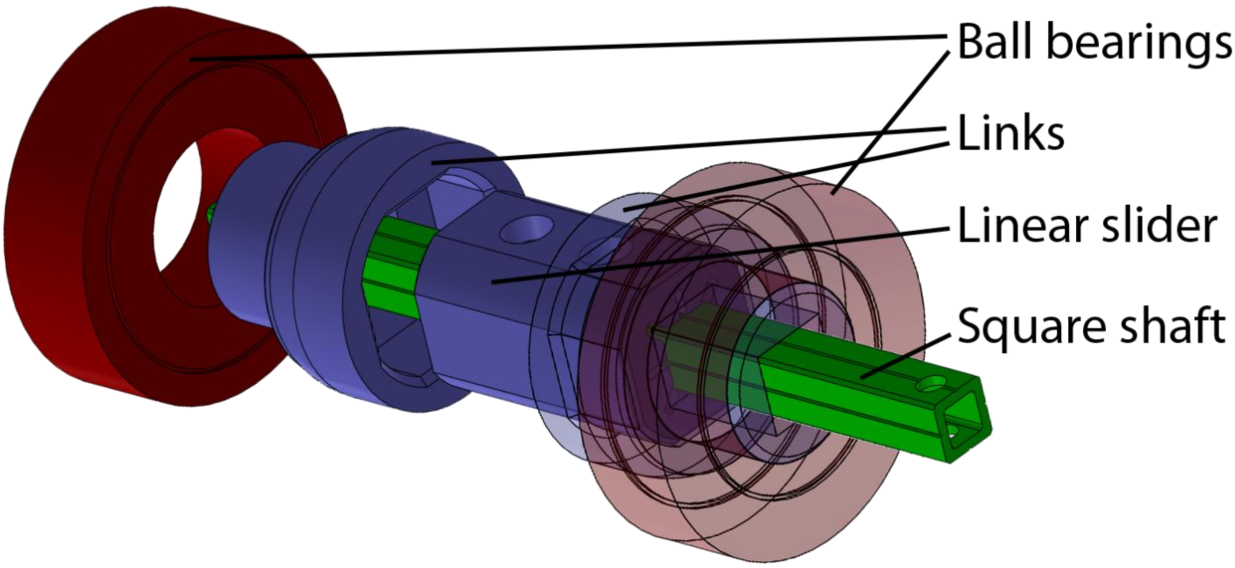

Figure 4.8 : Exploded view of large gear's support with color code of the kinematic diagram

The Cura settings used to print the gears were based on the experiments that were realised in section 3.5.2, with the idea of improving those results. The Figure 4.7 below shows parameters of the herringbone gear template used for this project for the large wheel, that were adapted in accordance to the reduction ratio previously defined. This template's geometry was also adapted with the chamfers and reductions stated in the design strategy of section 3.5.3.

Name	Value / Equation	Evaluates to	Comments
Global Variables			
"Module"	= 1.9mm	1.9mm	User input
"NumTeeth"	= 47	47	User input
"PressureAngle"	= 25	25	User input
"HelixAngle"	= 21	21	User input
"TwistDirection"	= 0	0	User Input. 0: right hand gear; 1
"FaceWidth"	= 15	15	User input
"Offset"	= 0.1mm	0.1mm	User Input. Clearance to compe
"Addendum"	= "Module"	1.9mm	
"WholeDepth"	= 2.25 * "Module"	4.275mm	
"PitchDiameter"	= "NumTeeth" * "Module"	89.3mm	
"BaseCircleDiameter"	= "PitchDiameter" * cos ("PressureAn	80.9333	
"OutsideDiameter"	= "PitchDiameter" + 2 * "Addendum"	93.1mm	
"RootDiameter"	= "OutsideDiameter" - 2 * "WholeDep	84.55mm	
"PitchAngle"	= 360deg / "NumTeeth"	7.65957	
"Phi"	= sqr (("OutsideDiameter" / 2) ^ 2 -	0.568559mm	Used in definition of the param
"Clearance"	= 0.25 * "Module"	0.475mm	
"FilletFull"	= "Clearance" * cos ("PressureAngle"	0.675744	
"FilletHalf"	= 0.5 * "Clearance" * cos ("PressureAı	0.337872	
"TwistAngle"	= (180 / pi) * "FaceWidth" * tan ("He	3.69437mm	
"CircularPitch"	= pi * "Module"	5.96903mm	Just for reference (not used in t
"Dedendum"	= 1.25 * "Module"	2.375mm	Just for reference (not used in t

Figure 4.7 : Solidworks herringbone gears template parameters modified for FDM printing

Concerning the overall quality, the printing parameters were refined compared to the previous ABS tests to obtain the final surface finish directly out of the Ultimaker, because the space between gear's teeth were too small to provide good post-processing here. The gears were thus printed with a layer height of 0.1 mm and speeds of 50 and 25 mm.s^{-1} respectively for infill and wall in order to limit under-extrusion and vibration issues on the final surface. The chosen infill was a grid at 45 % and the wall thickness was set at 1.3 mm, which is according to the tests a good compromise between part strength and sensitivity to printing defects related to cooling that can appear for a 100% infill.

For the large wheel whose bigger diameter is 93.1 mm, those settings imposed a print of more than 10 hours. With those time and dimensions for an ABS print, the part is highly exposed to warping. A good compromise to avoid this phenomenon is to slightly increase the bed temperature as well as printing with a brim in order to increase the build plate adhesions, as displayed on Figure 4.9. However, this brim also modifies the side surface of the print, here being the teeth profiles, by adding a small flood hard to cut even when the brim is removed. To fix this problem, the applied procedure was to add a chamfer on the bed touching surface, so the flood of the brim does not modify the structure of the first layers on the useful surface of the teeth.

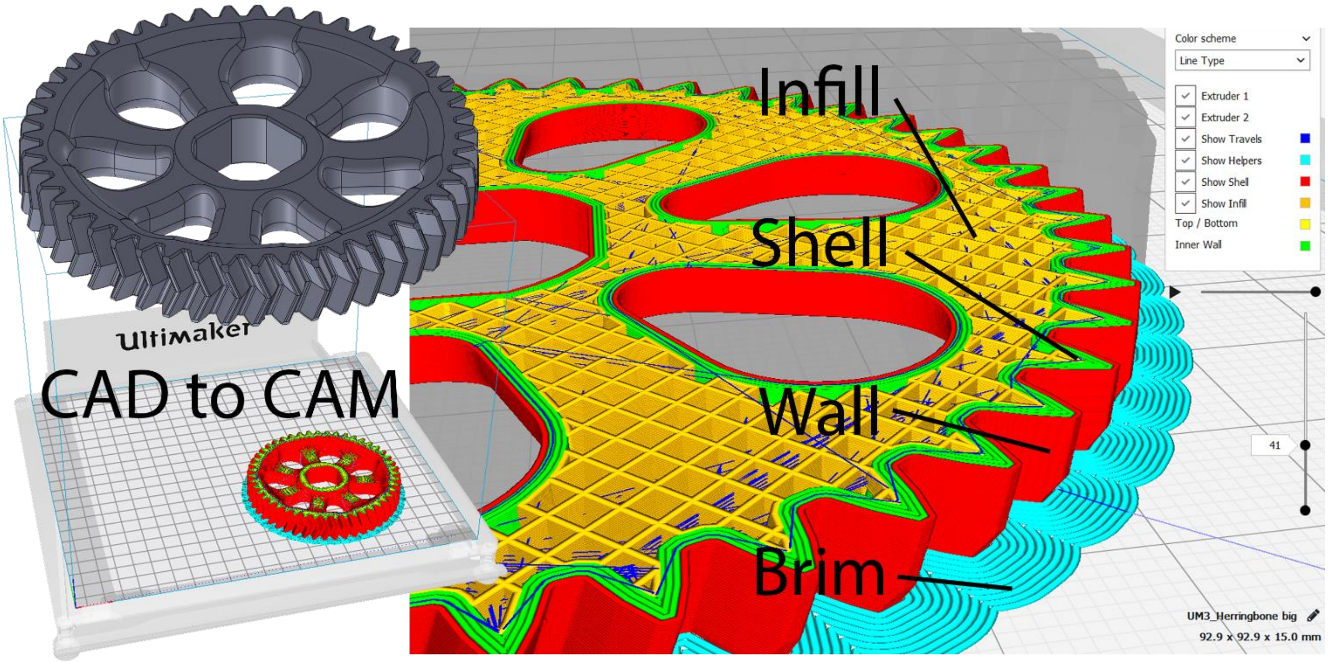

Figure 4.9 : Adaptation step between design and slicing for the large wheel

Even though the printing settings were made for the large wheel to be less likely to crash, the part warped a bit as shown on Figure 4.10. Fortunately, it did it without layer shifting and the dimensions remained unchanged in the X Y plan, making this issue non-disruptive for the part functionality.

This experienced demonstrates that printing a gear with a build plate adhesion ensured by a raft should not be a problem. Even if the surface of the object linked to the raft will be poorly finished, it can be insignificant regarding the useful surface when designed with chamfers, and there are better chances to avoid warping. In the end, the pinion was printed with the same parameters and came out with significantly better finishing than the one printed during tests, as well as a the one that was used in the Lulzbot Mini.

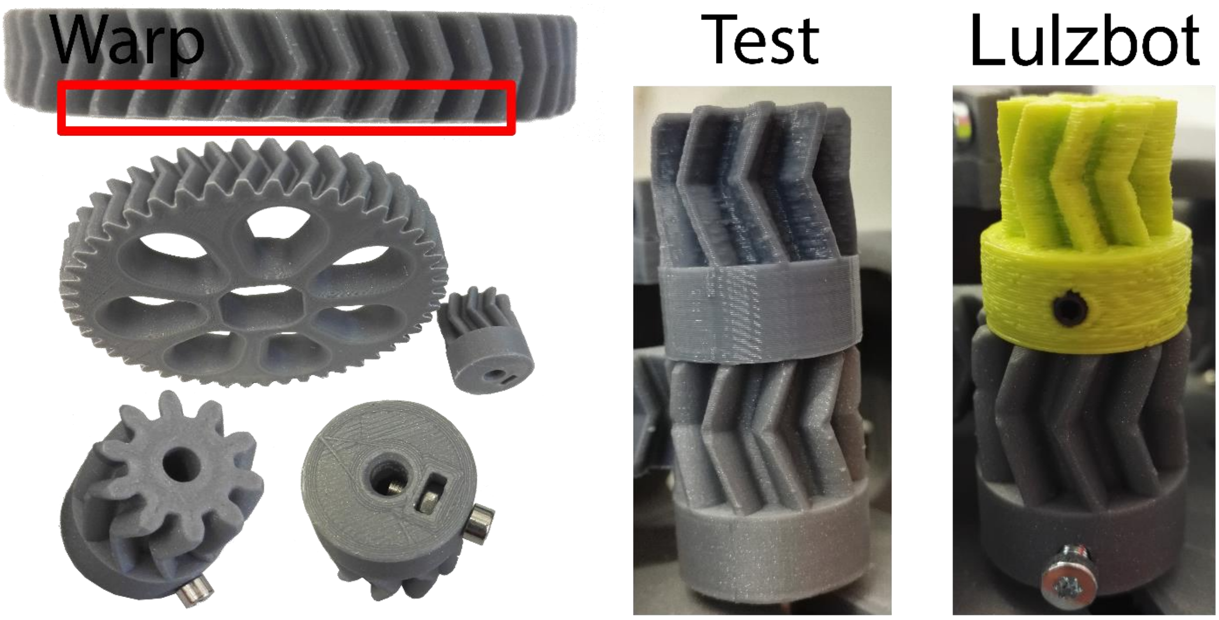

Figure 4.10 : Printed gears compared to tested gears and Lulzbot Mini gears

4.2.3 Improvements of version 1.3

This version comes at the time of printing the first parts of the prototype and is mainly an improvement in original design. With the first prints, some dimensions that couldn't be estimated regarding the entire Lulzbot Mini frame were adjusted. This is particularly the case for bottom body part, were the positioning of a couple of screws impeach its correct fitting to the X carriage and thus need a few adjustment cuts (A). More important the X sensors adjustment was made to ensure the safe motion of the carriage. When it travels along the X axis, the carriage detects stops thanks to two identical abutment contact sensors, one being mounted on the carriage and the other one being triggered by it. The first problem was that the estimated positioning of the sensor on the bottom body part was offset from the stop stud mounted on the frame (B). The second one was that the stud on the body was not long enough in X direction to trigger the sensor and avoid collision between the top body parts and the frame (C). The Figure 4.11 below shows the newly designed bottom body to be printed.

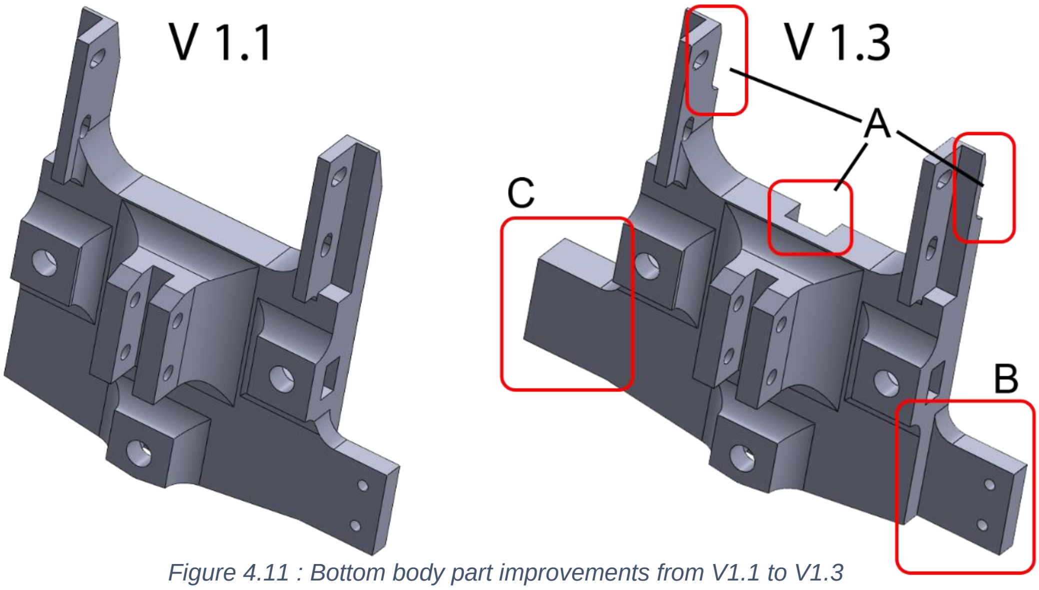

Figure 4.11 : Bottom body part improvements from V1.1 to V1.3

After the bottom body part, the top 1 and top 2 pieces have been firstly adapted to those last dimensions. Then they were lightened and simplified before gaining some fillets and rounded shapes, according to the strategies stated in 3.2.1. This in order to strengthen the parts by playing on thickness, improving the overall quality by reducing the amount of necessary support and reducing fail chances by providing shapes that are less sensitive to warping or layer shifting.

This version is also the one where the first needle protection was printed, on the model of the sliding segment and glued nut, found in section 3.6.1.1. In the initial iteration the space let for the nut was too tight and the proportion of the inner straight hole did not prove to be ergonomic to use with the needle already mounted on the syringe. It was thus redesigned with an added flaring to the trough hole and more space for the nut and its welded wire. The other amelioration provided at that stage was the integration of the round thread of the chuck that was designed and tested but abandoned in section 3.3.2. This in order to allow a more precise and easier tuning to each needles, while preventing the part to fall and potentially harm the glued nut and welded wire.

At the same time, the printing of the different parts continued, with a few printing mistakes even after an adapted design. For instance, with optic to save manufacturing time, the printing settings of the Top 1 body piece were changed, particularly concerning the speeds. This led to failure as shown on Figure 4.12 (A), where cracks, warping, layer shifting and detachment appeared, thus wasting a 6 hours print. Then another error appeared, still in order to win time the layer orientation was changed but the part was thus too fragile and cracked while assembling (B), wasting another 6 hours. Finally, a few print fails were due to mistakes in the calibration of machines that were used by many and which could also differ from a material to another. In the case of a fail like the common one show below with flexible filament (C), fast-to-print objects like the green one were used to check machines calibration.

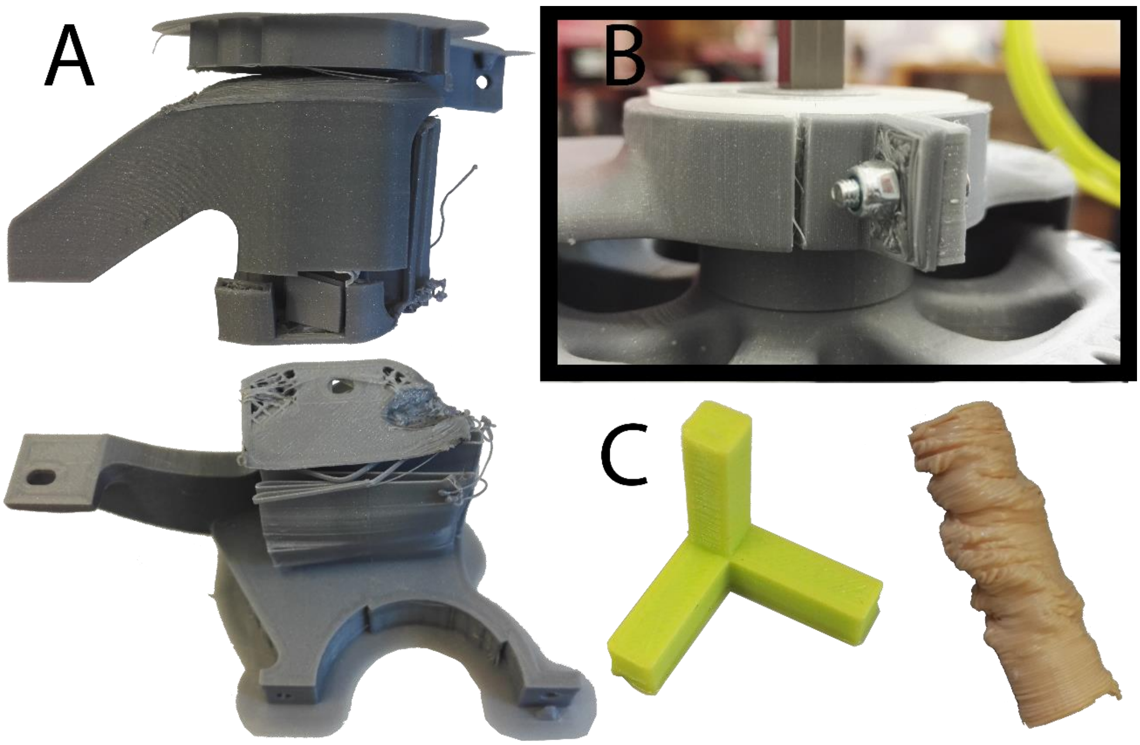

Figure 4.12 : Defaults corrected with printing settings and strengthen in V1.3 CAD files

4.3 Functional prototype

4.3.1 Printed version

Because version 1.3 improvements were done during the first prints, the current functional prototype is a hybrid version made of large components from 1.2 on which are attached the latest sub-solutions updates from 1.3. Parts are still in production at the moment with a focus on print quality, to successively replace pieces that are already assembled and come to the entire 1.3 version. The Figure 4.14 and Figure 4.13 show the currently used prototype and the CAD of the full next version.

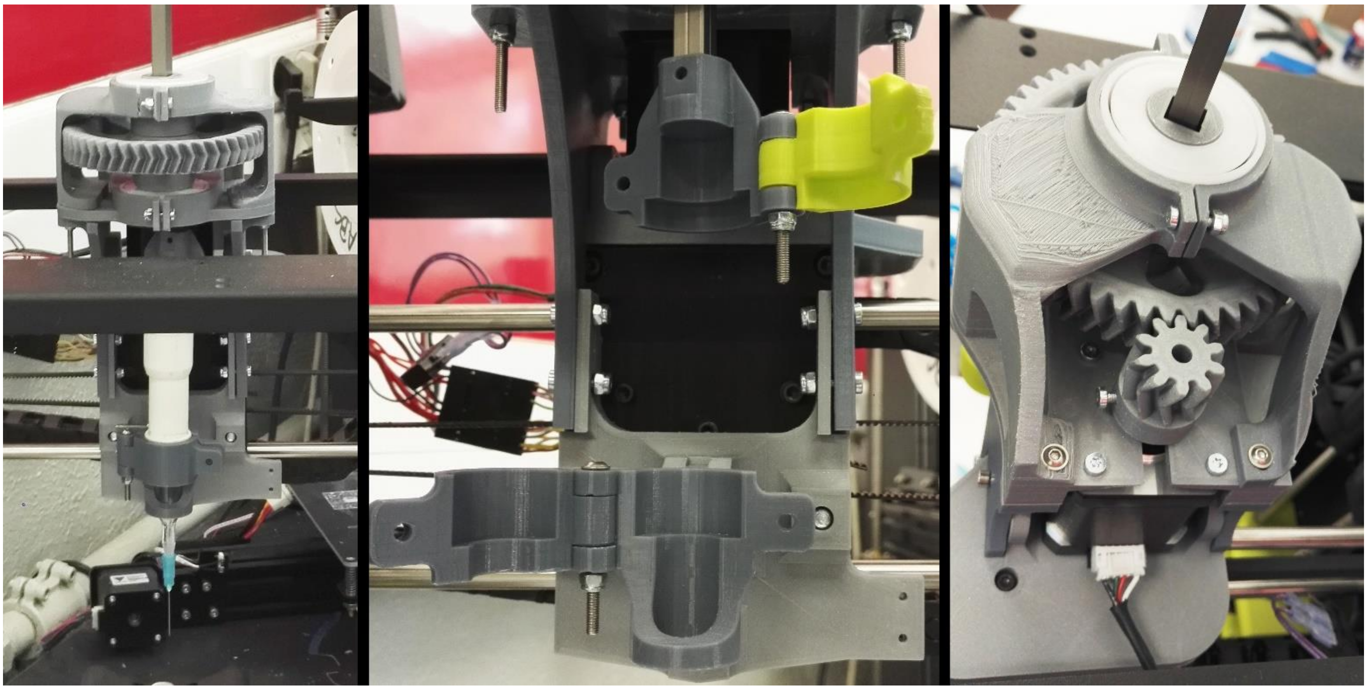

Figure 4.14 : Currently printed functional prototype, a hybrid of 1.2 and 1.3 CAD files

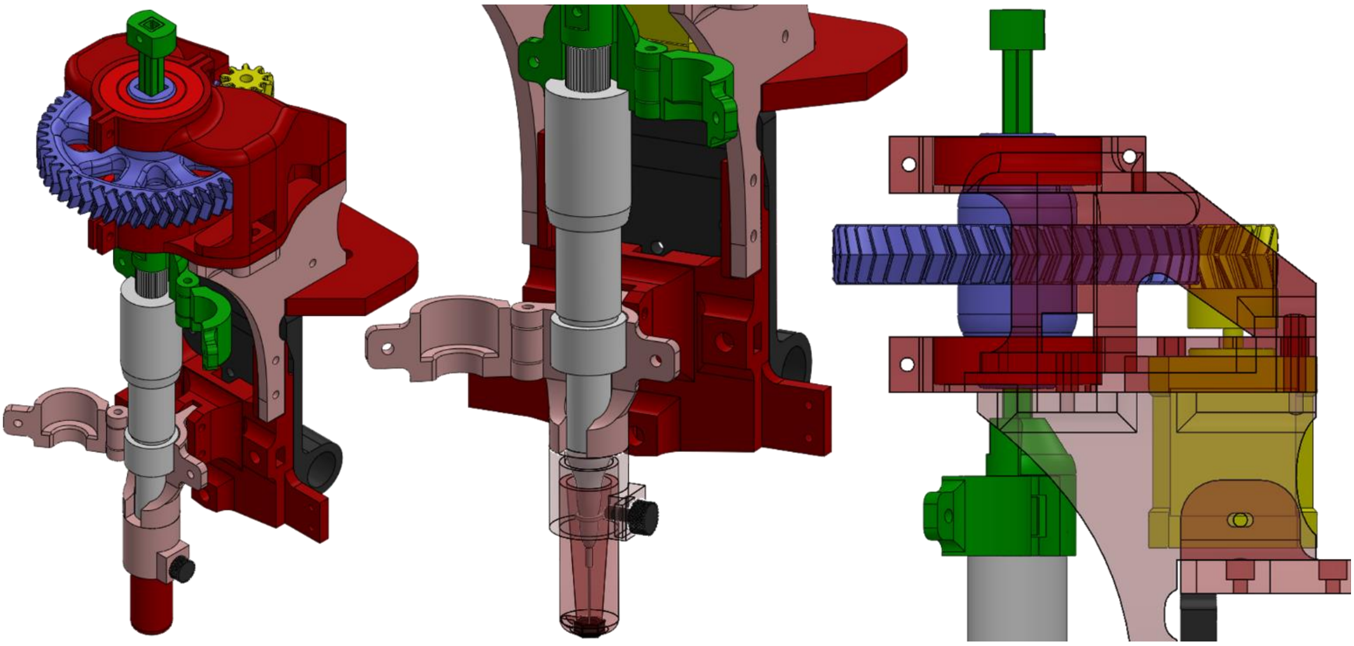

Figure 4.13 : 1.3 CAD version, next upgrade of the currently manufactured prototype

4.3.2 Manufacturing costs

Finally, it was interesting to estimate the production costs in terms of time and materials to improve the manufacture of future versions. The Table 4.1 groups the expenses of printed parts estimated with Ultimaker materials retail price of 0.0462 €/g. The parts were thus printed in 48h 03min for a cost of 12,13€, to which are added the ordered 14,72€ square shaft, the 13,28€ slider and the two 14,92€ ball bearings. However, those estimations do not count the setup time, fails, delivery costs and delays, fasteners costs, nor the 3D printer's tool head wear and maintenance. Nonetheless, when this data is crossed with the CAD files, we can learn from it the importance of shape and support on the printing time here. Indeed, the table shows that a heavy but simple-shaped parts can be faster than a lighter complex-shaped pieces using supports, for similar range of printing speeds.

Table 4.1 : Production expenses for the first functional version of the prototype

Function	Part	Time	Material	Layer height (mm)	Infill (%)	Mass (g)	Cost (€)
Gears	Wheel	10h 48	ABS	0,10	45	42	1,94
	Pinion	2h 09	ABS	0,10	45	7	0,32
Clamps	Main back	1h 59	PLA	0,15	45	12	0,55
	Main front	0h 51	PLA	0,15	30	5	0,23
	Top back	1h 40	PLA	0,15	45	10	0,46
	Top front	0h 47	PLA	0,15	30	5	0,23
Links	Bearing (X2)	1h 38	ABS	0,15	45	9	0,42
	Shaft stop	0h 14	PLA	0,20	30	2	0,09
Needle cover	Slider	0h 51	ABS	0,15	45	5	0,23
	Clamp link	1h 09	PLA	0,15	45	7	0,32
Body	Bottom	6h 13	ABS	0,15	30	38	1,76
	Middle	4h 46	ABS	0,15	30	33	1,52
	Top 1	6h 37	ABS	0,15	30	39	1,80
	Top 2 (X2)	6h 05	ABS	0,15	30	31	1,43
	Support (X2)	2h 16	PLA	0,20	30	18	0,83
Total		**48h03**				**263**	**12,13**

4.4 Test and validation of the experimental rig

After the assembly of modified version 1.2 of the extruder, the objective was to test and characterise the capacities of the experimental rig to work with fluids, to demonstrate its ability to test future ceramic pastes.

The first test concerned the syringe positioning on the bed and allowed to show an important design mistake. When adapting the X sensors position on the bottom body part, the overall location of the printing end changed on the X-carriage with an offset of about 16 mm in the negative X direction, as shown on the Figure 4.15. That impeach the auto-levelling function of the machine, which can only be completed when the needle protection is able to touch the 4 washers of the bed.

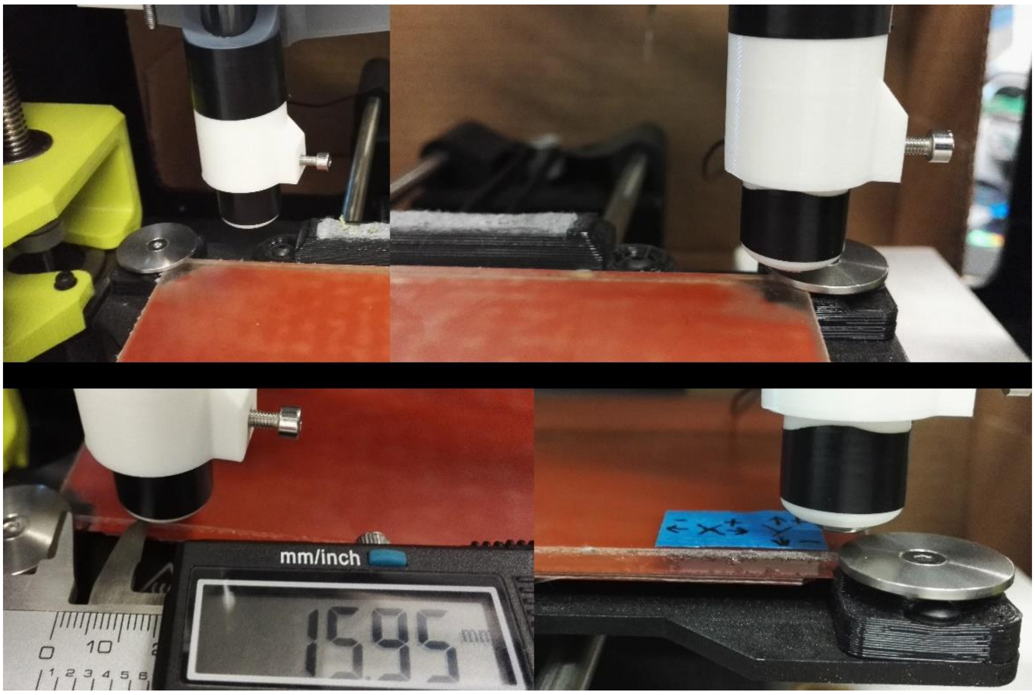

Figure 4.15 : Bed positioning error due to design adaptation mistake

The second experiment concerned the way of driving the prototype, with the monitor mode of the Lulzbot Cura slicer. So far the only connectivity present on the machine is a USB link and the way to drive the machine is to send gCode lines thanks to a command console. The manual control of the Cura monitor allows to separately move every axis for a given distance. However, to put the syringe in rotation and extract paste, the idea is to ask for virtual filament extraction since the software was built for FDM printing. To do so, a software security imposes to heat up the previous FDM hot end until reaching 120°C to avoid extruder damages because of cold filament extraction. That requires to keep the hot end, the thermistor and the 5V fan of the original extruding head permanently connected to the experimental rig, which connections are sensitive to sudden movements and therefore weakens the overall prototype and brakes its ergonomic. When the hot end reaches 150°C it becomes possible to drive the whole prototype uniquely with gCode lines, where the commands are sent first by stating the desired movement function then by axis displacements length, material extrusion length and speed required for this function (RepRap 2018).

After succeeding driving each element separately, the second test was to bring everything together in movement with a succession of gCode commands to ensure the layer printing protocol. As displayed on Figure 4.16, that was done by extracting shampoo, which has a more homogeneous composition and is consequently less viscous than the ceramic suspension. The drawn lines are placed in diagonal compared to the axis alignments and shows a constant thickness. This proves the ability of the rig to extract liquid at constant speed while traveling on both X and Y axis, which answers the requirements of ceramic paste printability testing. Another observation concerns the use of two different needles with cut bevels, where the quality of extraction did not present major observable differences with shampoo. However, inequalities might appear with ceramic paste but this factor can be overlooked by working with needles directly ordered without bevel. A problem related to shampoo bubbles in the syringe's reservoir also appeared after emptying half of the capacity. Contrary to the one displayed, this led to an inconstant flow of extracted fluid. As it could be a problem for future tests, it is thus recommended to load the ceramic paste by avoiding bubbles at the maximum. Finally, the printing end was manually placed on the bed thanks to the Lulzbot Cura controls, the layer height being visually placed with successive steps of 0,3 mm since there are no stop sensors on the Z axis positive direction. Then the automated movement of the machine were driven by the gCode displayed on the figure.

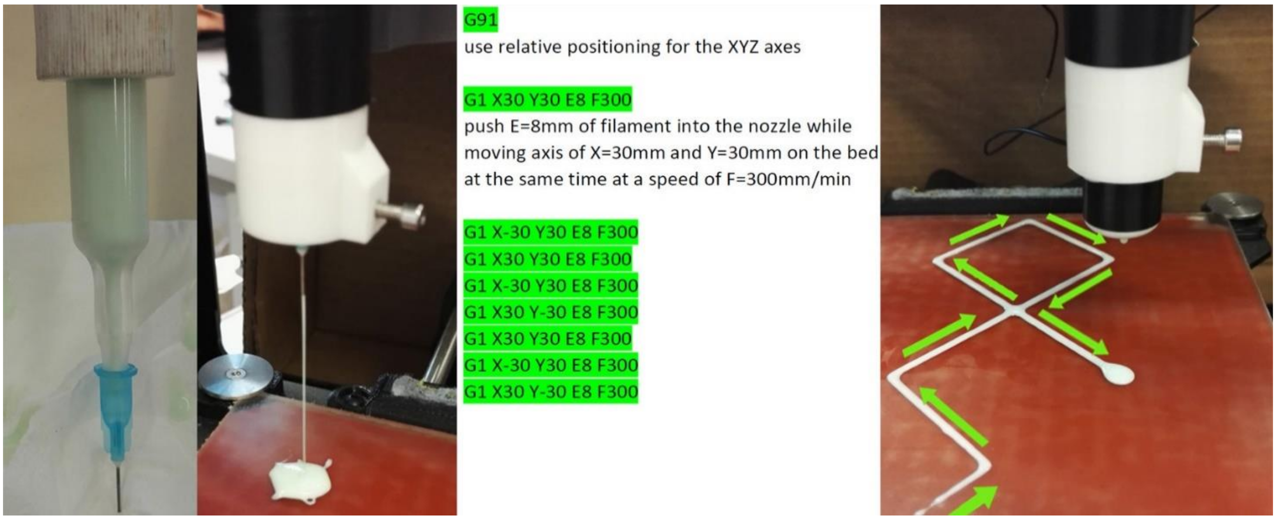

Figure 4.16 : Experimental rig printing test with shampoo

A last test concerned the mechanical fuse whose first design version has been printed in ABS with a layer height of 0,15 mm, see Figure 4.17. The fuse correctly inserted between the square shaft and the previously designed clamp and broke at the expected location. It also transmitted the torque with an empty reservoir but broke when the reservoir was filled with the shampoo, without being able to move the syringe. That is due to the print quality that provided a weaker fuse than expected, with a distinct infill in the central section instead of a full surface. It will be a problem in the future so a few tests will need to be led to determine better dimensions. Since those mechanical properties change with materials and printing settings, it is recommended to print a small batch at the same time with exactly the same parameters to form a stock. However, that does not provide a practical solution on the long term and contradicts the compactness improvements of the LDM extruder. A better solution will be to replace the mechanical fuse by an electrical breaker in the future, much more precise and repeatable.

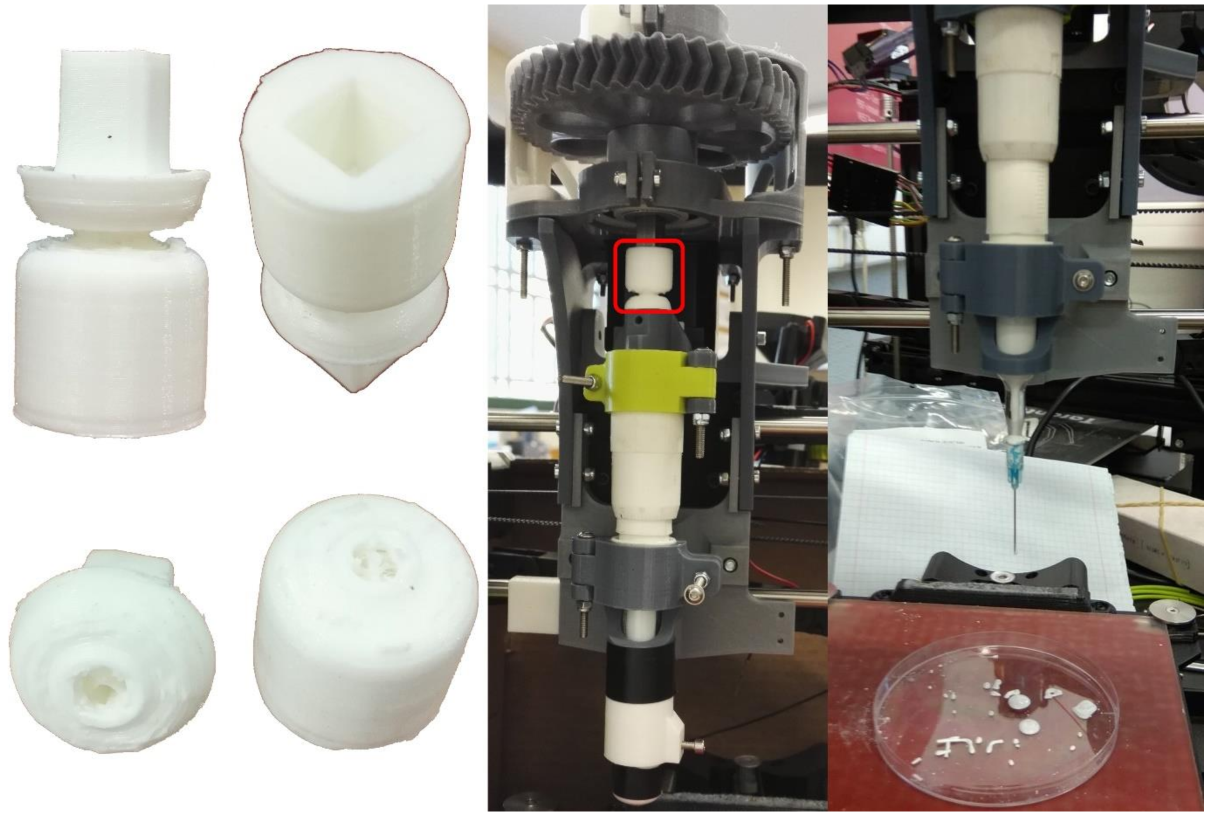

Figure 4.17 : Fuse insertion and breaking and early zirconia ceramic paste extraction test

During the first zirconia ceramic test, the custom paste showed a non-homogeneous composition as well as a shear-thickening rheological behaviour. That led to fail since the paste made the needle pop and could not pass through the gauge 23, the largest of the decided gauge range. The Figure 4.17 shows the second early version of the paste that worked with gauge 23 but could not pass through 29, which were the only two gauges that we had at disposal at that time. This second version had a better behaviour than the first paste, however it still did not show a constant extraction flow and sometimes formed small blasts. But those issues were only due to the paste composition that aims to be improved and since the tests with shampoo were conclusive, the rig's abilities proved to be valid for paste testing.

As an outcome, we can say the currently assembled version of the experimental rig fulfils the first function of fluid materials testing and allows mastery of X and Y directions, amount of extruded material and speeds while printing. However, it does not provide the overall functions of the FDM hardware, as for instance the auto-levelling. In that sense it is not ergonomic to use and a few improvements needs to be made both on the printed parts design in version 1.4 and on the software approach of the LDM printing process.

Chapter 5 - Conclusions & suggestions

5.1 Lessons and achievements

Throughout this project, theoretical knowledge was acquired until the experimental rig was designed as well as the necessary experience to manufacture and operate it. Firstly, by understanding the possibilities and limits of additive manufacturing methods, their strength and areas of specialisation. Then by perceiving the subtlety between theory and practice, particularly for the FDM process, allowing to put adapted design strategies in practice to obtain repeatable good quality prints. Finally, by assimilating this process and its correlations with robocasting, until overstepping it in order to configure the experimental rig using the LDM process.

The developed machine could find a multitude of use regarding the needs in the medical fields, particularly in dental applications where the use of ceramic materials is increasing. Those are usually costly elements, hard to produce with conventional machining, and the few additive manufacturing technique they can work with are still limited or expensive to use. The created experimental rig has therefore shown ability to operate with a thick fluid and print in X and Y directions at constant velocity. It was also able to extrude a zirconia-ceramic paste produced by the partner BioMat Research Group, thus fitting in the needs of testing better dental materials in the long run. The flowing speed of the early version of the ceramic paste was not precisely driven but the positioning and printing speeds proved to be mastered.

This LDM experimental rig was build adapting an existing FDM printer by replacing its tool head. The developed tool head works thanks to a standard micrometric syringe, which sleeve is actuated in rotation thanks to a geared interface actuated by a stepper. The necessary modifications were designed using as much of the original machine’s elements as possible, along with a maximum of 3D printed parts that were directly produced in the Lab2Prod. However, some parts were produced with available equipment for logistical reasons but their production was not justified from a cost study. Following a modularity concept for its assembly, it also possible to replace with ease specific part on this prototype, both for maintenance and printing process improvements.

Along with the prototype, sub-solutions and solved problems were individually documented on parts design, forming along with the adopted strategy a reliable process of designing for additive manufacturing. The identified achievements, as 3D printing gears, could be useful for similar issues clarification on coming projects within the Lab2Prod.

5.2 Future work

This section aims to take stock of some improvements that can be made in the short term, to make the prototype both easier to handle and safer. The following aspects of the experimental rig are listed here by order of usefulness.

5.2.1 Mechanical improvements

- Build an all-in-one body that will reposition the syringe on the X carriage to allow bed auto-levelling and for a more compact system, in order to win space in the build volume. This can also reduce the sensitivity of the prints to X axis dynamic motion, or get more room for a potential second extruder.
- Reduce mechanical slack in the mechanism by enlarging the linear sliding zone on the square shaft (interface C on Figure 3.3). This can be done by adding another plastic slider or considering a made to measure print with a tribological filament.
- For the case of a prototype with low plays, insert an angle corrector or homokinetic rotational joint to correct axis alignment between motored square shaft and the top clamp.
- Redesign gears in metal to improve its bulkiness for the same torque transmission. Ideally insert a gearbox to vary the reduction ration according to the chosen needle gauge.
- Place both abutment contact sensors on the Lulzbot Mini frame instead of keeping them on the X carriage, in order to simplify cabling and amount of fragile parts on the tool head.
- Add rubber pads on the main clamp to protect the syringe’s glass tank and improve adhesion. Redesign both clamps tightening systems considering wingnuts and quick closing arms of bike seat fasteners as described in section 3.3.2.
- Incorporate nut caps in every body part or consider the thermal threaded inserts that were discarded in section 3.2.1, to avoid using small tools as well as limit contact with glassware in the case of a laboratory use.
- Add stampers on motor steppers to reduce noise and vibration problems in prints.

5.2.2 Electrical securities

- Add and electrical breaker to replace the mechanical fuse for the protection of the needle (see section 3.6.2.1). This can protect the stepper from current overconsumption at the same time.
- Consider a fast to access stop button associated to a safe stop process, since this machine may need to run tests with unknown material reactions or hazardous outcome.
- Think about an enclosure or electrical protections against liquid projections in case of use in a laboratory environment.

5.2.3 Software adaptations

- Adapt the Lulzbot Cura software, or improve a free console as the Octoprint one, to obtain a user friendly interface. The goal is also to simplify the use of the hardware by getting rid of virtual FDM securities described in section 3.1.3.1. Ideally develop a custom made software that will be adapted to the experiments needs.
- Incorporate an automatic printing speed adaptation that will count the available volume of paste in the reservoir as well as the reduction ratio due to gears, syringe and the needle gauge in use.
- Create an environment that allows a maximum of printing settings as for FDM, for instance like support density and positioning. The idea is also to have an interface able to evolve with the hardware's improvements.

5.3 Prospective ameliorations

A few reinterpretations and changes in the long run can also be considered for this prototype, knowing that it embodies the first iteration of an experimental rig that could be used in several fields.

5.3.1 Process improvement

As for the previously described enhancements, a few ameliorations concerning the machine's hardware could act on the printing process itself:

- **Create a needle cutting tool** in the case of the needles would be ordered with a bevel. The idea here would be to have a cutting protocol leaving an output surface usable for printing and which could be as repeatable as possible to avoid calibration problems.
- **Replace the needle** to simplify auto-levelling, regulate the extrusion flow and improve the tool head bulkiness. It can be made quite simply as the manner of the permanent solution described in section 3.6.1.2, or outright by replacing the syringe by pressurised paste tank and endless screw, similarly to the DeltaWasp's system described in section 2.3.3.2. The advantage would be to have a largely more important amount of printable material at the same time, the suppression of air bubbles with the endless screw and the possibility to add a vacuum pump near the nozzle to simulate a FDM-like retraction for shear thinning printed materials.
- **Master the printing temperatures** by adding heating or cooling devices on both build plate and tool head. It can be done by plunging the bed in an oil bath or inserting a thermal liquid system around the extruder and fans on the tool head. With the optic of testing a maximum of liquid materials and since some pastes can react differently under several conditions there is also the idea of adding and electrolyte bath, UV lights or even vacuum pump and their related sensors.
- **Allow double extrusion** or create interchangeable heads to be able to print composite ceramics or test adaptive macro-structures.

5.3.2 Experimentation planning

Independently of the fields this experimental rig will be used in, a global planning scheme can be made to win time over printing settings tests, corresponding to the controllable parameters. The technique of defining and investigating all possible conditions with multiple factors in an experiment is known as the factorial design in the literature (Roy 2010). For a full factorial design, the number of possible designs is $N = L^m$ where m is the number of factors and L the number of associated levels. Since N grows exponentially, techniques such as fractional factorial plans are used to simplify the experiment by investigating only a small portion of all possible combinations. This approach saves considerable time and money but suffer from the following limitations:

- The experiments become unwieldy in cost and time when the number of variables is large.
- Two designs for the same experiment may yield different results.
- The interpretation of the experimental results with a larger number of factors may be difficult due to lack of standard design and analysis guidelines.

To overcome those issues, we can consider here the Taguchi method, advantage being the use of standardized experiment design methodology. The whole of the approach arise out of the idea that quality should be designed into the process and not inspected into it, where the best results are achieved by minimizing the deviation from a target. In engineering terms, this reconsideration of quality makes it measurable through consistency of performance, and is achieved when performance is close to the target with least variation. To improve quality, the strategy is thus to find the factor-level combination that reduces performance variability, then to adjust the factor levels that bring performance closer to the target. In practice that is done by planning experiments according to a standard specific set of tables called orthogonal arrays, which represent the smallest fractional factorials. That also allow to set a robust planning strategy to identify noise factors and thus study the loss functions and run signal-to-noise analysis. This strategy therefore corresponds to the search of suitable range of printing settings, independently of the controlled parameters.

For instance, this can be a productive first approach to identify settings with the greatest influence on printing quality, to set further, more advanced experiments. A typical application of the method will include the following five major steps:

- **Brainstorming** about quality characteristics, define tested factors and objectives. (ex: final printed dimension’s variation under 5%, printing speed and bed temperature as variables)
- **Designing** the experiment on standardised orthogonal arrays (ex: using software as KitTag)
- **Conducting** the experiment (in 3D printing several times to obtain reliable statistics)
- **Analysing** the results to determine the optimum conditions (and parameters interactions)
- **Running confirmatory test(s)** using the optimum conditions

References

3D Matter. 2017. “FDM 3D Printing Materials Compared | 3D Hubs.” 2017. https://www.3dhubs.com/knowledge-base/fdm-3d-printing-materials-compared.

ACMA. 2014. “Pros and Cons of Additive Manufacturing | Composites Manufacturing Magazine.” 2014. http://compositesmanufacturingmagazine.com/2014/10/pros-cons-additive-manufacturing/.

Afonso Vilar de Castro Paredes, Madalena. 2017. “Optimization of Zirconia-Based Pastes for Additive Manufacturing of Dental Prosthesis.” Instituto Superior Técnico.

André Mateus de Marques Frutuoso, Nuno. 2017. “Tool-Path Generation for a Multiple Independent Print Head System for Fused Deposition Modeling.” Instituto Superior Técnico.

Armstrong, Courtney. 2016. “Post Processing for FDM Printed Parts | 3D Hubs.” 2016. https://www.3dhubs.com/knowledge-base/post-processing-fdm-printed-parts.

ASTM International. 2012. “ASTM F2792 - 12a Standard Terminology for Additive Manufacturing Technologies (Withdrawn 2015).” West Conshohocken, PA. 2012. https://www.astm.org/Standards/F2792.htm.

Atala, Anthony, and Sean V Murphy. n.d. *Perinatal Stem Cells*. Vol. 9781493911.

Azari, Abbas, and Sakineh Nikzad. 2009. “The Evolution of Rapid Prototyping in Dentistry: A Review.” *Rapid Prototyping Journal* 15 (3): 216–25. https://doi.org/10.1108/13552540910961946.

Bird, Jane. 2012. “Exploring the 3D Printing Opportunity.” 2012. https://www.ft.com/content/6dc11070-d763-11e1-a378-00144feabdc0.

C. B. Dias Pinheiro, Francisco. 2018. “Development of a Functional Upper Limb Prosthesis,” no. May.

Cesarano, Joseph. 1998. “A Review of Robocasting Technology.” *MRS Proceedings* 542 (January): 133. https://doi.org/10.1557/PROC-542-133.

EngineersEdge. 2018. “External Metric Thread Table Chart and Fastener Sizes M1.6 - M18 | Engineers Edge.” 2018. https://www.engineersedge.com/hardware/metric-external-thread-sizes1.htm.

Graham, Michael. 2017. “A Practical Guide to FDM 3D Printing Gears – EngineerDog.” 2017. https://engineerdog.com/2017/01/07/a-practical-guide-to-fdm-3d-printing-gears/.

GrantaDesigns. 2015. “Granta Design:” 2015. http://www.grantadesign.com/education/edupack/tools.htm.

Haque, Rizwan. 2016. “Five Things You Need To Know About Injection Molding.” 2016. https://www.creativemechanisms.com/blog/five-things-you-need-to-know-about-injection-molding.

Hudson, Ben. 2016. “How to Design Parts for FDM 3D Printing | 3D Hubs.” 2016. https://www.3dhubs.com/knowledge-base/how-design-parts-fdm-3d-printing.

Ivoclar Vivadent. n.d. “IPS e.Max ZirCAD Properties.” Accessed July 2, 2018. http://www.ivoclarvivadent.com/en/p/all/products/all-ceramics/ips-emax-technicians/ips-emax-zircad.

Le, Van Thao, Henri Paris, and Guillaume Mandil. 2017. “Process Planning for Combined Additive and Subtractive Manufacturing Technologies in a Remanufacturing Context.” *Journal of Manufacturing Systems* 44 (June): 243–54. https://doi.org/10.1016/j.jmsy.2017.06.003.

Lewis, Jennifer A, James E Smay, and John Stuecker. 2006. “Direct Ink Writing of Three-Dimensional Ceramic Structures.” https://doi.org/10.1111/j.1551-2916.2006.01382.x.

Ligon, Samuel Clark, Robert Liska, Jürgen Stampfl, Matthias Gurr, and Rolf Mülhaupt. 2017. “Polymers for 3D Printing and Customized Additive Manufacturing.” *Chemical Reviews* 117 (15): 10212–90. https://doi.org/10.1021/acs.chemrev.7b00074.

Materialise Cloud. 2015. “STL Converter | Materialise Cloud.” 2015. https://cloud.materialise.com/tools/stl-converter.

MatWeb. 2007. “304 Stainless Steel.” 2007. http://matweb.com/search/DataSheet.aspx?MatGUID=abc4415b0f8b490387e3c922237098da&ckck=1.

Micallef, Joe. 2015. *Beginning Design for 3D Printing*. Apress. https://doi.org/10.1007/978-1-4842-0946-2.

Michalec, George. 1994. “Elements of Metric Gear Technology,” 1–124. http://scholar.google.com/scholar?hl=en&btnG=Search&q=intitle:ELEMENTS+OF+METRIC+GEAR+TECHNOLOGY#0.

NASA, and Quincy Bean. 2017. “ISS Science for Everyone.” https://doi.org/10.2514/6.2013-5439&SA=X&SCISIG=AAGBFM1B6WPTLFEC_RJHH9CIREQEXWSMLG&OI=SCHOLARALRT.

Peng, Erwin, Xiangxia Wei, Ulf Garbe, Dehong Yu, Brunet Edouard, Aihong Liu, and Jun Ding. 2018. “Robocasting of Dense Yttria-Stabilized Zirconia Structures.” *Journal of Materials Science* 53 (1): 247–73. https://doi.org/10.1007/s10853-017-1491-x.

RepRap. 2018. “G-Code - RepRap.” 2018. https://reprap.org/wiki/G-code.

Roy, Ranjit K. 2010. *A Primer on TheTaguchi Method*. Edited by Society of Manufacturing Engineers. Dearborn, Michigan 48121.

Russo, Lucio Lo, Khrystyna Zhurakivska, Domenico Speranza, Angelo Salamini, Domenico Ciavarella, Stefano Ciaramella, Massimo Martorelli, et al. 2018. “A Comparison among Additive Manufactured

Polymeric Complete Dental Models Resulting from Intraoral Scans: An in Vivo Study.” *International Review on Modelling and Simulations* 11 (1): 1–4. https://doi.org/10.15866/iremos.v11i1.14186.

Sarasota. 2017. “Zirconia Dental Implants vs Titanium Implants - Which Is the Best?” 2017. https://www.sarasotadentistry.com/dental-blog/zircona-dental-implants-vs-titanium-implants/.

Schoffer, Filemon. 2016. “How Expiring Patents Are Ushering in the next Generation of 3D Printing | TechCrunch.” 2016. https://techcrunch.com/2016/05/15/how-expiring-patents-are-ushering-in-the-next-generation-of-3d-printing/?guccounter=1.

Shen, James Zhijian. 2014. *Advanced Ceramics for Dentistry*. *Advanced Ceramics for Dentistry*. https://doi.org/10.1016/C2011-0-07169-7.

Simplify3D. 2018. “Print Quality Troubleshooting Guide | Simplify3D Software.” 2018. https://www.simplify3d.com/support/print-quality-troubleshooting/#warping.

Ultimaker. 2017. “Technical Data Sheet ABS.” https://ultimaker.com/download/67931/TDS ABS v3.012.pdf.

Xu, H.H.K., D.T. Smith, S. Jahanmir, E. Romberg, J.R. Kelly, V.P. Thompson, and E.D. Rekow. 1998. “Indentation Damage and Mechanical Properties of Human Enamel and Dentin.” *Journal of Dental Research* 77 (3): 472–80. https://doi.org/10.1177/00220345980770030601.

Zhang, Ya-Rong, Wen Du, Xue-Dong Zhou, and Hai-Yang Yu. 2014. “Review of Research on the Mechanical Properties of the Human Tooth.” *International Journal of Oral Science* 6 (2): 61–69. https://doi.org/10.1038/ijos.2014.21.